



DOCTORAL THESIS

Department of Pharmacy
Graduate School of Pharmaceutical Science, XXXIII Cycle

University of Naples Federico II

Design and synthesis of molecular hybrids between drugs for psoriasis treatment and H₂S donors

Ph.D. Thesis
FLAVIA GIORDANO

Approved by

Ph.D. Supervisor: Prof. Francesco Frecentese
Ph.D. Program Coordinator: Prof. Maria Valeria D'Auria



Summary of PhD thesis

According to PhD fellowship holder within the PhD Program PON RI 2014/2020, my PhD thesis is divided into three parts, the first one carried out at the Department of Pharmacy - University of Naples Federico II, the second one at the Department of Biosciences - University of Salzburg, and the last one at pharmaceutical industry Genetic s.p.a. in Fisciano (Italy).

The project has been principally focused on design, synthesis and characterization of molecular hybrids containing a portion pharmacologically active in the treatment of psoriasis and an H₂S-releasing moiety, with the aim to develop novel compounds able to modulate multiple targets in antipsoriatic therapy. Psoriasis is a chronic and relapsing immune-mediated inflammatory skin disease, characterized by uncontrolled keratinocyte proliferation and dysfunctional differentiation. Since H₂S has proven to be involved in inflammation, pruritus and cytoprotection, molecular hybrids have been developed for merging the beneficial effect of H₂S to pharmacological effect of the starting drug.

My attention has been paid to the synthesis and characterization of H₂S-releasing molecular hybrids, which are composed by glucocorticoids or retinoid derivatives as active drugs in treatment of psoriasis, and H₂S donors (4-hydroxythiobenzamide or TBZ, 4-isothiocyanatophenol or HPI, 5-(4-hydroxyphenyl)-3H-1,2-dithiole-3-thione or ADT-OH, and ethyl 4-hydroxybenzodithioate or HBTA). Topical corticosteroids are the most prescribed treatment for psoriasis worldwide, thanks to their relative potency, rapid efficacy, cosmetic acceptability, and versatility in use. They represent the first-line therapy in several inflammatory diseases. Among glucocorticoids, I have chosen Betamethasone 17-valerate and Triamcinolone acetonide as approved active drugs in psoriasis treatment, due to their wide both topical and systemic use. As the latter, also retinoid derivatives are commonly used in psoriasis therapy, such as Acitretin which is usually used as systemic drug, and Tazarotenic acid that represents the active form of the first topical receptor-selective retinoid prodrug, Tazarotene. Chemical synthesis of

the four series of molecular hybrids and their characterization are described in this thesis.

At the present, results relative to steroidal anti-inflammatory H₂S-releasing hybrids are the only one already disclosed due to the reduction in activity related to COVID-19, and the difficulties and costs behind working with animals for screening assays. However, the studies on retinoids derivatives are ongoing.

The corticosteroid derivatives have been evaluated *in vitro* for their H₂S releasing properties via amperometric assay by the research group of Professor Vincenzo Calderone. Moreover, the same research group have performed preliminary experiments on tissue viability and determination of cytokine levels, because of involvement of proinflammatory mediators at different stages of the disease. Triamcinolone acetonide hybrids resulted to be able to release a greater amount of H₂S than Betamethasone-17-valerate hybrids. Different H₂S releasing properties for the glucocorticoid molecular hybrids have been investigated by Professor Caterina Fattorusso through computer aided Structure-Activity Relationship studies that allow to demonstrate that the less flexible acetal substituent of positions 16 and 17 in Triamcinolone acetonide in comparison to the more flexible and bulky alkyl chain of Betamethasone 17-valerate limited the conformational freedom of the H₂S-releasing group and influenced the interactions of L-Cys with H₂S donor moiety.

The other *in vitro* assays have also confirmed the superior efficacy of Triamcinolone acetonide hybrid derivatives, analyzing the cytoprotective effect of compounds via MTT assay, and the anti-inflammatory activity with the cytokine levels assays. However, these represent only preliminary data, because the replicates number of experiments on tissue viability and quantification of cytokine levels does not allow now to report the significance.

Following, *in vivo* screening on two of Triamcinolone acetonide hybrid derivatives have been performed by research group of Professor Marcelo Muscarà, evaluating Psoriasis Area Severity Index (PASI), as degree of skin inflammation on the back of the animals, skin thickness, based on a daily measurement of ear thickness, itch behaviour, and quantification of splenocytes in a mouse model of imiquimod-induced psoriasis. The results showed that the tested hybrids had only a small and, in some cases, not significant improvement in comparison to Triamcinolone acetonide. This not significant

additive or synergistic efficacy of synthesized hybrids has been addressed to the already very high efficacy of glucocorticoids at the very low dose adopted. H₂S donors, instead, need higher dosage to ensure their full pharmacological effect.

Finally, due to the interest of Genetic s.p.a. towards respiratory diseases and the well-known anti-inflammatory pharmacological effect of glucocorticoids in the treatment of asthma in addition to the positive effect of H₂S on the respiratory tract, H₂S-releasing glucocorticoids have been also tested for their anti-asthmatic properties, evaluating the potential H₂S-releasing profile in the cytosol of bronchial smooth muscle cells (BSMCs), the inhibitory effect on mast cell degranulation and the ability to induce cell membrane hyperpolarization in BSMCs. The most active compounds resulted to be the molecular hybrids with HPI moiety. These effects should be further strengthened by *in vivo* models, but these preliminary data may already pave the way for exploiting the hybridization process with H₂S-donor moieties for increasing the pharmacological activity of already employed drugs or counteracting specific side effects.

In the second unit of the thesis, I discuss about my experience at the University of Salzburg. According to the PhD program, I spent 6 months at the Department of Biosciences to collaborate with the research group of Professor Chiara Cabrele.

During this experience I have had the opportunity to improve my skills in peptide synthesis (both manually and automatic), purification and characterization, learning the use and interpretation of UV and circular dichroism spectroscopies, and making a structural investigation by nuclear magnetic resonance spectroscopy, analyzing the NMR spectra (TOCSY, COSY, ROESY) of peptides.

The study was mainly focused to the synthesis of phosphopeptides and peptide models to investigate π -cation interactions. I accomplished the manual synthesis of a difficult peptide sequence of the Id3 protein in both the unphosphorylated and phosphorylated forms, to investigate the effect of phosphorylation on the helix-2 of Id3. I characterized the two forms by mass spectrometry, HPLC analysis, and circular dichroism spectroscopy under different conditions. What concerns the peptide models to investigate π -cation interactions, I synthesized them by automatic peptide synthesizer and purified some of them via semipreparative HPLC. I characterized them by mass spectrometry, HPLC analysis, and circular dichroism spectroscopy. Thus, I analyzed the

results of the syntheses to find a correlation between peptide sequence and synthesis outcome. Finally, I contributed to the synthesis of FRET-peptides as active substrates of bacterial serine protease HtrA, with the aim to determinate the activity of *H.pylori* HtrA. With this work on the fluorogenic peptides I have contributed to a recent publication on the peer-reviewed journal Scientific Reports. The synthesis of FRET-peptides was performed manually, and the peptides were characterized by mass spectrometry and HPLC analysis. One of them was selected and used for testing the activity of *H.pylori* HtrA via FRET-peptide assay. The results suggested that the FRET peptide as a substrate for HpHtrA is a highly sensitive and reliable approach to quantify HtrA activity.

The third unit focuses on my training experience at the pharmaceutical industry Genetic s.p.a. in Fisciano (Italy). I spent 6 months there, in which I looked at all the aspects of development of different pharmaceutical forms, including the development of analytical methods and their validation, thus the validation processes and finally the stability studies to ensure the safety, efficacy, and quality of a new drugs, and to determinate its shelf-life.

During the first months I focused my attention on studying the characteristic of dosage forms and learning the use of instruments in the R&D labs, applied on already active projects. Then, I designed potential formulations for the synthesized compounds that have shown more promising results. Further studies finalized to the evaluation of the active substances' stability, to the determination of the formulation's physicochemical stability and to the characterization of their *in vitro* performances will be carried out by Genetic s.p.a. on the developed formulations.

Publications

- Giordano F, Corvino A, Scognamiglio A, Citi V, Gorica E, Fattorusso C, Persico M, Caliendo G, Fiorino F, Magli E, Perissutti E, Santagada V, Severino B, Pavese RC, Petti F, Martelli A, Calderone V, Frecentese F. Hybrids Between H₂S-donors And Betamethasone 17-Valerate Or Triamcinolone Acetonide: *In Vitro* Effect In Asthma Treatment. *Submitted*.
- Bernegger S, Brunner C, Vizovišek M, Fonovic M, Cuciniello G, Giordano F, Stanojlovic V, Jarzab M, Simister P, Feller SM, Obermeyer G, Posselt G, Turk B, Cabrele C, Schneider G, Wessler S. A novel FRET peptide assay reveals efficient *Helicobacter pylori* HtrA inhibition through zinc and copper binding. *Sci Rep*. 2020;10(1):10563.
- Narayanaswami V, Tong J, Fiorino F, Severino B, Sparaco R, Magli E, Giordano F, Bloomfield PM, Prabhakaran J, Mann JJ, Vasdev N, Dahl K, Kumar JSD. Synthesis, in vitro and in vivo evaluation of ¹¹C-O-methylated arylpiperazines as potential serotonin 1A (5-HT_{1A}) receptor antagonist radiotracers. *EJNMMI Radiopharm Chem*. 2020;5(1):13.
- Ferrante MC, Di Vaio P, Magli E, Frecentese F, Meli R, Caliendo G, Corvino A, Fiorino F, Giordano F, Monnolo A, Saccone I, Santagada V, Severino B, Calabria G, Manzo C, Perissutti E. PCB levels in adipose tissue of dogs from illegal dumping sites in Campania region (Italy). *Chemosphere*. 2020;244:125478.
- Magli E, Severino B, Corvino A, Perissutti E, Frecentese F, Saccone I, Giordano F, Castro M, Brea J, Loza MI, Santagada V, Caliendo G, Fiorino F. New Serotonergic Ligands Containing Indolic and Methyl Indolic Nuclei: Synthesis and In Vitro Pharmacological Evaluation. *Med Chem*. 2020;16(4):517-530.
- Kędzierska E, Fiorino F, Gibuła E, Corvino A, Giordano F, Herbet M, Dudka J, Poleszak E, Właż P, Kotlińska JH. Anxiolytic-like effects of the new arylpiperazine derivatives containing isonicotinic and picolinic nuclei: behavioral and biochemical studies. *Fundam Clin Pharmacol*. 2019;33(3):254-266.

- Zaminelli T, Magli E, Frecentese F, Lescano CH, Campos R, Saccone I, Corvino A, Di Vaio P, Giordano F, Luciano P, Fiorino F, Perissutti E, Santagada V, Severino B, Caliendo G, De Nucci G. Synthesis and Pharmacological Screening of Pyridopyrimidines as Effective Anti-Diarrheal Agents through the Suppression of Cyclic Nucleotide Accumulation. *ChemistryOpen*. 2019;8(4):464-475.
- Ercolano G, De Cicco P, Frecentese F, Saccone I, Corvino A, Giordano F, Magli E, Fiorino F, Severino B, Calderone V, Citi V, Cirino G, Ianaro A. Anti-metastatic Properties of Naproxen-HBTA in a Murine Model of Cutaneous Melanoma. *Front Pharmacol*. 2019;10:66.
- Magli E, Fiorino F, Severino B, Corvino A, Perissutti E, Frecentese F, Giordano F, Saccone I, Luciano P, Zaminelli T, Santagada V, Caliendo G, de Nucci G. Synthesis of phenylpyrimidinones as guanylyl cyclase C inhibitors. *Pharmazie*. 2019;74(1):15-17.

Abbreviations

2-Abz	2-aminobenzoyl
3-MST	3-mercaptopyruvate sulfurtransferase
ACN	Acetonitrile
AD	Atopic dermatitis
ADT-OH	5-(4-hydroxyphenyl)-3H-1,2-dithiole-3-thione
AMCP	Antimicrobial Peptide
AMP	Adenosine Monophosphate
AOAA	aminooxyacetic acid
AP-1	Activator Protein 1
BB-UVB	broadband UVB
BCA	β -cyano-alanine
BMP2	Bone Morphogenic Protein
BMV	Betamethasone 17-valerate
Boc	tert-Butyloxycarbonyl
BSMCs	Bronchial Smooth Muscle Cells
C/EBPs	CCAAT-enhancer-binding proteins
cAMP	Cyclic Adenosine Monophosphate
CAT	Cystathionine Aminotransferase
CBS	Cystathionine β -synthase
CCHCR1	Coiled-coil alpha-helical rod protein 1
CD	Circular Dichroism
cGMP	Cyclic guanosine monophosphate
CSE	Cystathionine γ -lyase
CyA	Cyclosporin A
DAO	D-amino-oxidase
DCM	Dichloromethane
DDR	DNA damage response

DIPEA	N,N-diisopropylethylamine
DMAP	N,N-Dimethyl-4-aminopyridine
DMF	<i>N,N</i> -Dimethylformamide
DMSO	dimethyl sulfoxide
DNA	Deoxyribonucleic acid
DSBs	DNA double-strand breaks
EDC	N-(3-Dimethylaminopropyl)-N'-ethylcarbodiimide hydrochloride
EDT	1,2-ethanedithiol
ELISA	Enzyme-Linked Immunosorbent Assay
ERK	Extracellular Signal-Regulated Kinase
FAEs	Fumaric Acid Esters
FDA	Food and Drug Administration
FI	Fluorescence Index
FKBP	FK506 binding protein
Fmoc	9-Fluorenylmethoxycarbonyl
FRET	Fluorescence or Forster Resonance Energy Transfer
GR	Glucocorticoid Receptor
GSH	Reduced Glutathione
GSK-3 beta	Glycogen Synthase Kinase 3 beta
HBTA	ethyl 4-hydroxybenzodithioate
HBTU	2-(1H-benzotriazole-1-yl)-1,1,3,3-tetramethyluronium hexafluorophosphate
HLA-C	Human leukocyte antigen c
HLH	Helix-Loop-Helix
HOBt	N-hydroxybenzotriazole
HpHtrA	Helicobacter Pylori -High Temperature Requirement A
HPI	4-isothiocyanatophenol
HPLC	High-performance liquid chromatography
HSP	Heat Shock Proteins

Htra	High Temperature Requirement A
IFN γ	Interferon-gamma
IKK	I-kappa B kinase
IL-1 beta	Interleukin-1 beta
IL-12	Interleukin-12
IL-17	Interleukin-17
IL-17RA	Interleukin -17 receptor A
IL-23	Interleukin-23
IL-6	Interleukin-6
IMQ	Imiquimod
iNOS	Inducible nitric oxide synthase
LPS	Lipopolysaccharide
LR	Lawesson's reagent
MAPK	Mitogen-Activated Protein Kinase
MDC1	Mediator of DNA damage checkpoint protein 1
MHC	Major Histocompatibility Complex
mTOR	mammalian Target Of Rapamycin
MTT	3-(4, 5-dimethylthiazolyl-2)-2, 5-diphenyltetrazolium bromide
MTX	methotrexate
NADH	Nicotinamide Adenine Di Nucleotide Hydrogen
NADPH	Nicotinamide Adenine Dinucleotide Phosphate Hydrogen
NB-UVB	narrowband UVB
NFAT	Nuclear factor of activated T-cells
NF- κ B	Nuclear Factor- κ B
NMP	N-methyl-2-pyrrolidinone
OBzl	Benzyl ester
PASI	Psoriasis Area Severity Index
Pbf	Pentamethyl-2,3-dihydrobenzofuran-5-sulfonyl
PDE4	Phosphodiesterase 4

PGG	Propargylglycine
PIP	Piperidine
PLP	Pyridoxal 5'-phosphate
PPIs	Protein-protein interactions
PSORS	Psoriasis Susceptibility Locus
PUVA	Psoralen Plus UVA
RAR	Retinoid Acid Receptors
RXR	Retinoid-X-Receptors
SASA	Solvent Accessible Surface Area
SPI	Salford Psoriasis Index
TAA	Triamcinolone acetonide
TAK1	TGF-beta-activated Kinase 1
tBu	tert-Butyl
TBZ	4-hydroxythiobenzamide
TCIs	Topical Calcineurin Inhibitors
TFA	Trifluoroacetic acid
TFE	2,2,2-Trifluoroethanol
TGFβ	Transforming Growth Factor beta
Th1	T helper 1
Th17	T helper 17
TIA	Thioanisole
TIS	Triisopropylsilane
TNF	Tumor Necrosis Factor
Trt	Trityl
VDR	Vitamin D Receptor
VEGF	Vascular endothelial growth factor
Y(NO ₂)	3-nitro-tyrosine

INDEX

Unit 1

Design and synthesis of molecular hybrids between drugs for psoriasis treatment and H₂S donors

1. Introduction	2
1.1. Psoriasis	2
1.2. Histological features and clinical classification	2
1.3. Comorbidities	7
1.4. Etiopathogenesis	9
1.5. Treatment of psoriasis	11
2. Hydrogen sulfide (H₂S)	31
2.1. Hydrogen sulfide as “new” gaseous transmitter	31
2.2. Chemical and biological properties	31
2.3. H₂S biosynthesis	32
2.4. Biological activity of H₂S in skin disorders	34
3. Aim of project	39
4. Chemistry	44
5. Experimental Section	49
5.1. Materials and Methods	49
5.2. General procedure for the synthesis of 21-hemisuccinate glucocorticoids	49
5.3. Synthesis of compounds I-VIII	51
5.4. Synthesis of compounds IX-XII	57
5.5. Synthesis of compounds XIII-XVI	59
5.6. Molecular Modelling	61
5.7. Pharmacological procedures	62
6. Results and Discussion	71

6.1.	Amperometric evaluation of H ₂ S releasing properties	72
6.2.	Computer Aided Structure-Activity Relationship Studies	76
6.3.	Tissue viability	79
6.4.	Determination of cytokine levels	80
6.5.	PASI score and skin thickness.....	84
6.6.	Itch behaviour.....	85
6.7.	Quantification of splenocytes	86
6.8.	In vitro studies of H ₂ S-releasing glucocorticoids anti-asthmatic properties.....	87
7.	Conclusion.....	95
	References.....	99

Unit 2

Chapter 1: Intramolecular contacts to stabilize secondary structure

1.	Introduction	110
1.1.	Protein-protein interactions mediated by α -helices and β -strands	110
1.2.	Phosphorylated and non-phosphorylated Id3 protein	111
2.	Experimental Part	113
2.1.	Materials and methods.....	113
2.2.	Peptide synthesis.....	114
3.	Results and Discussion	117
3.1.	Analytical characterization of the peptides.....	117
3.2.	CD spectroscopy	121

Chapter 2: Synthesis of FRET-active substrates of bacterial serine protease HtrA

1.	Introduction	125
2.	Experimental Part.....	126

2.1. Materials and methods.....	126
2.2. Peptide synthesis and analysis.....	127
3. Results and Discussion.....	130
References.....	137

Unit 3

Design of novel formulations containing H₂S-releasing corticosteroid hybrids

1. Introduction.....	139
2. Aim.....	139
3. Topical formulation for the treatment of psoriasis.....	140
3.1. Cream features.....	141
3.2. Design and analysis of a cream for psoriasis disease treatment.....	143
4. pMDI in the asthma therapy.....	144
4.1. pMDI features.....	146
4.2. Design and analysis of pMDI for the treatment of asthma.....	147
4.3. Dosage Unit Sampling Apparatus or DUSA.....	149
4.4. Next Generation Impactor or NGI.....	150
References.....	152

Unit 1

**Design and synthesis of molecular hybrids
between drugs for psoriasis treatment and H₂S donors**

1. Introduction

1.1. Psoriasis

Psoriasis was originally defined as a disorder primarily of epidermal keratinocytes [1], resulting in aberrant keratinocytes activation and strong cell proliferation. However, it is now considered as one of commonest immune-mediate disorders [2]. Psoriasis is a chronic and relapsing immune-mediated inflammatory skin disease with a high incidence worldwide (2-4%) [3]. In Italy 2.9% of people suffer from psoriasis [4]. The data indicate that the factors which influence the occurrence of psoriasis include age, gender, geographic region, and ethnicity. Psoriasis has traditionally been considered to affect both genders equally and it is less common in children and more common in adults [5, 6]. It is predominant in white people and its prevalence seems to depend on the latitude, being more frequent in countries more distant from the equator because of beneficial effects of sunlight on the disease [3].

1.2. Histological features and clinical classification

Psoriatic disease is characterized by uncontrolled keratinocyte proliferation and dysfunctional differentiation. Histological features of psoriasis plaques (Figure 1) are acanthosis (epidermal hyperplasia), increased vascularity in the dermis, and inflammatory infiltrate composed of dermal dendritic cells, macrophages, T cells, and neutrophils [7, 8].

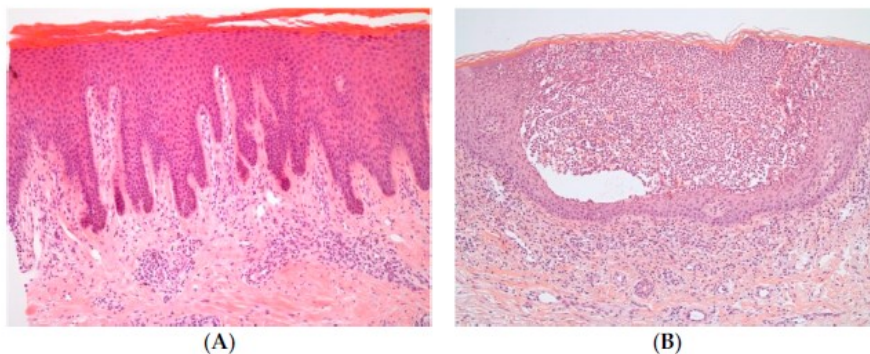


Figure 1. Histological features of psoriasis [8]. **A)** Psoriasis vulgaris. **B)** Pustular psoriasis.

Psoriasis is characterized by well-delineated papulosquamous plaques, that appear red and often covered by white or silver scales and may be painful and often severely pruritic. Plaques are usually distributed symmetrically and most commonly on the region of elbows and knees, scalp, lumbosacral region, umbilicus, palms of the hands, soles of the feet and genital region. However, different forms of psoriasis are distinguished depending on the type of lesion and localization [8, 9].

Psoriasis vulgaris

Psoriasis vulgaris is the commonest type of psoriasis, that affects about 90% of psoriatic individuals [9]. It is characterized by oval or irregular, red, sharply demarcated, raised plaques covered by silver-white scales and that can have different size, and it exists in different site-specific variants. It can be distributed in isolated patches but can also cover large areas of the skin (Figure 2).



Figure 2. A) Small plaque psoriasis. B) Localized thick plaque type psoriasis. C) Large plaque psoriasis [9].

Psoriasis vulgaris can be classified according to the age of onset, that distinguishes two type of psoriasis: type I psoriasis develops before 40th year and is related to genetic conditions, while type II psoriasis develops after 40th year [10].

The lesions may slowly enlarge (active lesions) especially on the legs and trunk or remain static (stable lesions) in advanced stage of disease. Almost 80% of psoriatic patients have mild to moderate disease and 20% have moderate to severe disease which affects more than 5% of the body surface area or well-defined areas of hands, feet, face, or genitals [10]. In the first stage of the disease the plaques developing in the upper layer of the dermis are not well evident; the blood vessels are dilated, allowing lymphocytes and neutrophils to emerge from their lumen and reach the epidermis. Afterwards, there is an uncontrolled proliferation and incomplete maturation of keratinocytes and consequent loss of the stratum granulosum and retention of nuclei in the stratum corneum (parakeratosis). In the advanced stage, disease develops with acanthosis, i.e. thickening of the stratum spinosum, and papillomatosis, i.e. elongation of the dermal papillae. Increased vascularity in the dermis, and inflammatory infiltrate composed of dermal dendritic cells, macrophages, T cells, and neutrophils characterize the psoriatic disease, which may sometimes resolve spontaneously [10].

Flexural (inverse) psoriasis

Flexural (inverse) psoriasis (Figure 3) is characterized by red plaques typically devoid of scales in the skin folds. The plaques are usually located in axillary, genital, perineal, intergluteal, and inframammary areas [9].



Figure 3. Flexural (inverse) psoriasis [7].

Guttate psoriasis

Guttate psoriasis is an acute form of psoriasis with small erythematous plaques with fine scales and appears on the trunk and upper arms and thighs. It usually occurs in children and adolescent. The manifestation of disease often has onset after a bacterial streptococcal infection and can disappear spontaneously or following topical treatment. Sometimes it can evolve in chronic or became into the plaque type [10].

Generalized pustular psoriasis

Generalized pustular psoriasis (Figure 4A) is an acute form of psoriasis characterized by small sterile cutaneous pustules and painful inflamed skin. In this form of psoriasis, a large amount of neutrophils infiltrate into stratum spinosum, being clinically appreciable it gives rise to sterile cutaneous pustules. It is an uncommon and severe form of psoriasis often associated with systemic inflammation symptoms, fever, fatigue, and neutrophils leukocytosis. It can be potentially fatal. Recent data has suggested that this disease has distinct etiology from the common psoriasis, also if it is still identified as a variant of psoriasis [10].



Figure 4. A) Generalized pustular psoriasis. B) Pustular psoriasis localized on the feet soles [8].

Palmoplantar pustulosis

Palmoplantar pustulosis is a localized pustular variant of psoriasis (Figure 4B). It presents yellow-brown, sterile pustules localized on palms and soles. Genetic analysis has shown that palmoplantar pustulosis and psoriasis vulgaris have different causes.

Furthermore, palmoplantar pustulosis predominantly affects women (9:1 female: male ratio) and either current or previous smokers (95%) [7].

Erythrodermic psoriasis

Erythroderma is an acute condition in which the whole-body surface is covered by a generalized erythema (affecting more than 75% of the body surface) and it is characterized by different degree of scaling. It affects 1-2.25% of patients with psoriasis, so it is extremely rare but is the most severe phenotype and can be potentially life threatening. Erythrodermic psoriasis can develop also systemic manifestations such as chills and hypothermia, limb oedema (due to generalized vasodilatation), myalgia, fatigue, and fever [10].

Psoriatic nail disease

Psoriatic nail disease (Figure 5) occurs in about 50% of patients and manifests itself with characteristic nail changes [9]: pitting (small pits in the nail plate), onycholysis (nail plate separation), subungual hyperkeratosis (in which yellow, keratinous material is collected under the nail plate), dystrophy, and the oil-drop sign (orange-yellow subungual discoloration). More than 90% of patient with psoriatic arthritis suffer by this disease. Fingernails are more frequently affected than toenails [11].



Figure 5. Nail changes in patients with psoriatic nail disease [9].

1.3. Comorbidities

Psoriasis main clinical manifestations include skin inflammation associated with pruritus and/or cutaneous pain that often leads to a severe emotional impact and social isolation and worsens patients' quality of life, due to the specific skin symptoms, the problems associated to the treatments ("treatment success") and their high costs, and the psycho-social implications of having to live with a very visible and disfiguring skin disease [3, 11, 12].

Psoriasis is associated also with psoriatic arthritis (an inflammatory arthropathy), that develops in the 40% of psoriasis patients and in the 10% of cases appears before skin manifestation of psoriasis [7, 8].

Moreover, psoriasis is associated with different systemic disorders, including autoimmune diseases, metabolic syndrome, and skin cancer. Psoriasis patients show increased hyperlipidemia, hypertension, coronary artery disease, type 2 diabetes, and increased body mass index. There is also an increased risk of cardiovascular disease [9, 13,14] and sometimes psoriatic individuals also show a higher prevalence of gastrointestinal, liver, and chronic kidney disease. An example is the association of psoriasis with the development of Crohn's disease [8].

Quality of life related to psoriasis

Several studies have proven that psoriasis has a strong negative impact on the life of patients affected by this disease. It has been demonstrated that psoriasis generates a significant detriment to quality of life. The possible causes can be that patients are embarrassed by their appearance because of stigmatized skin. This condition leads to depression and suicidal ideation in more than 5% of psoriatic individuals [11]. The data has shown patients have an increased risk of depression, anxiety, and suicidality, which is particularly elevated in younger patients [12]. About a third of people affect with psoriasis have lack of self-esteem that develops in pathological worries and anxiety and thus in a reduction of quality of life. All these aspects influence the interaction with others and carrying out physical responsibilities, both at work and at home. Avoidance behaviour and believing to be evaluated based on their skin disease produce stress in patients with psoriasis, that can have a deleterious effect on response to therapy. For this

reason, a psychological intervention may ameliorate the management of psoriasis, in addition to regular pharmacological therapy. In adjunct to the physical aspects of the disease (pain, itch, etc.) or the mental aspects of the disease (self-perception, social interaction, etc.), the "quality of life" of psoriatic patients is also influenced by the effects of the treatment on the disease ("treatment success") [11].

With the aim to provide a complete evaluation of disease, a specific scoring system has been validated to give a holistic measure of psoriasis severity, the Salford Psoriasis Index (SPI) [15]:

- S—Signs: a number from 0 to 10 reflecting physical severity of psoriasis based on the Psoriasis Area Severity Index (PASI score);
- P—Psychosocial disability: psychosocial impact of psoriasis on each patient measured as 0-10 on a visual analogue scale;
- I—Interventions: historical severity of disease and associated systemic therapies, episodes of erythroderma, etc.

Psoriatic arthritis

Psoriatic arthritis is a seronegative, chronic inflammatory rheumatoid arthritis [7, 8]. The disease occurs in presence or after severing cases of psoriasis and in about 10% of patients before psoriatic skin manifestation and the lesions usually can appear after 10-15 years after articular affection. Psoriatic arthritis often in associated also with nail disease. Its clinical manifestation consists in oedema, pain and stiff ness of the joints, ligaments, and tendons. Psoriasis and psoriatic arthritis seem not be completely genetically correlated. This disease can affect all the age without difference of gender. Five types of psoriatic arthritis can be distinguished: asymmetrical oligoarthritis, distal interphalangeal predominant, polyarthritis, spondylitis, and arthritis mutilans [7, 16].

Cardiovascular disease

Several studies have shown that patients with psoriasis express an increased risk of cardiovascular disease [9, 13-14]. An increase of myocardial infarction and stroke has been identified only in individuals with severe psoriasis. This systemic manifestation is probably correlated to increase of hyperlipidemia, hypertension, obesity, insulin

resistance that have been registered to be higher in psoriasis patients rather than patients without psoriasis. This comorbidity is mostly elevated in younger patients with severe psoriasis, and it has been demonstrated that the treatment with methotrexate and tumor necrosis factor (TNF) inhibitors may decrease the cardiovascular events.

1.4. Etiopathogenesis

Psoriasis is a complex disease, and its pathogenesis involves genetic, environmental, and immunological factors that alter the normal mechanism of skin growth favouring the formation of the characteristic erythematous patches [8, 10, 17, 18]. The data on family, twin, and relatives' studies suggest that the individuals with psoriasis are genetically predisposed, in fact the incidence is higher in first- and second-degree relatives of psoriatic patients, in which a dysregulated immune response takes place [8]. Nine chromosomal loci of psoriasis have been mapped using linkage method on genome-wide. These loci are known as *psoriasis susceptibility locus* (PSORS1-9). They correspond to regions where genes involved in inflammatory processes or genes involved in the differentiation phases of the proteins that make up the epidermis are localized. The major genetic determinant of psoriasis is PSORS1, which is located in the MHC on chromosome 6p. This region contains three genes of interest related to psoriasis vulgaris: HLA-C, variant HLA-Cw6 allele, encodes a class I MHC protein; CCHCR1, variant WWCC, encodes the coiled-coil x-helical rod protein, that is overexpressed in psoriatic epidermis; CDSN, variant allele 5, encodes corneodesmosin, a protein of the stratum granulosum and corneum of epidermis, important in the terminal stage of epidermis differentiation, that is upregulated in psoriasis. PSORS1 is probably responsible for 35-50% of heritability of the disease and HLA-C is capable to regulate both innate and adaptative response [7, 10].

The alteration of innate and adaptative cutaneous immune system is responsible for the development of psoriatic inflammation [8]. Psoriasis appears as an autoimmune and autoinflammatory disease. A variety of innate and adaptive immune cells and proinflammatory mediators are involved at different stages of the disease. The development of the psoriatic plaque depends on the interaction of keratinocytes with innate and adaptive immune cells which span the dermal layer of the skin.

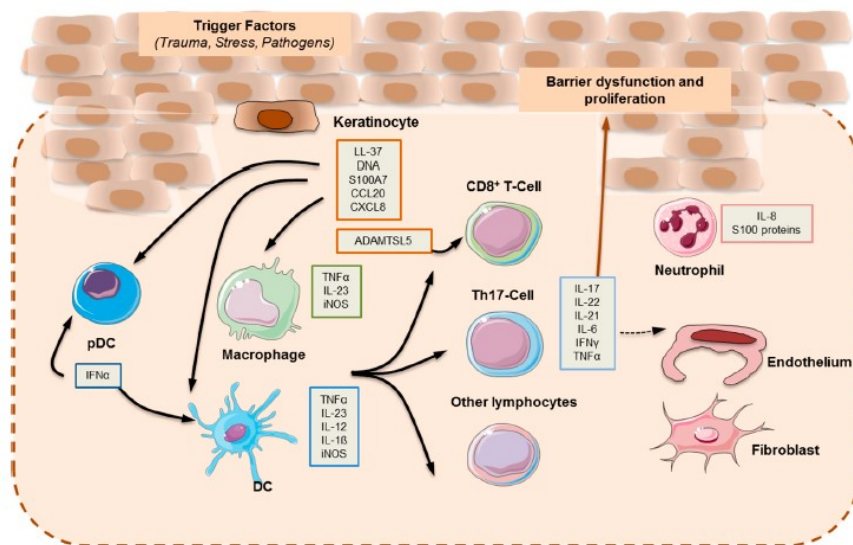


Figure 6. Pathogenesis of psoriasis [8].

Following exposure to certain environmental triggers which may contribute to psoriasis development, such as physical trauma (Koebner phenomenon), infections, drugs, smoking, alcohol, and stress [10], keratinocytes release the cationic antimicrobial peptide (AMCP) LL-37, that forms complexes with genetic material [8] (Figure 6). This event activates the dendritic cells (antigen-presenting cells) which play a significant role in the initial stages of disease. Therefore, a series of signalling pathways is triggered and leads to production of several cytokines involved in the pathogenesis of psoriasis, including $TNF\alpha$, IL-23 and IL-12, with the latter two modulating the differentiation and proliferation of Th17 and Th1 cell subsets, respectively. The activation of the adaptive immune response through the different T cell subsets is responsible of the maintenance phase of psoriatic inflammation. Th1 and Th17 cells secrete a series of pro-inflammatory cytokines that promote the development of psoriasis. Activated Th17 cells can secrete IL-17, IL-22, $TNF\alpha$, and $IFN\gamma$, concentrate neutrophil and promote the proliferation of keratinocytes, leading to the development of psoriasis [8].

The $TNF\alpha$ –IL-23–Th17 is the inflammatory pathway that characterizes plaque-type psoriasis. The IL-17 cytokine family is composed of six members: IL-17A–F. IL-17A and IL-17F are clinically relevant signalling in psoriasis. IL-17A exerts a stronger effect than IL-17F and binds to its trimeric receptor complex composed of two IL-17RA

subunits and one IL-17RC subunit, which interacts with ACT1 adaptor protein, leading to the activation of a series of intracellular kinases including: extracellular signal-regulated kinase (ERK), p38 MAPK, TGF-beta-activated Kinase 1 (TAK1), I-kappa B kinase (IKK), and glycogen synthase kinase 3 beta (GSK-3 beta). These kinases enable NF κ B, AP-1, and C/EBP transcription of pro-inflammatory cytokines, chemokines, and antimicrobial peptides [8].

Drugs targeting TNF α , IL-23, and IL-17 are effective in the clinical management of psoriasis.

1.5. Treatment of psoriasis

Psoriasis is a complex disease that has no definitive cure, and its treatments have only the aim to decrease disease activity and improve the symptoms. The main symptoms of psoriasis include dry or red patches of skin covered by silver-white scales, skin lesion, cracking of skin, inflammation, itching, pain.

The pharmacological therapy for psoriasis is usually chosen according to the clinical manifestations and degree of disease severity, the site of lesions and their extent. Three degrees of severity are distinguished depending on the percentage of affected body surface area: mild psoriasis affects less than 5% of body's surface area, moderate psoriasis affects 5-10%, and severe psoriasis affects more than 10% [19]. Furthermore, the choice of the right therapy is also made based on comorbidities and patient quality of life. In general, mild to moderate psoriasis is usually treated topically with a combination of glucocorticoids, vitamin D analogues, and phototherapy, while moderate to severe psoriasis needs to a systemic treatment.

A statistically data suggest that the variability of the treatment depends on the different countries. For instance, corticosteroids are the favourite topical treatment in the USA, while dithranol is more used in Europe and ciclosporin is preferred in Italy [19].

Psoriasis is a chronic disease that is also influenced by environmental triggers. These exacerbating factors, like stress, alcohol, smoke, drugs (as β -blocking agents, lithium carbonate, antimalarials, and interferon), should be avoided by patients [19]. Hence, proper behaviour along with appropriate therapy and adequate hydration of the psoriatic skin with emollients represent a good treatment of the disease.

From a therapeutic point of view, the last 20 years have seen a radical change in the approach to the psoriatic patient. Traditionally available treatments are topical agents, phototherapy, and systemic agents. The use of topical and systemic corticosteroids, among other drugs, is suggested [20]. In the more severe forms of the disease, systemic therapy with immunosuppressive and chemotherapeutic agents (e.g., cyclosporine, methotrexate, and retinoids) is also recommended. However, the adverse effects produced by the systemic treatments are often severe and a significant number of patients do not respond satisfactorily to them [21]. Thus, complementary therapies are still wanted.

The traditional local and systemic therapy is flanked by an important armamentarium of biological drugs (immunomodulating therapy based on monoclonal antibodies) [19, 22]. The therapy must be tailored to the subject and is therefore always individual and subjective, but the common goal is the remission of lesions and the improvement of the patient's quality of life.

Topical treatment

Topical therapy is the most utilized treatment of psoriasis, especially in patients with mild disease. Different vehicles are available for the correct penetration of medications: creams, lotions, foams, sprays, ointments, gels, solutions, shampoos, and so on. The choice of vehicle depends on different application sites on the body or patient compliance, that uses more gladly a less greasy preparation during the daytime than the night, in which can also use a less cosmetically appealing preparation but more effective [23]. Topical treatment of disease also includes the use of emollients in combination with pharmaceutical therapy, with the aim to maintain correct hydration of the skin.

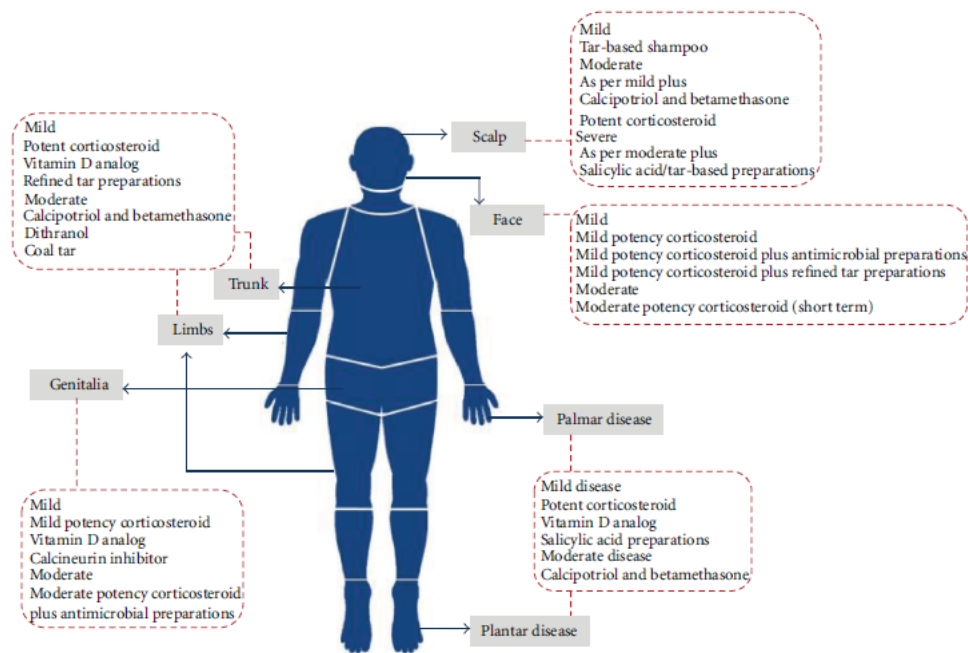


Figure 7. Topical therapy for the treatment of psoriasis [25].

In addition, topical drugs can be used as a monotherapy or in combination, an example is the combination of betamethasone dipropionate and calcipotriol [24]. Moreover, topical agents can be also adjuvant for moderate or severe psoriasis, simultaneously treated with either ultraviolet light or systemic medications, because of their potentially capacity to reduce the amount of phototherapy or systemic agent required to achieve satisfactory disease control.

Topical antipsoriatic drugs available for mild-to-moderate psoriasis include topical corticosteroids, coal tar, vitamin D₃ derivatives (calcitriol, tacalcitol, and calcipotriol), topical retinoids (tazarotene), dithranol (or anthralin), keratolytics (salicylic acid, urea), calcineurin inhibitors (pimecrolimus and tacrolimus) [23].

Topical corticosteroids

Topical corticosteroids are the most prescribed treatment for psoriasis worldwide, thanks to their relative potency, rapid efficacy, cosmetic acceptability, and versatility in use [23]. They are generically used in the treatment of all disease degrees, as a

monotherapy in case of mild psoriasis or in combination with the systemic therapy in case of moderate-to-severe psoriasis [23].

Topical corticosteroids have become the first-line treatment of various dermatological disease including psoriasis, due to their vasoconstrictive, antiproliferative, anti-inflammatory, and immunosuppressive action. Their mechanism of action consists in binding to intracellular glucocorticoid receptor (GR), which is located in the cytoplasm linked to the heat shock proteins HSP90 and HSP70, when the ligand is absent. After binding to GR, this complex GR-HSP is broken, and the complex corticosteroid-glucocorticoid receptor migrates in the nucleus and triggers the transcription of genes with anti-inflammatory functions, like annexin A1 (also known as lipocortin 1) and I κ B- α (protein that has the function to inhibit the NF- κ B transcription factor). Moreover, the complex corticosteroid-glucocorticoid receptor negatively regulates gene transcription of numerous genes, which encode for pro-inflammatory agents, for example, cytokines, growth factors, adhesion molecules, nitric oxide, prostanoids, and other hormones. The complex interacts with nuclear factor- κ B (NF- κ B) leading to its transrepression, inhibiting pro-inflammatory genes transcription [25].

The glucocorticoids enhance the transcription of anti-inflammatory genes and decrease the transcription of inflammatory genes, producing an overall anti-inflammatory effect. Moreover, they repress maturation, differentiation, and proliferation of all immune cells, including dendritic cells and macrophages, giving an immunosuppressive effect. The antiproliferative action is due to their antimitotic activity, that produce a beneficial effect in a disease characterized by elevated cell turnover rate of skin, as psoriasis [25].

Their limitations are due to the occurrence of cutaneous adverse effects such as skin atrophy, telangiectasia, striae distensae, and purpura, and potential systemic adverse effects such as iatrogenic Cushing's syndrome and hypothalamic-pituitary-adrenal axis suppression, that limit their long-term and extensive utilization [23]. To reduce these complications, several strategies have been introduced such as use at weekends only, combination with other topical non-steroidal agents, and transition to drugs of weaker potency when initial clinical response has been obtained. This type of therapy may also improve their efficacy and safety profile and facilitate their use for longer periods [19].

Clobetasol propionate, halobetasol propionate, fluticasone propionate, betamethasone dipropionate, betamethasone valerate and triamcinolone acetonide (Figure 8) are some

examples of effective corticosteroids used in the treatment of psoriasis. They are usually prescribed at 0.05-0.5% concentration [25].

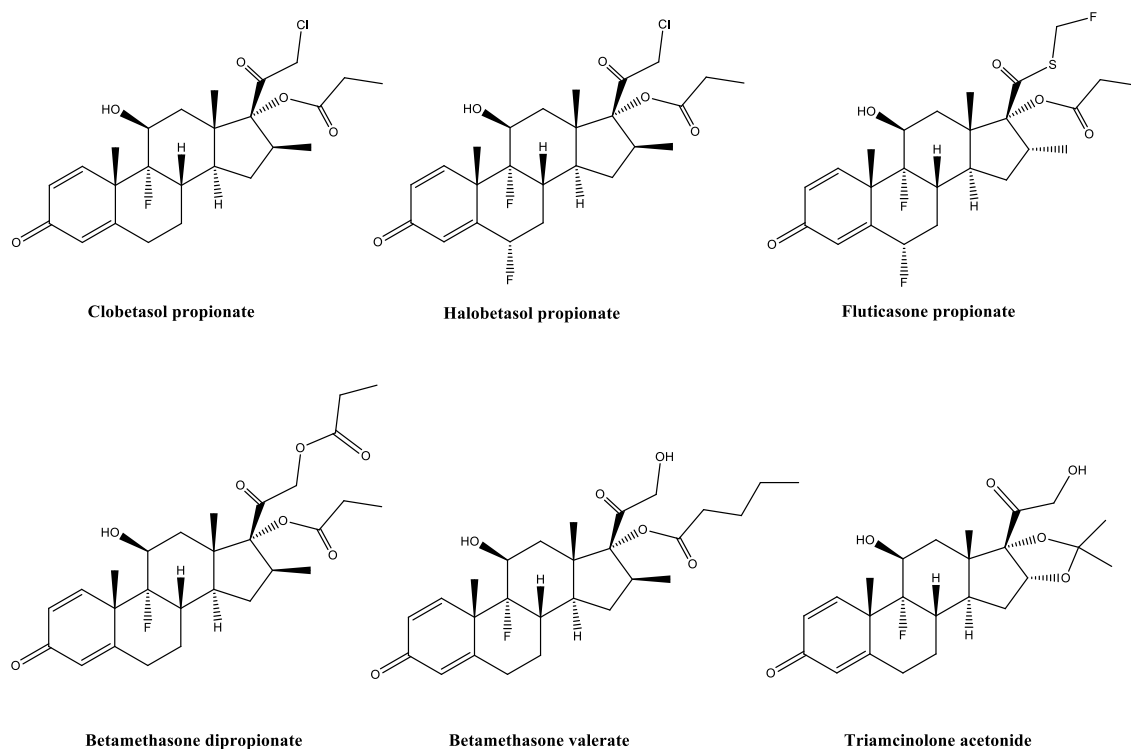


Figure 8. Corticosteroids for the treatment of psoriasis.

Anthralin (Dithranol)

Anthralin (Figure 9) represents one of the oldest and most effective topical treatments of psoriatic plaques [23]. It is usually used for the localized treatment of scaly plaques of psoriasis on the body or the scalp that have not been removed with other treatments. Its use is limited by skin irritation, that depends on concentration of drug on skin. In fact, anthralin may be prescribed as a short contact therapy. It has been demonstrated that the applications of high-dose anthralin for up to 30–60 min a day produce similar effect to longer and twice-daily applications of calcitriol ointment. However, a study on patients treated with short contact anthralin and vitamin D analogues has shown that patients preferred the therapy with vitamin D analogues, because of skin irritation given by anthralin. For this reason, its use has fallen gradually with the onset of more cosmetically suitable drugs [19]. The use of anthralin is recommended during the night and with a concentration of 1% and an application for no more than 1 h. Moreover,

Triethanolamine applied after the removal of anthralin, prevents irritation and neutralizes any anthralin residue remaining on the skin [23].

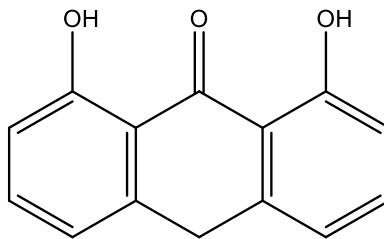


Figure 9. Chemical structure of anthralin.

Anthralin accumulates in keratinocyte mitochondria and creates a dysfunction of mitochondrial membrane inducing apoptosis and causes endogenous cytochrome c release. In its mechanism of action, in which is also involved its capacity to produce free radicals, it reduces keratinocyte proliferation, prevents T-cell activation and restores cell differentiation [26].

Coal Tar

Coal tar is one of the oldest substances used in the treatment of psoriasis. It is available in ointments, shampoos, and solutions, and is commonly used in hospital or day-care settings. Its efficacy improves when associated with UVB exposure. Therapeutic action is due to suppression of DNA synthesis, reduction of cell division of basal layer in epidermis. Odour, staining, irritant contact dermatitis, erythema, stinging, folliculitis, formation of keratoacanthomas, and risk of skin cancer represent its main side effects [19].

Salicylic acid

Salicylic acid is a topical keratolytic agent that now is used in association with other topical drugs for psoriasis (like topical corticosteroid or calcineurin inhibitors) to increase their penetration [23]. Its application determinates the desquamation of corneocytes reducing intercellular cohesiveness of the horny cells and the pH of the stratum corneum, as a result increasing hydration and softening. Its application should

be avoided on large body surfaces and areas with thin stratum corneum, as genitals, the mucous membrane, and the eyes. The principal side effects are the potential chronic or acute systemic intoxication and the consequent symptoms of oral mucosa burning, frontal headache, central nervous system symptoms, metabolic acidosis, tinnitus, nausea, and vomiting [23].

Topical retinoids

Tazarotene is the first topical receptor-selective retinoid prodrug, derived from Vitamin A, used for the management of mild to moderate plaque psoriasis and efficacious also in dealing of acne vulgaris, and photoaging [27]. It is available as a gel or cream at concentration of 0.1% or 0.05% and it is moderately effective as a monotherapy, reducing in plaque elevation, scaling, and erythema, and usually used in combination with Vitamin D analogues or topical corticosteroids, with the aim to reduce steroid atrophogenicity. Tazarotene is even used in association with phototherapy, as UVB and PUVA, accelerating the clinical response and reducing the cumulative UVB or PUVA exposure load. It has been also demonstrated its effectiveness in the treatment of nail psoriasis, reducing onycholysis and pitting [28].

The most common side effects of tazarotene are localized skin irritation, erythema and dryness and it does not give systemic side effects. Tazarotene may be used such as a short contact therapy (30-60 min) and in low concentration, with the aim to minimize symptoms. Moreover, it cannot be used in sensitive areas, like face, flexures, and genitals. After its application, the exposure to sunlight must be avoid. Tazarotene is contraindicated in women who are pregnant because of its risk of teratogenicity [28].

Following topical application, Tazarotene as a prodrug is converted by cutaneous esterases to its active form, the cognate carboxylic acid of tazarotene (Figure 10). Thanks to their polyaromatic structures, both are rigid and nonisomerizable molecules due to the two rings and the linear triple bond system. This characteristic gives to tazarotenic acid an improved retinoid receptor affinity [27, 28].

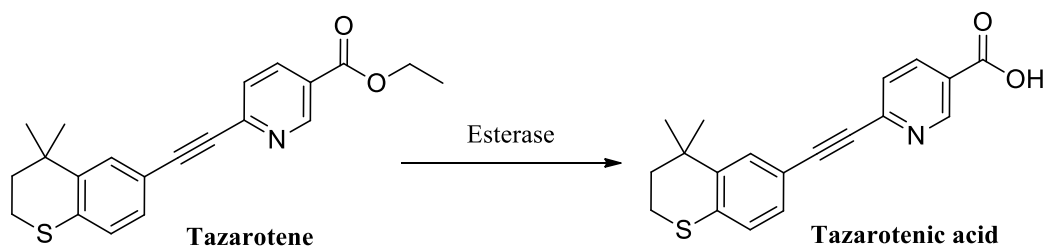


Figure 10. Cutaneous activation of tazarotene to tazarotenic acid.

Topical tazarotene acts on retinoic acid receptors (RAR) and retinoid-X-receptors (RXR). Retinoic receptors are located within nucleus and exist in different isoforms (3 distinct subtypes, α , β , and γ), which have a different distribution in tissues. RAR α is expressed in many embryonic and adults' tissues. RAR β is located in dermal fibroblasts. RAR γ is expressed in adult human epidermis and it is considered the key mediator of retinoid effects on keratinocytes. Tazarotene interacts especially with the RAR family and selectively binds to β , and γ retinoic receptors, making a complex ligand-receptor which migrates in nucleus and regulates the transcription of genes in a direct and indirect manner [28].

The interaction of Tazarotene with retinoic receptors resulting in altered gene expression of inflammatory cytokines and inhibition of keratinocyte proliferation. The results are reduction of epidermal hyperproliferation (antiproliferative effects), normalization of keratinocyte differentiation, and decrease of inflammation [28].

Vitamin D analogues

Vitamin D analogues represent the first-line therapy in treatment of chronic plaque psoriasis, either as monotherapy or in combination and are generally applied once or twice daily. They may be used as long-term therapy thanks to their safety profile. They have proven effective also in the treatment of nails psoriasis. Topical synthetic vitamin D analogues calcitriol, tacalcitol and calcipotriol (Figure 11) have been developed to improve the antipsoriatic effects of vitamin D and decrease hypercalcemic action (because they are rapidly converted into inactive metabolites) [19]. These compounds are commercialized as creams, ointments, or solutions. Calcipotriol is slightly more

effective than calcitriol or tacalcitol and has shown a potency comparable to that of some topical corticosteroids. It is more tolerated than calcitriol and tacalcitol due to less power on calcium homeostasis, even though in general clinically relevant hypercalcemia and para thyroid hormone suppression are rarely noticed for all three vitamin D analogues [23]. Calcipotriol is sold as cream, ointment, and scalp lotion. It is generally used for moderate-severe scalp psoriasis and for plaque psoriasis. Calcitriol is the synthetic form of the vitamin D active metabolite. It is better tolerated than calcipotriol in the treatment of more sensitive areas of body surface, like face, hairline, and flexures [23]. It is usually available as an ointment. Tacalcitol exists as ointment and lotion and although it is resulted less potent than calcipotriol, clinical data suggest that it is a safe, well tolerated, and efficacious long-term treatment for chronic plaque psoriasis and does not show systemic side effects [23].

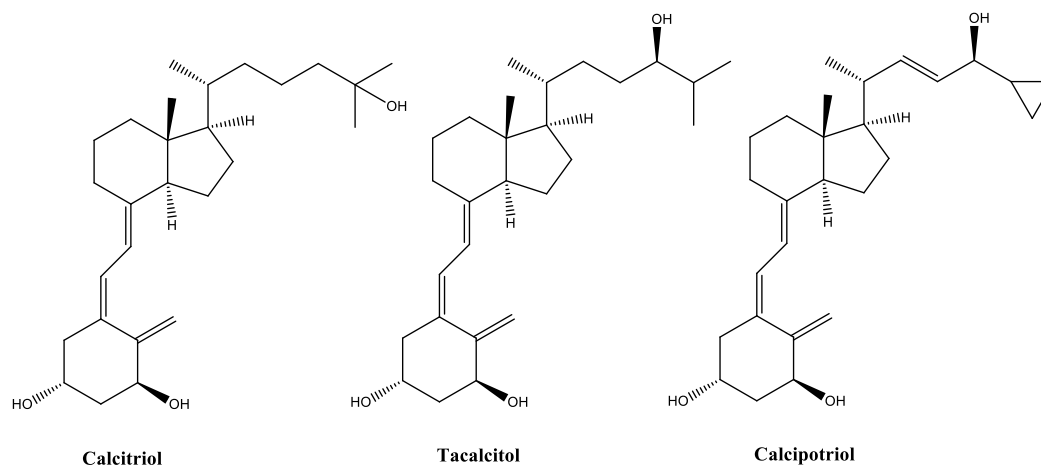


Figure 11. Vitamin D analogues.

These compounds may be used in combination therapy with the aim to reduce the dose and the application time of others antipsoriatic agents. Several studies have been demonstrated that the combination therapy of vitamin D analogues with other antipsoriatic treatment improves the risk-benefit ratio [19]. For instance, the formulation containing calcipotriol and betamethasone dipropionate has proven marked benefits, superior efficacy, and reduction of side effects of both drugs [24].

Vitamin D analogues are overall safe and have few side effects, which occur as skin irritation on or around psoriasis plaques, manifesting as pruritus, burning, oedema, peeling, dryness, and erythema. Hypercalcemia, hypercalciuria, and parathyroid

hormone suppression represent the systemic adverse effects, but are very rare under well controlled doses.

Vitamin D analogues inhibit keratinocytes proliferation and induce keratinocyte differentiation, regenerating healthy skin structure and function. In their mechanism of action Vitamin D analogues bind to the intracellular Vitamin D receptor (VDR), forming the complex ligand-receptor which enter in the nucleus and then binds to vitamin D response elements in the promoter regions of target genes and regulates the genes involved in epidermal proliferation, inflammation, and keratinization [29].

Topical immunomodulators

Topical calcineurin inhibitors (TCIs), tacrolimus, pimecrolimus, and the most recent sirolimus have proven effective in the treatment of psoriasis, even though their use in psoriasis is off label. In fact, they are approved for in the treatment of mild to moderate atopic dermatitis [23].

The data on topical tacrolimus and pimecrolimus in treating psoriasis based on double-blind and open studies have shown that these drugs are efficacious in the treatment of psoriasis, particularly for facial, genital, and intertriginous areas. The studies have suggested a superiority of topical tacrolimus action to placebo and to topical calcitriol, and a superiority of topical pimecrolimus to vehicle, but lower efficacy than calcipotriol or clobetasol ointment. Pimecrolimus has proven effective for inverse psoriasis [30].

Tacrolimus is available as ointment (0.03% and 0.1%) and pimecrolimus as cream (1%). Unfortunately, because of large molecular size and the inability to penetrate thick psoriatic plaques, their efficacy in the treatment of psoriasis is limited. For these reasons, they may be used under occlusion to enhance the penetration, or by combining these agents with salicylic acid, or on the thinner skin of the face, intertriginous areas, or genitals. However, newer vehicles of topical tacrolimus have been developed to improve its penetration into thick psoriatic plaques.

Skin irritation and a usually transient stinging sensation are the most common side effects, along with the theoretical risk of cancer with long term usage. Moreover, they are generally not considered teratogenic due to their low systemic absorption [23].

The molecular mechanisms of action of calcineurin inhibitors involve inhibition of critical signalling pathways that regulate T cell activation.

Tacrolimus is a macrolide lactone antibiotic that was first isolated from the *Streptomyces tsukubaensis*. It binds FKBP proteins and forms a complex tacrolimus–FKBP12. This complex inhibits action of calcineurin phosphatase which is therefore unable to dephosphorylate the transcription factor NFAT (inhibition of NFAT activation). As a result, NFAT remains in the cytoplasm and is unable to transactivate genes involved in T-cell activation. It blocks intracellular signalling pathways that are essential to produce cytokines by lymphocytes, that are important in causing skin lesions in psoriasis [31].

Pimecrolimus is an ascomycin macrolactone derivative, that binds to FKBP12 protein forming the complex ascomycin–FKBP12, and therefore blocks calcineurin activity. In the same way of tacrolimus, it blocks the production of inflammatory substances [31].

Sirolimus (rapamycin) is a macrolide antibiotic, isolated from a fungus. It binds to FKBP12 protein but unlike tacrolimus and pimecrolimus, does not inhibit calcineurin. Instead, sirolimus inhibits a multifunctional serine-threonine kinase, mammalian target of rapamycin (mTOR) that is involved in a different pathway of T-cell activation [31].

The data have proven tacrolimus, pimecrolimus and sirolimus inhibit the proliferation of cultured keratinocytes at therapeutically relevant concentrations [31].

Phototherapy

Phototherapy is one of the most effective treatment modalities for psoriasis. It is used when a large area of the body surface is affected by psoriasis and plaques are small and thin [32]. In the past the exposure to natural sunlight has represented an effective cure in the treatment of psoriasis and it may give benefit in selected psoriatic patients. Phototherapy represents an appropriate treatment for elderly patients, after the topical ones, due to its minimally invasive nature. The treatments are initially required on average 2 or 3 times per week with cautious dose escalation and reduction in frequency with clinical response. The frequency of phototherapeutic treatments in the authorized centers makes the treatment inconvenient for many patients. Moreover, the therapy can sometimes be expensive.

Phototherapy is available as psoralen plus UVA (PUVA), broadband UVB (BB-UVB), and narrowband UVB (NB-UVB) and excimer laser [32].

UVB is having a wavelength in the range of 290-320 nm and is safe, effective, and cost-effective. The most effective UVB wavelength for psoriasis is given with the dose of 300-313nm (narrowband UVB), thus NB-UVB has proven clinically superior to BB-UVB. Narrow band UVB are best tolerated, and it reduced the photo carcinogenic risk in long term therapy. Furthermore, it is safe in pregnancy and mostly applicable for large BSA (body surface area) cure. Only recently a TL-01 UVB fluorescent tube which gives 83% of the UV-emission at the 311 ± 2 nm is made available [32]. Therefore NB-UVB is more expensive than BB-UVB, because of the cost of replacement bulbs.

The UVB (either broadband or narrowband) are often used in combination with tazarotene, vitamin D₃ analogues, or systemic treatments. Additionally, phototoxic and photo allergic drug reactions are less frequent with broadband UVB than with UVA light in photochemotherapy. In using UVB phototherapy, it is very important to determinate the degree of erythema considering the individual patients' Fitzpatrick skin types I-IV to establish the correct UVB dose [19, 32].

UVA is having a wavelength in the range of 320-400 nm and its therapeutic effect alone is limited. For improving its therapeutic effect, it is used in combination with photosensitizing psoralen (PUVA). PUVA photochemotherapy involves ingestion or application of psoralen (5-methoxy psoralen, 8-methoxy psoralen or trioxalen), and subsequent exposure to UVA irradiation. Dose of UVA depends on the presence or absence of erythema. Antipsoriatic effect is given by suppression of DNA synthesis by cross linking to DNA strand and conjugate protein [32].

PUVA therapy has proven very efficacious in many patients with psoriasis, with potential for long remissions. It is more effective of UVB phototherapy, even though NB-UVB therapy avoids some of the PUVA side effects. In fact, the ingestion of psoralen may produce nausea and headache and is contraindicated in pregnancy. Moreover, PUVA induces photoaging and other skin changes including lentiginos, skin burning, and photosensitivity. A long-term PUVA treatment may cause an increased risk of squamous cell carcinoma and possibly malignant melanoma. These side effects may occur mostly in fair-skinned individuals who have received more than 250 treatments. Thus, it is important selecting patients for PUVA therapy, especially if the

patient has pale skin (skin type I or II), a history of skin cancer, or current immunosuppressive therapy. Topical treatment that consists in immersion in a bath or shower of diluted psoralen before exposure to UVA has been developed with the aim to reduce side effects. Moreover, PUVA may be used in association with topical retinoids to reduce the side effects of both treatments. However, with the introduction of NB-UVB, use of PUVA has fallen worldwide [19, 32].

The excimer laser therapy requires the use of monochromatic xenon-chloride (excimer) laser and other phototherapeutic appliances, that delivers high-energy UVR radiation of 308 nm. The treatment time is shorter than traditional UVR and the possibility to focus directly on skin affected zone represents one of the biggest advantages. The most common side effects are erythema and blistering at treatment sites and residual hyperpigmentation [32].

Systemic treatments

Traditional systemic agents for the treatment of psoriasis includes methotrexate (MTX), cyclosporin A, and retinoids, which are effective in treating moderate to severe psoriasis. All compounds can be administered as oral drugs except for methotrexate, which is also available for subcutaneous administration [8]. In addition to the traditional agents, newer systemic drugs have been approved for psoriasis: dimethyl fumarate and apremilast [8].

Methotrexate (MTX; 4-amino-N¹⁰ methyl pteroylglutamic acid) was first approved systemic drug for psoriasis by the Food and Drug Administration in 1971, and despite the advent of new therapies, methotrexate continues to play a central role as a potent immune modulating drug in the treatment of moderate to severe psoriasis. MTX is a folic acid antagonist which inhibits the dihydrofolate reductase, therefore blocks the conversion of dihydrofolate to tetrahydrofolate, a cofactor for the formation of De Novo synthesis. MTX interferes with thymidine and purine biosynthesis and thus inhibits DNA synthesis and cell replication [19]. Moreover, MTX has also specific T-cell suppressive activities. It has recently been discovered that MTX inhibits aminoimidazole carboxamide ribotide transformylase, following in accumulation of adenosine, which is a T-lymphocyte toxin and may be responsible for

immunosuppressive action [32]. The typical side effects of methotrexate are nausea, leukopenia, liver transaminase elevation, mucosal ulceration, stomatitis, and bone marrow suppression (which risk may be potentiated by sulphonamides and their derivatives). In addition, pulmonary fibrosis is an extremely rare adverse effect, while hepatic fibrosis and cirrhosis may occur with long-term therapy. Among its major side effects MTX is teratogen, abortifacient and decreases sperm count. In fact, the administration of methotrexate is absolutely contraindicated in pregnant women, and pregnancy should be avoided for at least 3 months after discontinuing treatment. Moreover, also men whose partners are considering conception should avoid methotrexate for this period [19]. Because of its potential severe side effects, it is necessary to be careful in monitoring of patients. Despite what, MTX remains a frequently used cost-effective first-line drug in the treatment of moderate to severe psoriasis.

Cyclosporin A (CyA) is an immunosuppressant agent, member of calcineurin inhibitors. It is very effective against psoriasis, for its remission and as maintenance therapy. It is useful as an intermittent short-term therapy for moderate to severe psoriasis [19].

The major potential side effects are impaired renal function, hypertension, non-melanoma skin cancer, and nephrotoxicity related to the duration of treatment and the dose. Cyclosporin is usually used in combination or in rotation with other treatments for psoriasis, like as low-dose methotrexate or acitretin, mycophenolate mofetil, fumarates, sulfasalazine, and biological agents [19]. Because of its immunosuppressive power, it has had a significant impact on transplant medicine and the management of inflammatory disorders of skin, joints, and bowel. Cyclosporin is a macrocyclic immunosuppressant. The molecular mechanism of action of cyclosporin A is like the other calcineurin inhibitors. Cyclosporin binds to an intracellular protein, called cyclophilin (cyclophilin A) and inhibits calcineurin phosphatase activity and thereby inhibits activation of the transcription factor NFAT. Therefore, it blocks T-cell activation [31].

Oral retinoids (vitamin A derivatives) have proven efficacious in the treatment of psoriasis. They act binding to nuclear retinoid receptors (RAR and RXR), therefore altering gene transcription, normalizing keratinocyte proliferation and differentiation, and having anti-inflammatory effects (as described in “*Topical retinoids*” section) [19].

Etretinate has been the first oral effective retinoid approved for the treatment of psoriasis [33]. It has been early replaced by acitretin, which is its natural metabolite, because of its limited usage due to its unfavourable pharmacokinetic profile. Etretinate has a higher lipophilicity than acitretin considering that etretinate is the ethyl-ester prodrug of acitretin (Figure 12), which is its main active metabolite. In fact, etretinate is stored in fat tissues and has a long elimination half-life of more than two months and requires about two years for its complete elimination after the discontinuation of therapy [33].

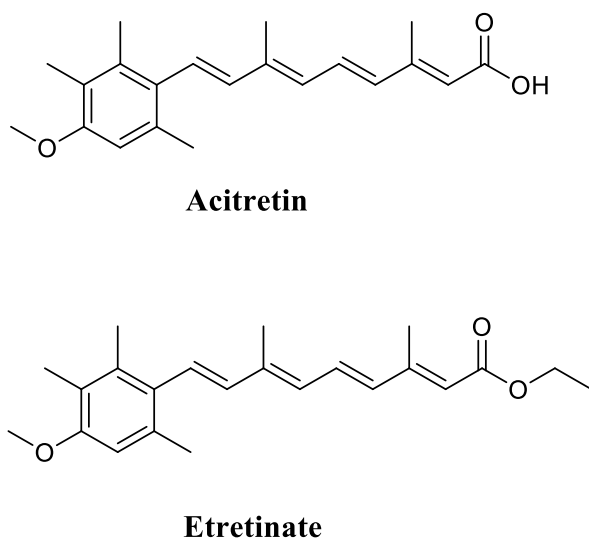


Figure 12. Acitretin and etretinate chemical structures.

Acitretin is the commonly oral retinoid used in the treatment of psoriasis [33]. It has shown a similar effectiveness to etretinate with a better pharmacokinetic profile, indeed acitretin has a half-life of about 2 days (50 h). Acitretin modulates the cellular differentiation of the epidermis, acting on RAR receptors. As a result, a decrease of scaling, erythema and thickness of the plaques occurs. Acitretin has proven to reduce the thickness of the stratum corneum and to have an anti-inflammatory effect in the epidermis and dermis. It is not immunosuppressive, for that reason it may be riskless treatment for patients with moderate to severe psoriasis, who need to an adequate systemic therapy and are affected by chronic infection such as HIV, hepatitis B, hepatitis C or malignancy, in whose is contraindicated the systemic immunosuppressive therapy. Acitretin represents one of the most effective treatments

for erythrodermic and pustular psoriasis. It can be used as a monotherapy, although has a lower efficacy, or in combination with other agents, with the aim to enhance effectiveness of therapy and reduce treatments' doses. It is usually associated with phototherapy (UVB or PUVA) or with many other systemic and biological agents. Acitretin, especially at low doses, is generally safe for long term use [33]. The ingestion of alcohol with acitretin is contraindicated because of the transesterification conversion of acitretin to etretinate. The most common side effects usually are dose dependent. Among principal adverse effects there are cheilitis, conjunctivitis, skin dryness, hair loss, effluvium, hepatitis (rare), hyperlipidemia, and teratogenicity. Because of their teratogenicity, retinoids should be avoided in pregnancy and according to FDA the contraception in women must be kept for three years after discontinuing the treatment with acitretin [33].

Fumarates (fumaric acid esters - FAEs) are small molecules with immunomodulatory and anti-inflammatory properties [34]. They are used in Germany as oral systemic drugs for the treatment of severe psoriasis [35]. Pharmaceutical preparations contain a mix of salts of different fumaric acid ethyl esters and dimethyl fumarate in various doses. Dimethyl fumarate is main active compound and often is associated with monoethyl fumarate [8]. Antipsoriatic effects are due to NF- κ B inhibition and T-cell apoptosis [34, 35]. Despite FAEs have not severe adverse side effect, they may cause unpleasant gastrointestinal symptoms such as abdominal cramps, diarrhoea, and nausea, along with other adverse effects as flushing, fatigue, and pruritus. These effects generally resolve over time and are probably dose dependent and usually slightly severe [8].

Apremilast is a recently developed drug for the treatment of moderate to severe psoriasis and psoriatic arthritis [36]. It is a small molecule inhibitor, administered orally, and selective for phosphodiesterase 4 (PDE4). Inhibition of PDE4 impedes the hydrolyzation of the second messenger cAMP to AMP, causing an increase of intracellular cAMP levels, thus inhibiting the production of pro-inflammatory cytokines (TNF- α , IFN γ , and IL-12), and increased levels of anti-inflammatory cytokines as IL-10 [36]. Apremilast has proven to have anti-inflammatory effects on keratinocytes, fibroblasts, and endothelial cells. The side effects are generally mild and self-resolve over time. The most common ones are nausea and diarrhoea and infections on the upper respiratory tract and nasopharyngitis [8].

Biological drugs

Biological drugs represent an innovative treatment of moderate to severe psoriasis for patients who do not respond well to traditional systemic therapy or do not well tolerate its side effects [22]. Biological agents may inhibit the occurrence and development of the disease and may be effective in the treatment of moderate to severe psoriasis and psoriatic arthritis [22]. They are administered subcutaneously or intravenously [8], and target specific inflammatory pathways, such as TNF- α , IL-17, IL-12 and IL-23, and pathogenic T cells [8, 22].

Table 1. Biological drugs for the treatment of psoriasis.

Drug	Mechanism	Application
Etanercept	Human recombinant fusion protein mimicking TNF- α receptor	s.c.
Infliximab	Chimeric monoclonal IgG1 antibody that binds to soluble and transmembrane forms of TNF- α	i.v.
Adalimumab	Human monoclonal IgG1 antibody that binds to soluble and transmembrane forms of TNF- α	s.c.
Certolizumab pegol	Fab portion of humanized monoclonal antibody against TNF- α conjugated to polyethylene glycol	s.c.
Ustekinumab	Human IgG1j monoclonal antibody targeting the common p40 subunit of IL-12 and IL-23	s.c.
Guselkumab	Human IgG1 λ monoclonal antibody that selectively binds p19 subunit of IL-23	s.c.
Tildrakizumab	Human IgG1 κ monoclonal antibody that selectively binds p19 subunit of IL-23	s.c.
Risankizumab	Human IgG1 monoclonal antibody that selectively binds p19 subunit of IL-23	s.c.
Secukinumab	Human IgG1 κ monoclonal antibody that selectively targets IL-17A	s.c.
Ixekizumab	Humanized IgG4 monoclonal antibody that selectively binds and neutralizes IL-17A	s.c.
Brodalumab	Human IgG2 monoclonal antibody targeting IL-17 receptor type A	s.c.

Biological agents presently used in clinical practice are TNF- α inhibitors (etanercept, infliximab, adalimumab, and certolizumab pegol) [8, 22], IL-12/23 p40 antagonist (ustekinumab), IL-23 p19 antagonists (guselkumab, tildrakizumab, and risankizumab), IL-17A antagonists (secukinumab and ixekizumab), and IL-17 receptor A antagonist (brodalumab) [8, 22] (Table 1).

TNF- α inhibitors

TNF- α inhibitors have been the first biological drugs approved in the treatment of psoriasis and psoriatic arthritis and are used as standard drug to evaluate drug efficacy in psoriasis clinical research [8].

Etanercept is a human recombinant fusion protein formed by the soluble human TNF- α type II receptor portion linked to the Fc region of an IgG1 antibody. It can competitively bind soluble TNF- α in serum and mimicking TNF- α receptor, it inhibits TNF- α biological activity [22]. Etanercept was the first TNF- α inhibitors approved by Food and Drug Administration (FDA) for psoriasis [8]. It is administered by subcutaneous injection.

Infliximab is a chimeric monoclonal IgG1 antibody formed by murine variable (Fab) region and human constant (Fc) region. It binds to soluble and transmembrane forms of TNF- α preventing TNF- α linkage to its receptor, and thus inhibits TNF- α activity [22]. It is administered by intravenous infusion. Infliximab has proven more efficacious than other TNF- α inhibitors and its chimeric nature should give it a higher immunogenic potential, which influences drug survival [8].

Adalimumab is a fully human monoclonal IgG1 antibody, which acts with the same mechanism of action of infliximab, binding soluble and transmembrane forms of TNF- α . It is administered by subcutaneous injection [22].

Certolizumab pegol is a pegylated protein. It is formed by a Fab portion of a humanized monoclonal antibody against TNF- α linked by covalent conjugation to polyethylene glycol. This characteristic gives it biopharmaceutical improvements, such as increase of half-life and reduction of immunogenicity [37]. Certolizumab has firstly been used in the treatment of Crohn's disease and then its use has been extended to psoriatic arthritis and recently to plaque psoriasis. Certolizumab pegol may be used during pregnancy and

breastfeeding because of it has not Fc domain, and thus cannot cross the placenta [8]. It is administered by subcutaneous injection.

IL-23 inhibitors

IL-23 inhibitors have been developed after TNF- α inhibitors due to the involvement of IL-23 in expansion of Th17 cells. Inhibitors currently approved are ustekinumab, guselkumab, tildrakizumab, and risankizumab.

Ustekinumab is a fully human IgG1j monoclonal antibody targeting the common p40 subunit of IL-12 (a dimer composed of p40 and p35 subunits) and IL-23 (a dimer composed of p40 and p19 subunits), that is overexpressed in psoriatic plaques. The binding to p40 inhibits IL-23 and IL-12 effects and thus the blocking of T cell activating mechanisms occurs and the initial T cell differentiation to a Th1 and Th17 cell does not take place [22]. Ustekinumab is administered by subcutaneous injection. It is also efficacious in the treatment of psoriatic arthritis and Chron's disease [8]. It has a safe clinical profile and the most common side effects are nasopharyngitis, upper respiratory tract infections, fatigue, and headache, and in only two cases tuberculosis has been reported [8].

Since the data suggest that IL-23 has a crucial role in Th17 response, and Th1 signalling is important for the response against bacterial and viral pathogens, and IL-12 to obtain a protective effect in psoriatic inflammation, more selective biologics targeting exclusively IL-23 have been developed [8]. Guselkumab [22], tildrakizumab [8], and risankizumab [8] are fully human IgG1 monoclonal antibodies, which bind selectively p19 subunit of IL-23. They block effects of IL-23 in inflammatory reaction ensuring an antipsoriatic effect. They are administered by subcutaneous injection. A phase 2 trial that compared the activity of risankizumab versus ustekinumab for treatment of moderate to severe plaque psoriasis has shown that the selective blockade of IL-23 with risankizumab has given superior clinical responses rather than the treatment with ustekinumab [38], confirming that the binding to the p19 subunit rather than p40 gives a more complete inhibition of interleukin-23 activity, which potentially results in increase efficacy in the treatment of plaque psoriasis. Moreover, Guselkumab has shown clinical superiority compared to adalimumab [39, 40].

IL-17 inhibitors

As a result of the success of biological treatment of psoriasis with IL-23 inhibitors, researchers have developed IL-17 inhibitors. IL-17A is a potent cytokine in the IL-17 family and high levels of IL-17 correlated with disease severity has been found in skin lesions and in the blood of patients with psoriasis [41]. Three IL-17 inhibitors are currently being evaluated for the treatment of moderate to severe psoriasis [41].

Secukinumab is a fully human IgG1 κ monoclonal antibody which selectively targets IL-17A, and prevents its interaction with receptors, therefore reducing inflammation. It was the first IL-17A inhibitor approved for psoriasis therapy in 2015, has shown a rapid onset of action and is administered by subcutaneous injection [41].

Ixekizumab is a humanized IgG4 monoclonal antibody that selectively binds and neutralizes IL-17A. Thus, it has proven greatly efficacious in alleviating psoriasis skin lesions [41]. It is administered by subcutaneous injection.

Brodalumab is a human IgG2 monoclonal antibody targeting IL-17 receptor type A (IL-17RA). It antagonizes the biological activity of IL-17A, IL-17F, interleukin-17A/F, and interleukin-17E. It has shown a satisfactory and safety profile in the treatment of psoriasis [41]. It is administered by subcutaneous injection.

Since IL-17 signalling is crucial for the defence against extracellular bacterial and fungal infections, IL-17 inhibition may result in infectious adverse effects. However, the most common side effects include nasopharyngitis, headache, upper respiratory tract infection, and arthralgia [41].

2. Hydrogen sulfide (H₂S)

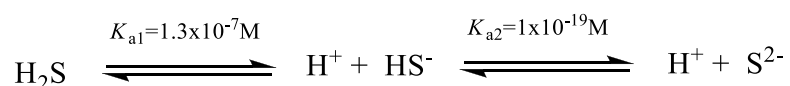
2.1. Hydrogen sulfide as “new” gaseous transmitter

Hydrogen sulfide (chemical formula H₂S) is a colourless gas with the characteristic smell of rotten eggs. H₂S was initially known for its toxicity [42], however Abe and Kimura were the first who suggest H₂S as an endogenous neuromodulator, describing its enzymatic mechanism of production in the brain, its biological effects at physiological concentrations, and its specific cellular targets [43]. Following studies have shown that along with other two still known gasotransmitters, nitric oxide (NO) and carbon monoxide (CO), H₂S is involved in several physiological and pathological functions in mammalian tissues, and now it can be considered the third endogenously produced gaseous transmitter of pharmacological interest [44, 45].

2.2. Chemical and biological properties

Hydrogen sulfide is a gas, less polar than water due to the presence of sulfur, which has a lower electronegativity than oxygen, and with a boiling point of -60.7°C, because of the weak intermolecular forces exist for H₂S.

Hydrogen sulfide is weakly acidic, and in aqueous solution it dissociates into hydrogen cation (H⁺) and hydrosulfide anion (HS⁻), which then dissociates into H⁺ and sulfide anion (S²⁻) according to the following reaction:



At physiological conditions, about one-third of hydrogen sulfide is in its undissociated form and two-thirds dissociate into H⁺ and HS⁻, which needs to higher pH values for dissociating than the physiological ones. Thus, significant amounts of H₂S and HS⁻ coexist and both species contribute directly to the biological action of H₂S. Because of its lipophilicity, H₂S easily crosses the biological membranes and penetrates cells, giving to H₂S a high biological potential [46].

2.3. H₂S biosynthesis

H₂S is synthesized at considerable amounts in most tissues, such as brain, cardiovascular system, liver, and kidney [47]. In mammals, endogenous H₂S is produced by enzymatic reactions [48], even though a minor endogenous source of H₂S is non-enzymatic [49, 50].

The endogenous production of H₂S via non-enzymatic processes may occur from glucose, glutathione, inorganic and organic polysulfides (present in garlic), and elemental sulfur as precursors. For instance, H₂S can be produced by reduction of elemental sulfur using reducing equivalents obtained from the oxidation of glucose, or by direct reduction of glutathione in presence of NADH and NADPH [49]. In addition, organic polysulfides present in garlic and garlic-derived one can be converted in H₂S with a thiol-dependent mechanism, in presence endogen thiols, such as reduced glutathione (GSH) [50] (Figure 13).

Enzymatic synthesis of H₂S can be occurred by three enzymes: cystathionine γ -lyase (CSE), cystathionine β -synthase (CBS) and 3-mercaptopyruvate sulfurtransferase (3-MST) [48] (Figure 11).

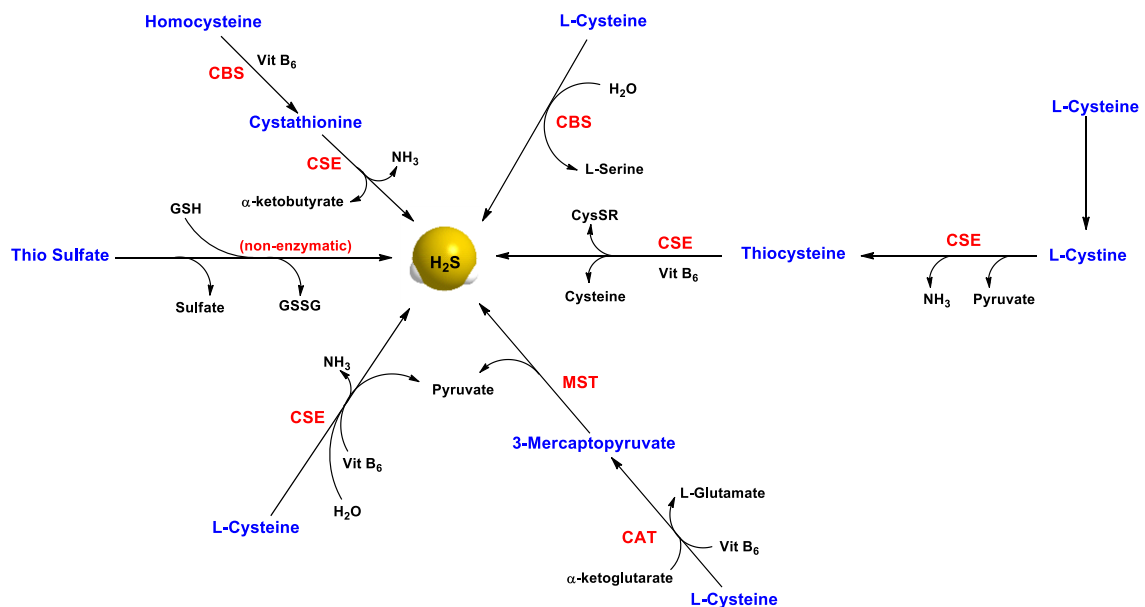


Figure 13. Biosynthesis and transformation of H₂S in mammalian cells.

CBS and CSE are pyridoxal 5'-phosphate (PLP)-dependent (the active form of vitamin B₆) enzymes which are localized in the cytosol and convert L-cysteine into H₂S. 3-MST is more localized in mitochondria where converts 3-mercaptopyruvate into H₂S, using α -ketoglutarate as a co-factor. 3-mercaptopyruvate is generated from L-cysteine through another enzyme, cystathionine aminotransferase (CAT) [48].

L-cysteine is the key substrate for enzymatic generation of endogenous H₂S. It is a sulfur-containing amino acid derived from alimentary sources, synthesized from L-methionine through the so-called "trans-sulfuration pathway" with homocysteine (Hcy) as an intermediate, or liberated from endogenous proteins [46].

Moreover, H₂S can be also released through a "desulfhydration" reaction, consisting of the removal of the cysteine sulfur atom without its oxidation, catalyzed by CBS and CSE [46].

CBS and CSE are the principal enzymes responsible for the endogenous production of H₂S in mammalian tissues. They are expressed in different tissues. CBS is predominant in the central nervous system, although its expression has also been observed in other organs, such as kidney, liver, lymphocytes, uterus, placenta, and pancreas islets [51]. Indeed, CSE is more expressed in cardiovascular system and respiratory system, moreover it is also dominant in liver, kidney, uterus, and pancreatic islets [51]. 3-MST, like CBS and CSE, is expressed in a lot of tissues and particularly in cardiac cells, pericentral hepatocytes in the liver, and proximal tubular epithelium of the kidney [51]. Moreover, the precise localization of the H₂S-generating enzymes in the different cell types of the skin has not yet been determined. However, the expression of both CSE and 3-MST enzymes has been demonstrated by Western blot analysis in homogenates of human cutaneous tissue and another study has proven expression of the enzymes CSE and CBS in normal human keratinocytes [52].

CBS produces H₂S from L-cysteine and homocysteine to form L-cystathionine and H₂S [53, 54]. Furthermore, through β -replacement reaction CBS generates H₂S and L-serine from L-cysteine [54].

CSE catalyzes cystathionine α,γ -elimination reaction to obtain L-cysteine, ammonia, and α -ketobutyrate [55]. Moreover, CSE also uses L-cysteine and/or homocysteine as substrate to produce H₂S. It has proven that at a physiological concentration of L-

cysteine and homocysteine, about 70% of H₂S is obtained by α - and β -elimination of L-cysteine CSE-catalyzed [56].

Another pathway involves the enzyme cysteine aminotransferase (CAT), that produces 3-mercaptopyruvate from L-cysteine and α -ketoglutarate in the presence of reductants transferring the amine group from cysteine to a keto acid. Thereby, the enzyme 3-mercaptopyruvate sulfurtransferase (3-MST) generates H₂S from 3-mercaptopyruvate [57]. It has recently proven that also the enzymes D-amino-oxidase (DAO) may produce 3-mercaptopyruvate from the amino acid D-cysteine, and then 3-MST generates H₂S from 3-mercaptopyruvate [58].

After its enzymic synthesis, H₂S can be either immediately released or stored and subsequently released, in response to a physiological signal. It can be stored in two different forms in the cells: acid-labile sulfur (H₂S is released under acidic conditions) and as bound sulfane sulfur (H₂S is released under reducing conditions) [59, 60].

Some compounds have been developed as inhibitor of H₂S biosynthesis which act on CBS and CSE. The most common agents include propargylglycine (PGG), β -cyanoalanine (BCA), aminooxyacetic acid (AOAA), trifluoroalanine and hydroxylamine (HA) [44, 61]. PGG and BCA have proven to be specific inhibitors of CSE, while AOAA is often used as a selective CBS inhibitor. Although their low potency, poor selectivity, and limited cell-membrane permeability, these inhibitors have been used with the aim to verify the effects of inhibition of H₂S production.

2.4. Biological activity of H₂S in skin disorders

Potential beneficial effects of balneotherapy containing sulfur have been used for centuries as a folk medicine procedure for treatment and relief of several conditions including wound healing, acne, rosacea, scabies, atopic dermatitis (AD), psoriasis, and urticaria. It was evident that mineral waters could have intrinsic “pharmacological properties”, such as H₂S contained in sulfurous waters which has obtained greater scientific attention [52].

Knowledge of the biological functions of endogenous H₂S is constantly expanding. H₂S plays an important role in many physiological responses including neuromodulation [43], oxidative stress reduction [62], hypertension [63], oedema [64], haemorrhagic

shock [65], pain perception [66], gastric mucosal integrity [67], vascular tone [68], cell proliferation [69], apoptosis [70], and inflammation [71, 72]. Many studies in the literature have highlighted the role of hydrogen sulfide in the physiological regulation of various organs and systems, including cardiovascular, respiratory, central nervous, gastrointestinal, immune, and reproductive systems, and the skin [52, 73, 74]. Variations in endogenous H₂S production underlie the pathogenesis of several skin diseases, including inflammation, infection, and cancer [52].

Among the several pathological and physiological condition in which H₂S appears to be involved, my attention has been focused on the H₂S role in skin pathophysiology, and on its involvement in inflammation, pruritus and cytoprotection, goal-orienting, particularly on psoriasis.

Endogenous H₂S has proven to be involved in the regulation of important functions in the skin, such as vasodilatation [75], cell proliferation [76], apoptosis [77], inflammation [78], and pruritus [79, 80] (Figure 14).

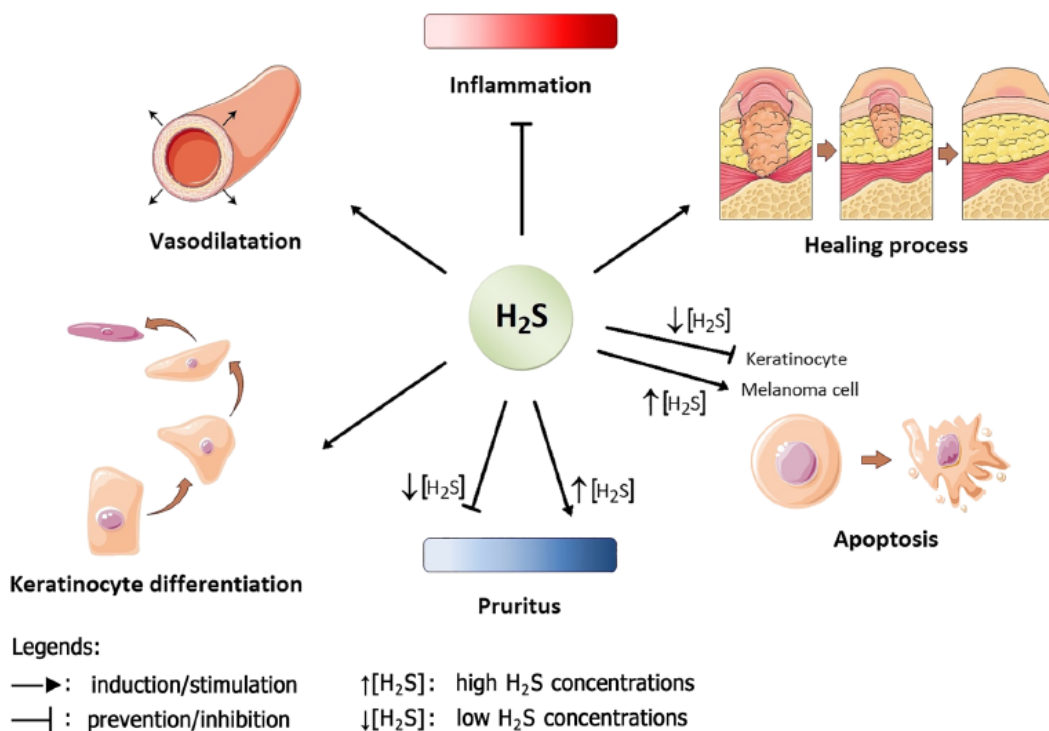


Figure 14. Effects of H₂S in the skin [52].

H₂S mediated effects have been observed to be dose dependent. In fact, the exogenous administration of H₂S at low concentration, using sodium hydrosulfide (NaHS) as H₂S donor, has stimulated keratinocyte proliferation [76]. On the other hand, at high concentrations, H₂S alters keratinocyte cell proliferation and adhesion. It has been observed that H₂S has induced proapoptotic effects, reducing clonal growth, cell proliferation, and cell adhesion of NCTC 2544 human keratinocytes [77]. This effect has been mediated by inhibition of mitogen-activated protein kinase signalling, and the reduction of sulfide-treated cells adhesion has been associated to a down-regulation of the expression of β 4, α 2, and α 6 integrins (necessary to promote cell adhesion as well as anti-apoptotic and proliferative signalling in normal keratinocytes). The dose-dependent effect of H₂S, very similar to that observed for NO, is a consequence of the affinity of this gasotransmitter for wide array of molecular targets.

Several in vitro and in vivo studies have shown the anti-inflammatory effects of H₂S. The exposure of the normal human keratinocytes to sub-cytotoxic formaldehyde has shown the involvement of CSE and CBS in promoting the resolution of cutaneous inflammation. In this regard, it has been observed that both enzymes were up-regulated in response to toxic stimuli. In addition, the produced H₂S inhibited the formation of pro-inflammatory mediators [78].

Further studies have shown that H₂S alleviates skin inflammation by increasing NO release, which results in a subsequent decrease in VEGF release in keratinocytes [81], or by inhibiting IL-8 expression in keratinocytes (a key event in the pathogenesis of psoriasis) [82]. The data have demonstrated that exogenous application of H₂S donors (NaHS and GYY4137) on human keratinocytes has produced a significant increase of NO release due to the rapid Akt activation, which consequently has stimulated iNOS expression, responsible of NO rise. NO has inhibited ERK1/2 activation resulting in the reduction of vascular endothelial growth factor (VEGF) release. These findings have demonstrated the central role of Akt and ERK1/2 in H₂S effects, showing a possible molecular mechanism of H₂S and its anti-inflammatory proprieties. This study suggests that H₂S donors may be promising therapeutic agents for the treatment of chronic inflammatory diseases of the skin, such as psoriasis [81]. In addition, mitogen-activated protein kinase (MAPK) (extracellular signal-regulated kinases (ERK) 1 and 2) activity has proven increased in injured psoriatic skin and it represents a key event for IL-17-

induced IL-8 synthesis by keratinocytes. Therefore, a study conducted on both primary psoriatic lesion and NCTC human keratinocytes has shown that the H₂S donor NaHS reduced basal expression and secretion of IL-8, and impaired also IL-17 and IL-22 induced IL-8 production by reducing ERK phosphorylation levels, both in vitro and in vivo [82].

An in vitro study conducted with the aim to investigate the role of H₂S in psoriasis and its potential anti-inflammatory effect, has shown that the serum levels of H₂S in psoriasis patients were significantly lower than in healthy controls, and the levels of several inflammatory cytokines (TNF α , IL-6, and IL-8) were increased significantly [83]. Furthermore, it has been reported that H₂S could inhibit TNF α -induced inflammatory responses in keratinocytes in a dose dependent manner and may exert anti-inflammatory effect via suppressing the activation of p38 MAPK, ERK and NF- κ B pathways. Thus, H₂S may have a protective role in the pathogenesis of psoriasis.

H₂S also plays an important role on the pruritogenic response. The data suggest that inhibition of endogenous H₂S synthesis with β -cyano-L-alanine (a CSE/CBS inhibitor) has exacerbated scratching behaviour induced by compound 48/80 in mice, along with increased neutrophil recruitment and myeloperoxidase activity compared to the control group treated with saline. Moreover, the intradermal injection of low doses of H₂S donors, sodium sulfide (Na₂S) and Lawesson's reagent (LR), has reduced histamine or C48/80-induced skin inflammation and pruritus conferring a protective effect, and these effects seemed in part mediated by stabilization of mast cells [79]. Another study has shown that H₂S donors may also decrease non-histaminergic mediated itching in mice. In this regard, the pruritus has been induced by the activation of PAR2 (proteinase-activated receptor 2) with the peptide agonist SLIGRL-NH₂. Co-injection of SLIGRL-NH₂ with either the slow-release H₂S donor GYY4137 or the spontaneous donor NaHS significantly reduced pruritus, via K_{ATP} channel opening and involving NO in a cGMP-independent manner [80]. On the other hand, high concentrations (within $\mu\text{mol}\cdot\text{kg}^{-1}$ range) of H₂S donors NaHS and Na₂S may induce pro-pruriceptive effects by the activation of T-type calcium channels in a dose-dependent manner [84]. These contradictory data can be explained keeping in mind that endogenous H₂S production

follows a slow kinetic profile, while the administration of spontaneous H₂S donors leads to a sudden production of mediator in high amounts, which are not physiological.

Among the multiple beneficial effects of H₂S in the skin, its cytoprotective effects have also been highlighted. In vitro studies on HaCaT cell cultures have shown that NaHS reduced hypoxia-induced cell injury and the inflammatory responses, and NSHD-1 (an N-mercapto-based H₂S donor) was able to protect HaCaT cells from methylglyoxal-induced injury and dysfunction [85, 86].

3. Aim of project

Considering the growing interest in the therapeutic application of hydrogen sulfide, many H₂S-releasing agents have been developed during the years.

Retrospective analysis of the literature has revealed that H₂S donors can be compounds that either directly release H₂S when in solution (such as NaHS, Na₂S, Lawesson's reagent, GYY4137) or function as precursors for endogenous H₂S synthesis (N-acetylcysteine, L-cysteine). Although sodium hydrogen sulfide (NaHS) is widely used in most pharmacological studies, it releases H₂S too quickly, therefore, it is unable to mimic the in vivo slow and continuous physiological release of H₂S. This uncontrolled and rapid release can cause serious damages [46]. Considering these disadvantages, H₂S-releasing slow kinetic molecules have been developed with the aim of mimicking the physiological conditions [87], including garlic-derived organic polysulfides (DADS and DATS), Lawesson's reagent and derivatives (GYY4137), 1,2-dithiol-3-thiones (DTT) such as ADT-OH, some isothiocyanates, thioamide derivatives or dithioesters (such as TBZ, HBTA).

These H₂S donors may be used alone or chemically conjugated to active pharmacological compounds with the aim of improving their therapeutic profile [88] (some examples are reported in Figure 15). Some of them have achieved good results in clinical practice.

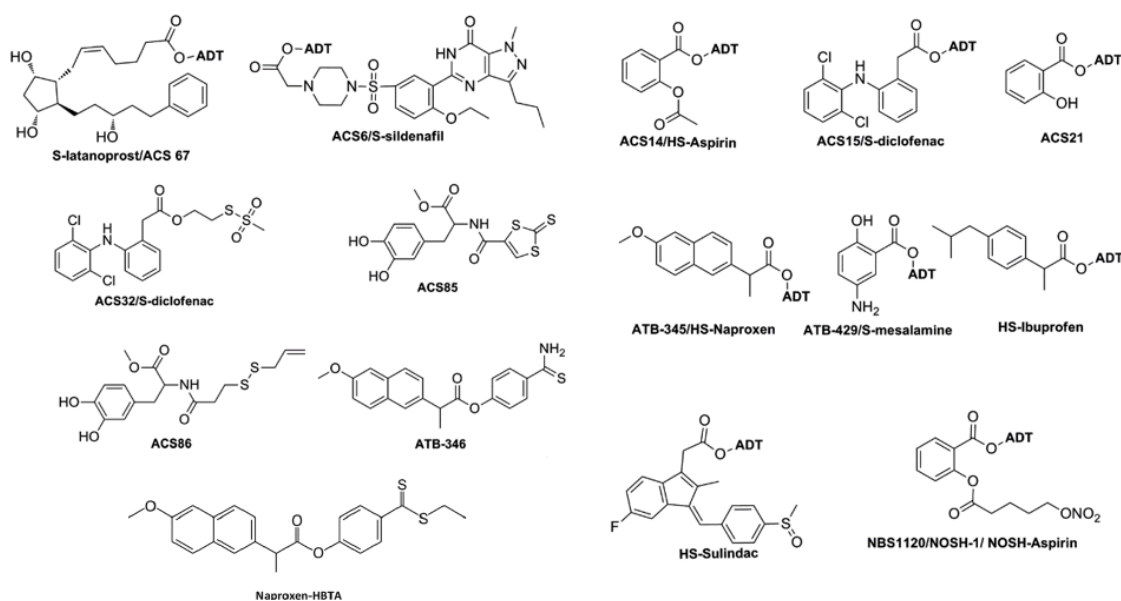
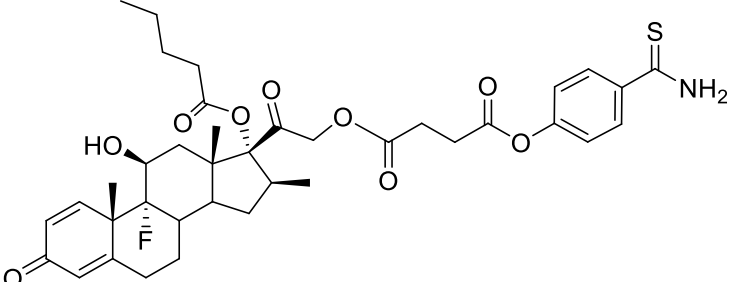
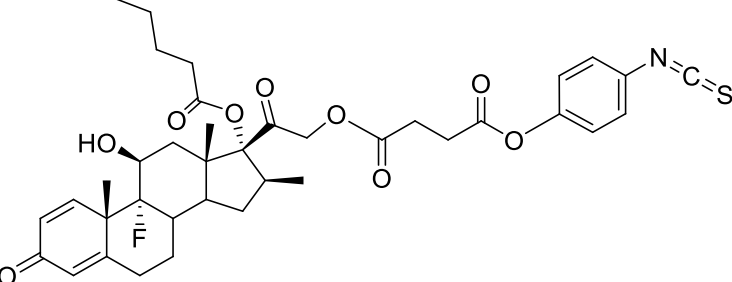
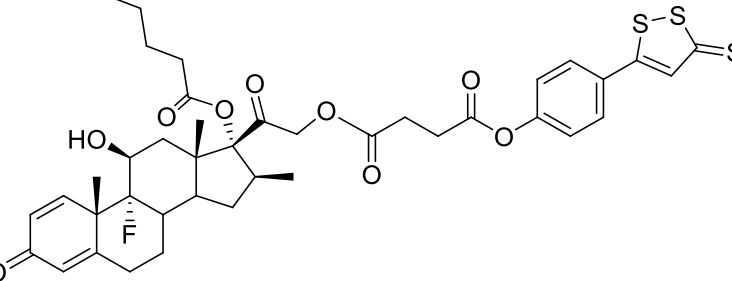
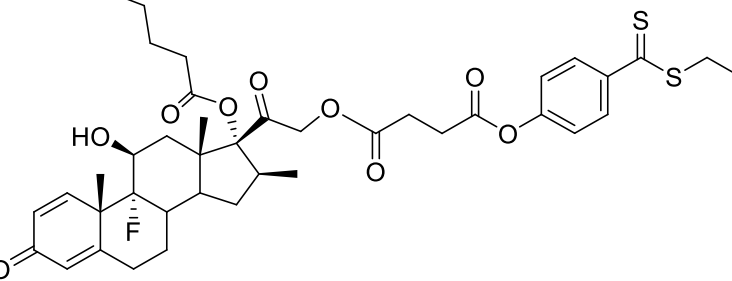
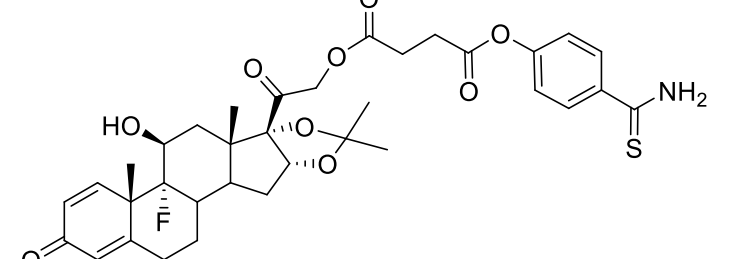


Figure 15. Structures of H₂S-releasing agents conjugate to active drugs.

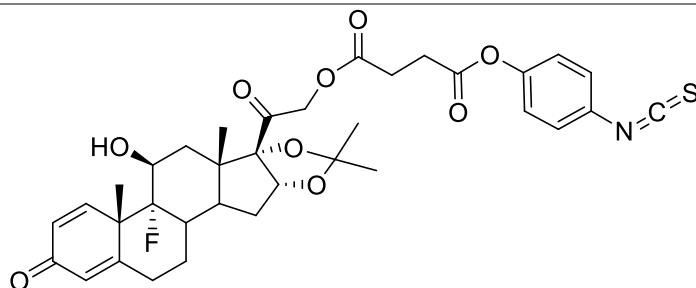
Considering the involvement of this gasotransmitter in several pathophysiological conditions of the skin [52], the aim of my project is design, synthesis, and characterization of H₂S-releasing molecular hybrids, containing active pharmacological compounds in psoriasis treatment and H₂S donors, that could improve therapeutic activity. The choice is derived from the purpose of conjugating the pharmacological properties of the starting drug and the beneficial effects of H₂S.

My attention has been paid to the synthesis of H₂S-releasing molecular hybrids, which are composed by glucocorticoids, acitretin, or tazarotenic acid as active drugs in treatment of psoriasis, and H₂S donors (TBZ, HPI, ADT-OH, and HBTA). The choice of these active drugs is due to their wide use for treating psoriasis (as shown above). Synthesized compounds are shown in Table 2.

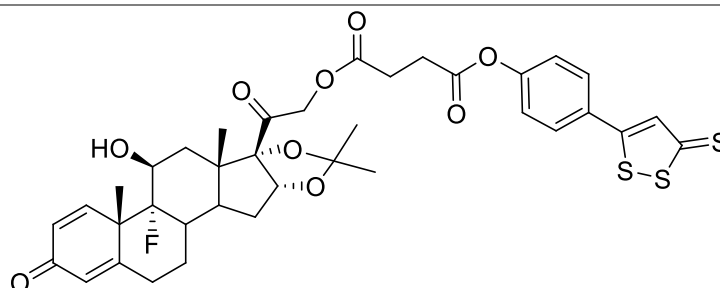
Table 2. Synthetized H₂S-releasing molecular hybrids.

Name/Label	Chemical structure
Betamethasone 17-valerate- 21-succinate TBZ (I)	
Betamethasone 17-valerate- 21-succinate HPI (II)	
Betamethasone 17-valerate- 21-succinate ADT (III)	
Betamethasone 17-valerate- 21-succinate HBTA (IV)	
Triamcinolone acetonide 21-succinate TBZ (V)	

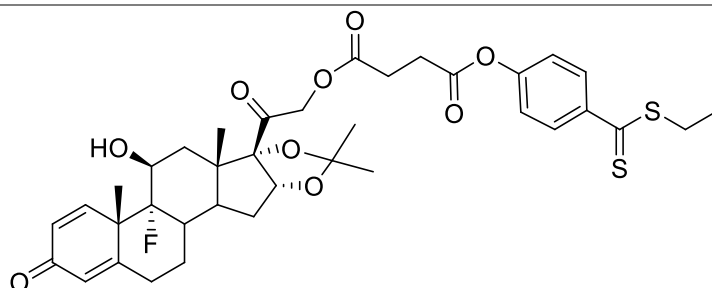
Triamcinolone
acetone
21-succinate
HPI
(VI)



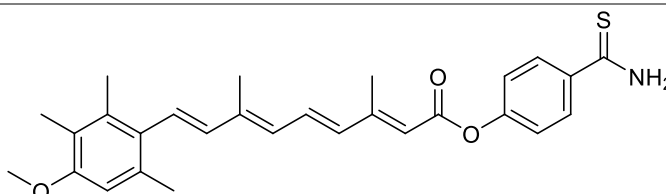
Triamcinolone
acetone
21-succinate
ADT
(VII)



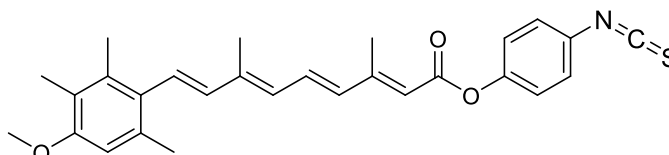
Triamcinolone
acetone
21-succinate
HBTA
(VIII)



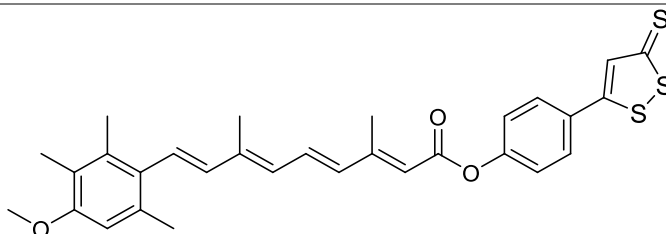
Acitretin
TBZ
(IX)



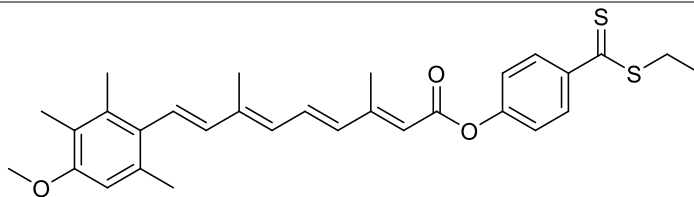
Acitretin
HPI
(X)



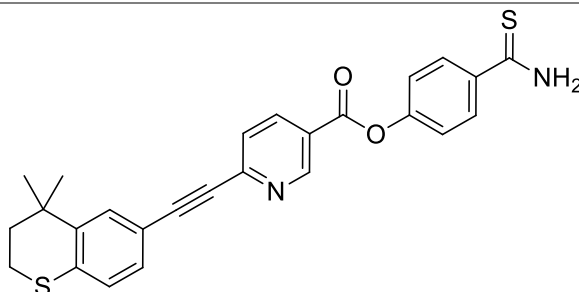
Acitretin
ADT
(XI)



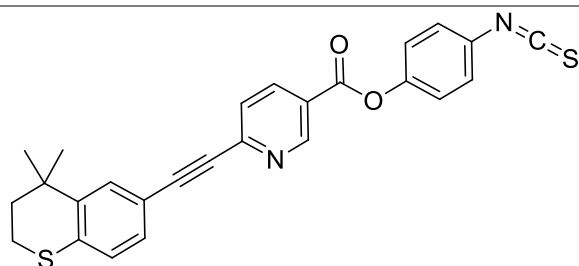
Acitretin
HBTA
(XII)



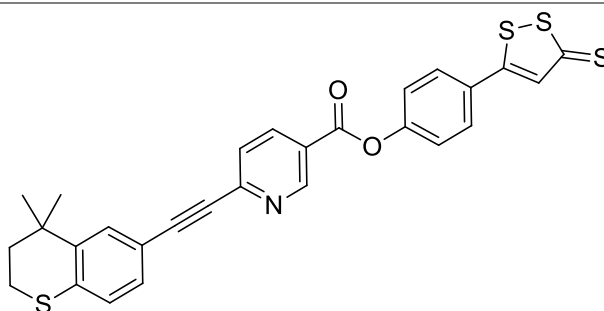
Tazarotene
TBZ
(XIII)



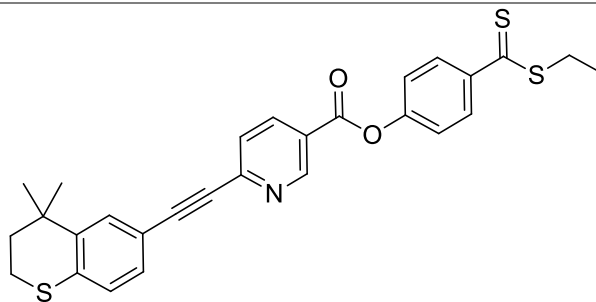
Tazarotene
HPI
(XIV)



Tazarotene
ADT
(XV)



Tazarotene
HBTA
(XVI)



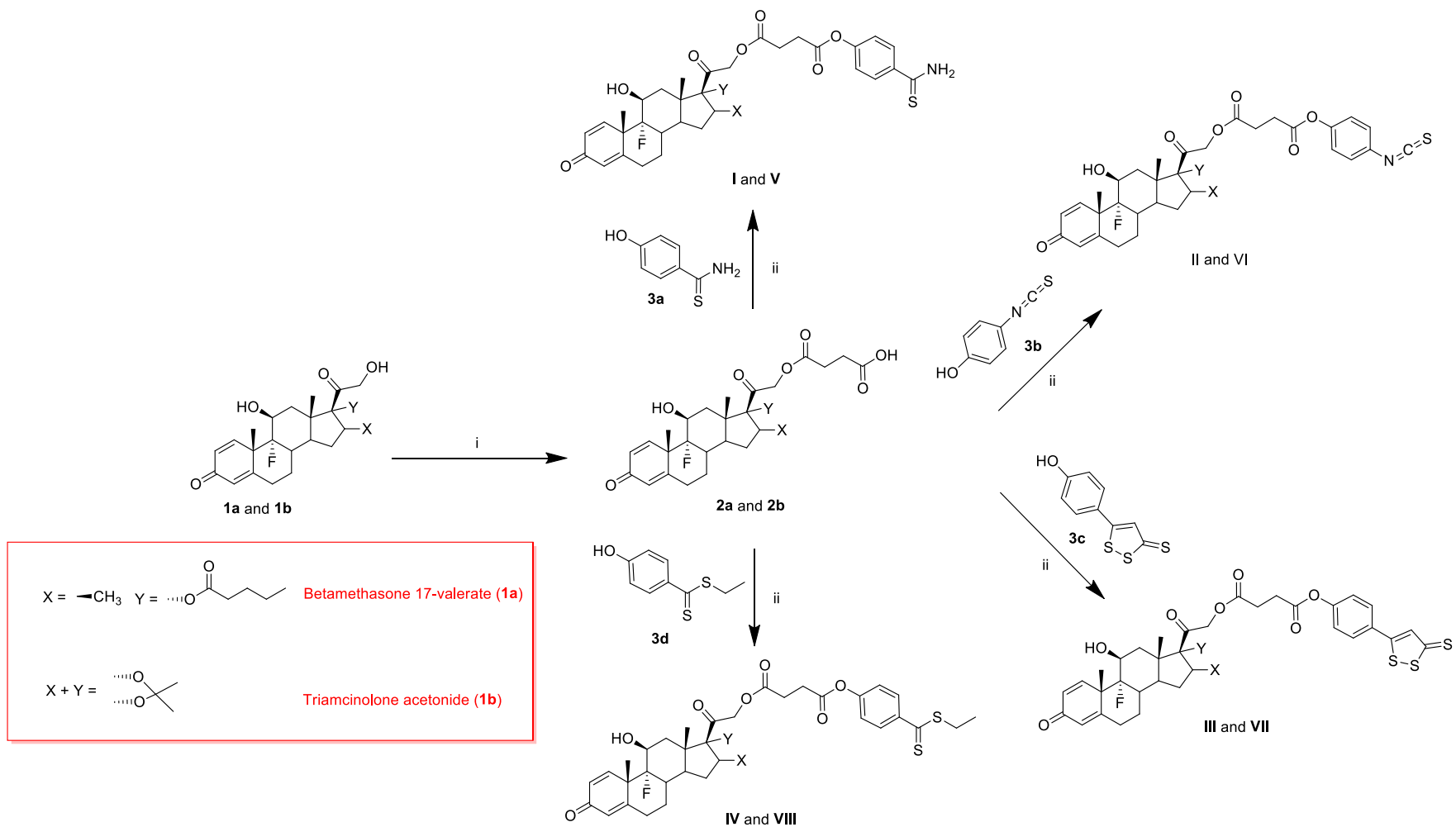
4. Chemistry

Chemical structures of compounds **I-XVI** are reported in Table 2 and the synthetic strategy for their synthesis is reported in schemes hereinafter.

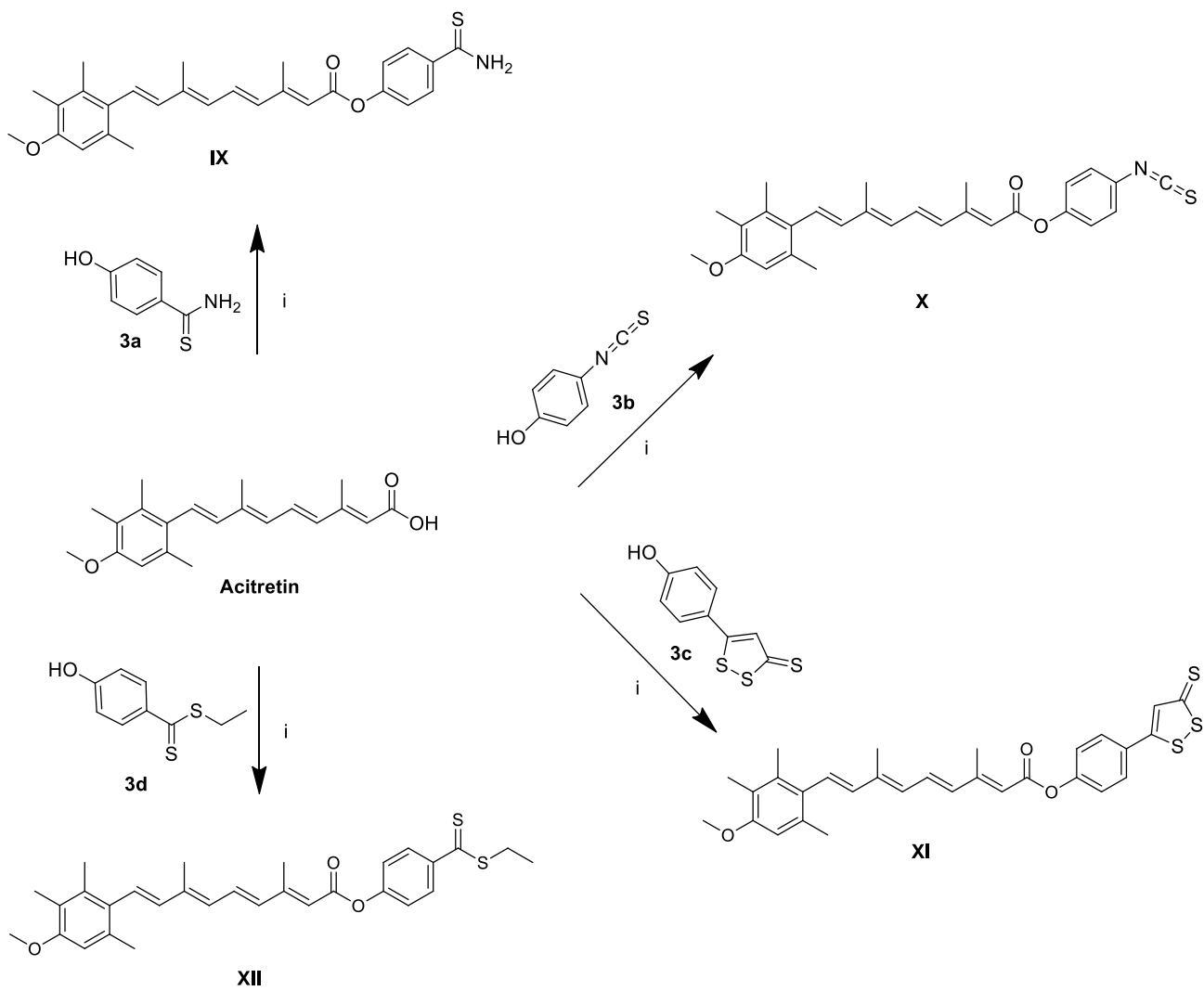
The synthetic procedure for the preparation of glucocorticoids hybrid derivatives (compounds **I-VIII**, Scheme 1) has been based on the conversion of Betamethasone 17-valerate (**1a**, BMV) or Triamcinolone acetonide (**1b**, TAA) into the corresponding hemi-succinated esters, by treatment with an excess of succinic anhydride in the presence of catalytic amount of DMAP in anhydrous pyridine.

The intermediates **2a** and **2b** were subjected to a condensation reaction between the carboxylic function and the phenolic function of the different H₂S-donors (**3a-3d**), via EDC in the presence of DMAP, thus obtaining the final compounds **I-VIII**.

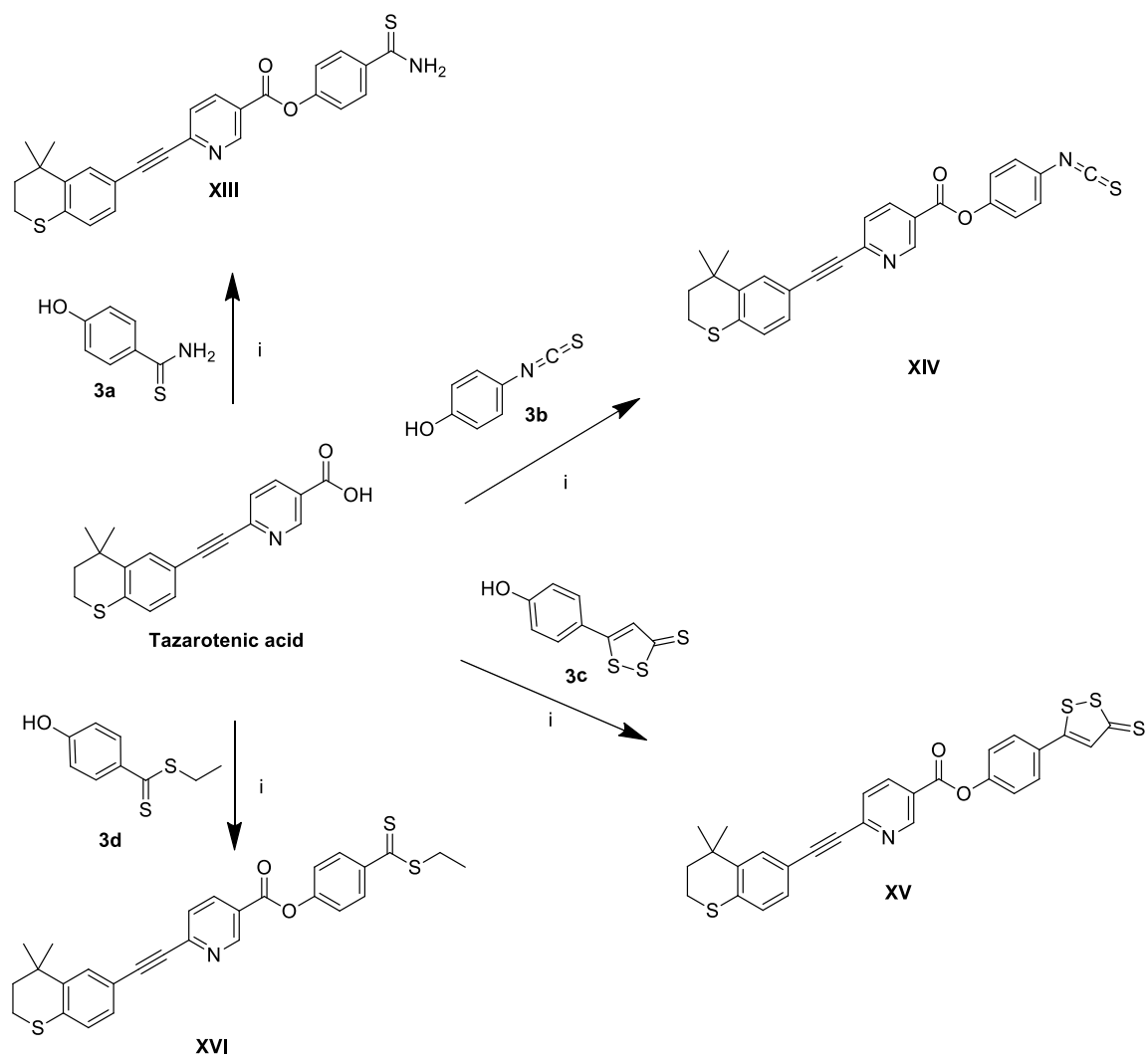
Synthesis of acitretin and tazarotenic acid hybrid derivatives (compounds **IX-XVI**) was performed by acitretin (Scheme 2) or tazarotenic acid (Scheme 3) coupling with the different H₂S donors (**3a-3d**), via EDC in the presence of DMAP.



Scheme 1. Synthesis compounds **I-VIII**. Reagents and conditions: i) succinic anhydride (3 eq.), DMAP (0.1 eq.) anhydrous pyridine, rt, 12h; ii) EDC (1.5 eq.), DMAP (0.1 eq.), anhydrous THF, rt, 12h.

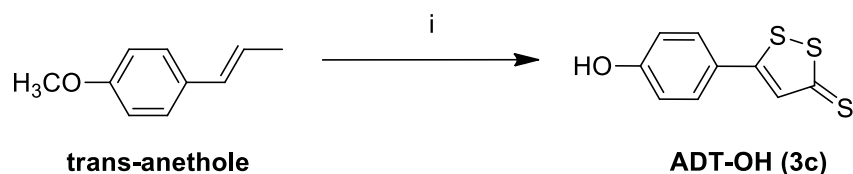


Scheme 2. Synthesis of compounds **IX-XII**. Reagents and conditions: i) EDC (1.5 eq.), DMAP (0.1 eq.), anhydrous THF, rt, 12h.



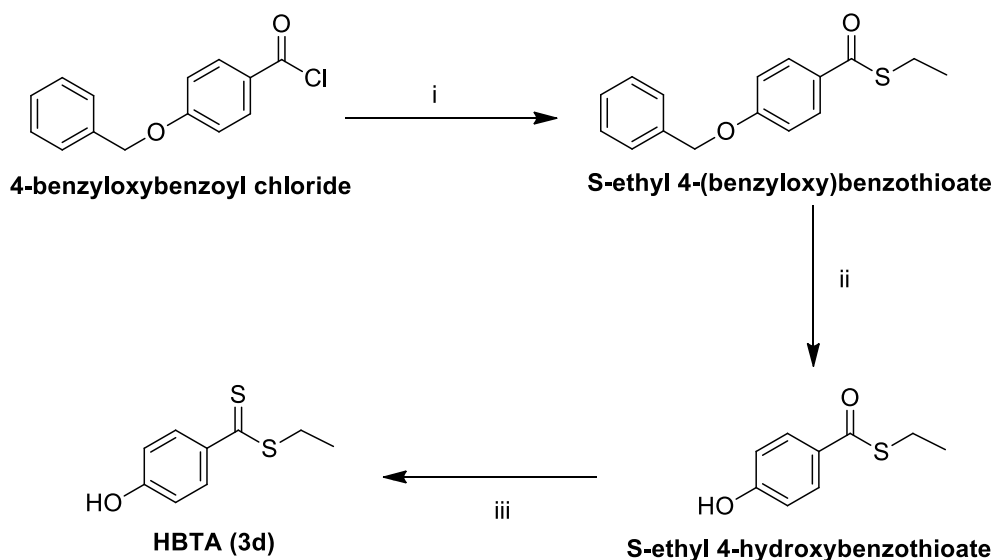
Scheme 3. Synthesis of compounds **XIII-XVI**. Reagents and conditions: i) EDC (1.5 eq.), DMAP (0.1 eq.), anhydrous THF, rt, 12h.

H₂S-donors **3a** and **3b** (4-hydroxythiobenzamide or TBZ, and 4-isothiocyanatophenol or HPI, respectively) are commercially available; compound **3c** (5-(4-hydroxyphenyl)-3H-1,2-dithiole-3-thione or ADT-OH) was obtained following with modifications a synthetic procedure previously described [89], based on the reaction between trans-anethole and sulfur in DMF (Scheme 4).



Scheme 4. Synthesis of ADT-OH: i) sulfur (5.5 equiv.), DMF, 140°C.

H₂S-donor **3d** (ethyl 4-hydroxybenzodithioate or HBTA) was synthesized using recently published procedures [90] (Scheme 5).



Scheme 5. Synthesis of HBTA. Reagents and conditions: i) CH₃CH₂SH (1.5 equiv.), triethylamine, anhydrous CH₂Cl₂, MW (300W, 50°C), 8 min; ii) 1,2,3,4,5-pentamethylbenzene (10 equiv.), BCl₃ (8 equiv.), anhydrous CH₂Cl₂, -78 °C; 30 min; iii) Lawesson's reagent (0.6 equiv.), toluene, MW (500W, 110°C), 1h.

5. Experimental Section

5.1. Materials and Methods

Betamethasone 17-valerate, Triamcinolone acetonide, Acitretin and Tazarotenic acid were purchased from Carbosynth Ltd (UK); all the reagents, solvents or other chemicals were obtained from Merck.

Solutions were concentrated with a Buchi R-114 rotary evaporator at low pressure. All reactions were followed by TLC carried out on Merck silica gel 60 F254 plates with fluorescent indicator on the plates and were visualized with UV light (254 nm). Preparative chromatographic purifications were performed using silica gel column (Kieselgel 60). Melting points, determined using a Buchi Melting Point B-540 instrument, are uncorrected and represent values obtained on re-crystallized or chromatographically purified material. Mass spectra of final products were performed on LTQ Orbitrap XL™ Fourier transform mass spectrometer (FTMS) equipped with an ESI ION MAX™ (Thermo Fisher, San José, USA) source operating in positive mode. Elemental analyses were carried out on Carlo Erba model 1106; analyses indicated by the symbols of the elements were within $\pm 0.4\%$ of the theoretical values. $^1\text{H-NMR}$ and $^{13}\text{C-NMR}$ spectra were recorded on Varian Mercury Plus 400 MHz instrument. Spectra of Betamethasone 17-valerate, Triamcinolone acetonide and Tazarotenic acid hybrid derivatives were recorded in $\text{DMSO-}d_6$, while in CDCl_3 for Acitretin hybrid derivatives. Chemical shifts are reported in ppm. The following abbreviations are used to describe peak patterns when appropriate: s (singlet), d (doublet), dd (double doublet), t (triplet), m (multiplet), bs (broad singlet).

5.2. General procedure for the synthesis of 21-hemisuccinate glucocorticoids

Betamethasone 17-valerate-21-succinate (2a)

1.0g (2.10 mmol) of Betamethasone 17-valerate **1a** was dissolved in anhydrous pyridine (30 mL) and 0.63g (6.30 mmol) of succinic anhydride and 0.1 eq of DMAP were then added. After being stirred overnight at room temperature, the mixture was evaporated under reduced pressure. The resulting residue was then treated with 20 mL of water and

the mixture was stirred for 20 min and then centrifuged. The obtained precipitate was washed again with H₂O and filtered. Product **2a** (1.12 g) was obtained as a white powder (yield 93%). m.p. 191.1-192.5°C.

¹H NMR (DMSO-d₆) δ 12.26 (bs, 1H, COOH), 7.27 (d, J=10.1, 1H), 6.22 (dd, J = 10.1, 1.8 Hz, 1H), 6.03 (bs, 1H), 5.53 (d, J=4.3, 1H), 4.70 (d, J=16.8, 1H), 4.48 (d, J=16.8, 1H), 4.22 (m, 1H), 2.63 (t, J=5.8, 2H), 2.61-2.58 (m, overlapped, 1H), 2.49 (t, J=5.8, 2H), 2.39 (m, 2H), 2.35 (m, 1H), 2.23 (m, 1H), 2.07 (m, 1H), 1.88-1.85 (m, 2H), 1.71 (d, J=13.3, 2H), 1.52 (m, overlapped, 2H), 1.50 (s, 3H), 1.38-1.36 (m, 1H), 1.35 (t, overlapped, J=7.4, 3H), 1.27-1.22 (m, overlapped, 7H), 1.12-1.06 (m, 1H), 0.86-0.81 (m, overlapped, 6H). ¹³C NMR (DMSO-d₆) δ 14.03, 16.66, 20.01, 22.12, 23.41 (d, ³J_{C-F} = 5.4, C-18), 26.53, 28.03, 28.83, 29.34, 30.63, 33.42 (d, ²J_{C-F} = 19.2, C-8), 34.15, 34.88, 36.66, 46.65, 47.87, 48.20 (d, ²J_{C-F} = 22.8, C-10), 68.11, 70.50 (d, ²J_{C-F} = 35.6, C-11), 93.89, 101.39 (d, ¹J_{C-F} = 175.5, C-9), 124.60, 129.50, 152.96, 167.17, 171.74, 173.60, 174.41, 185.70, 198.70. ESI-MS [M+H]⁺ m/z calc. 576.65 for C₃₁H₄₁FO₉ found 577.2

Triamcinolone acetonide-21-succinate (2b)

The desired product **2b** has been obtained following the same procedure reported for compound **2a** starting from 1.0 g (2.30 mmol) of Triamcinolone acetonide **1b**, 0.69g (6.90 mmol) of succinic anhydride and 0.1 eq DMAP. White powder (yield 1.15g, 93%). m.p. 183.2-184.6°C.

¹H NMR (DMSO-d₆) δ 12.36 (bs, 1H, COOH), 7.29 (d, J = 10.1 Hz, 1H), 6.24 (dd, J = 10.1, 1.8 Hz, 1H), 6.02 (s, 1H), 5.48 (d, J = 3.9 Hz, 1H), 5.16 (d, J=17.8, 1H), 4.87 (d, J=5.1, 1H), 4.76 (d, J=17.8, 1H), 4.20 (m, 1H), 2.68 (t, J=5.8, 2H), 2.64 (m, 1H), 2.52 (t, J=5.8, 2H), 2.50-2.45 (m, overlapped, 2H), 2.34 (dd, J=13.5, J=3.6, 1H), 2.03 (d, J=13.5, 1H), 1.94 (m, 1H), 1.82 (m, 1H), 1.72 (d, J=12.9, 1H), 1.59 (m, 1H), 1.54 (m, 1H), 1.49 (s, 3H, CH₃), 1.37 (m, overlapped, 1H), 1.35 (s, 3H, CH₃), 1.14 (s, 3H, CH₃), 0.83 (s, 3H, CH₃). ¹³C NMR (DMSO-d₆) δ 16.52, 23.29 (d, ³J_{C-F} = 5.6, C-18), 25.89, 26.72, 27.84, 28.80, 29.09, 30.50, 30.90, 32.89 (d, ²J_{C-F} = 19.5, C-8), 33.51, 36.26, 43.00, 45.55, 48.16 (d, ²J_{C-F} = 22.4, C-10), 67.62, 70.54 (d, ²J_{C-F} = 38.3, C-11), 81.67,

97.48, 101.43 (d, $^1J_{C-F} = 176.5$, C-9), 111.35, 124.72, 129.57, 152.70, 167.05, 172.05, 173.61, 186.35, 203.49. ESI-MS $[M+H]^+$ m/z calcd 534.57 for $C_{28}H_{35}FO_9$; found 535.2.

5.3. Synthesis of compounds I-VIII

4-carbamothioylphenyl-(2-((9R,10S,11S,13S,16S,17R)-9-fluoro-11-hydroxy-10,13,16-trimethyl-3-oxo-17-(pentanoyloxy)-6,7,8,9,10,11,12,13,14,15,16,17-dodecahydro-3H-cyclopenta[a]phenanthren-17-yl)-2-oxoethyl) succinate
(Betamethasone-17-valerate-21-succinate-TBZ, I)

To a solution of **2a** (1.0 g, 1.7 mmol) in anhydrous tetrahydrofuran (30 mL), 4-hydroxythiobenzamide (TBZ, 0.26 g, 1.7 mmol) and DMAP (0.02 g, 0.17 mmol) were added. The reaction mixture was kept on ice bath stirring under nitrogen for 10 min and EDC (0.49 g, 2.85 mmol) was then added. The mixture was stirred under nitrogen atmosphere at room temperature for 12 hours. The solvent was evaporated, and the residue was purified by silica gel column chromatography (ethyl acetate/n-hexane, 6/4, v/v). Compound **I** was crystallized from diethyl ether/n-hexane (1/1, v/v). Yellow powder. Yield 0.87 g, 72%. m.p. 120.3–122.1 °C.

1H NMR (DMSO- d_6) δ 9.87 (bs, 1H, NH_2), 9.50 (bs, 1H, NH_2), 7.91 (d, $J=8.6$, 2H), 7.28 (d, $J=10.2$, 1H), 7.15 (d, $J=8.6$, 2H), 6.22 (dd, $J = 10.1, 1.8$ Hz, 1H), 6.00 (bs, 1H), 5.53 (d, $J=4.3$, 1H), 4.74 (d, $J=16.7$, 1H), 4.53 (d, $J=16.7$, 1H), 4.22 (m, 1H), 2.88 (t, $J=5.8$, 2H), 2.80 (t, $J=5.8$, 2H), 2.61-2.58 (m, 1H), 2.39 (m, 2H), 2.35 (m, 1H), 2.25 (m, 1H), 2.08 (m, 1H), 1.87-1.83 (m, 2H), 1.74 (d, $J=13.2$, 2H), 1.52 (m, overlapped, 2H), 1.50 (s, 3H), 1.38-1.36 (m, 1H), 1.35 (t, $d=7.4$, 3H), 1.27-1.22 (m, overlapped, 7H), 1.12-1.06 (m, 1H), 0.86-0.81 (m, overlapped, 6H). ^{13}C NMR (DMSO- d_6) δ 14.03, 16.66, 20.01, 22.12, 23.41 (d, $^3J_{C-F} = 5.4$, C-18), 26.53, 28.03, 28.83, 29.34, 30.63, 33.42 (d, $^2J_{C-F} = 19.2$, C-8), 34.15, 34.88, 36.66, 46.65, 47.87, 48.20 (d, $^2J_{C-F} = 22.8$, C-10), 68.11, 70.50 (d, $^2J_{C-F} = 35.6$, C-11), 93.89, 101.43 (d, $^1J_{C-F} = 175.8$, C-9), 121.63, 124.60, 129.19, 129.50, 137.50, 152.96, 153.07, 167.21, 170.93, 171.74, 174.41, 185.70, 198.80, 199.50. ESI-MS $[M+H]^+$ m/z calc. 711.28 for $C_{38}H_{46}FNO_9S$ found 712.0

2-((9R,10S,11S,13S,16S,17R)-9-fluoro-11-hydroxy-10,13,16-trimethyl-3-oxo-17-(pentanoyloxy)-6,7,8,9,10,11,12,13,14,15,16,17-dodecahydro-3H-cyclopenta[a]phenanthren-17-yl)-2-oxoethyl (4-isothiocyanatophenyl) succinate (Betamethasone-17-valerate-21-succinate-HPI, II)

Compound **II** has been obtained following the same procedure reported for **I**, starting from **2a** (1.0g, 1.7 mmol) and 4-hydroxyphenyl isothiocyanate (HPI, 0.26 g, 1.7 mmol). The residue was purified by silica gel column chromatography (CHCl₃/ethyl acetate, 8/2, v/v). The obtained compound **II** was crystallized from n-hexane. White solid. Yield 0.80 g, 66 %. m.p. 89.5–92.0°C.

¹H NMR (DMSO-d₆) δ 7.48 (d, J=8.6, 2H), 7.28 (d, J=10.2, 1H), 7.12 (d, J=8.6, 2H), 6.22 (dd, J = 10.1, 1.8 Hz, 1H), 6.00 (s, 1H), 5.53 (d, J=4.3, 1H), 4.74 (d, J=16.7, 1H), 4.53 (d, J=16.7, 1H), 4.22 (m, 1H), 2.88 (t, J=5.8, 2H), 2.80 (t, J=5.8, 2H), 2.61-2.58 (m, 1H), 2.39 (m, 2H), 2.35 (m, 1H), 2.25 (m, 1H), 2.08 (m, 1H), 1.87-1.83 (m, 2H), 1.74 (d, J=13.2, 2H), 1.52 (m, overlapped, 2H), 1.50 (s, 3H), 1.38-1.35 (m, 1H), 1.27-1.22 (m, overlapped, 7H), 1.12-1.06 (m, 1H), 0.86-0.81 (m, overlapped, 6H). ¹³C NMR (DMSO-d₆) δ 14.02 16.65, 19.99, 22.10, 23.40 (d, ³J_{C-F} = 5.4, C-18), 26.53, 28.04, 28.82, 29.30, 30.63, 33.40 (d, ²J_{C-F} = 19.1, C-8), 34.14, 34.87, 36.65, 43.70, 46.65, 47.85, 48.16 (d, ²J_{C-F} = 22.6, C-10), 68.05, 70.42 (d, ²J_{C-F} = 35.2, C-11), 93.86, 101.37 (d, ¹J_{C-F} = 175.6, C-9), 123.77, 124.59, 127.62, 128.00, 129.43, 134.13, 159.78, 153.97, 167.17, 170.91, 171.73, 174.48, 185.60, 198.88. ESI-MS [M+H]⁺ m/z calc. 709.82 for C₃₈H₄₆FNO₉S found 710.6

2-((9R,10S,11S,13S,16S,17R)-9-fluoro-11-hydroxy-10,13,16-trimethyl-3-oxo-17-(pentanoyloxy)-6,7,8,9,10,11,12,13,14,15,16,17-dodecahydro-3H-cyclopenta[a]phenanthren-17-yl)-2-oxoethyl-(4-(3-thioxo-3H-1,2-dithiol-5-yl)phenyl) succinate (Betamethasone-17-valerate-21-succinate-ADT, III)

Compound **III** has been obtained following the same procedure reported for **I**, starting from **2a** (1.0 g, 1.7 mmol) and 5-(p-hydroxyphenyl)-1,2-dithione-3-thione (ADT-OH, 0.39g, 1.7 mmol). The obtained residue was purified by silica gel column chromatography (ethyl acetate/n-hexane, 6:4, v/v). Compound **III** was crystallized from n-hexane. Orange powder. Yield 0.81g, 61%. m.p. 105.5–107.0 °C.

^1H NMR (DMSO- d_6) δ 7.97 (d, $J=8.6$, 2H), 7.83 (s, 1H), 7.32 (d, $J=8.6$, 2H), 7.29 (d, $J=10.1$, 1H), 6.24 (dd, $J = 10.1$, 1.8 Hz, 1H), 6.02 (s, 1H), 5.56 (d, $J=4.3$, 1H), 4.74 (d, $J=16.7$, 1H), 4.53 (d, $J=16.7$, 1H), 4.22 (m, 1H), 2.88 (t, $J=5.8$, 2H), 2.80 (t, $J=5.8$, 2H), 2.61-2.58 (m, 1H), 2.39 (m, 2H), 2.35 (m, 1H), 2.25 (m, 1H), 2.08 (m, 1H), 1.87-1.83 (m, 2H), 1.74 (d, $J=13.2$, 2H), 1.52 (m, overlapped, 2H), 1.50 (s, 3H), 1.38-1.35 (m, 1H), 1.27-1.22 (m, overlapped, 7H), 1.12-1.06 (m, 1H), 0.86-0.81 (m, overlapped, 6H). ^{13}C NMR (DMSO- d_6) δ 14.02, 16.66, 20.00, 22.11, 23.42 (d, $^3J_{\text{C-F}} = 5.4$, C-18), 26.54, 28.03, 28.83, 29.38, 30.63, 33.43 (d, $^2J_{\text{C-F}} = 19.2$, C-8), 34.15, 34.87, 36.66, 43.69, 46.65, 47.87, 48.18 (d, $^2J_{\text{C-F}} = 22.6$, C-10), 68.11, 70.50 (d, $^2J_{\text{C-F}} = 35.3$, C-11), 93.89, 101.38 (d, $^1J_{\text{C-F}} = 175.8$, C-9), 123.49, 124.63, 129.08, 129.31, 129.50, 136.26, 152.95, 153.85, 167.21, 170.86, 171.77, 173.15, 174.38, 185.64, 198.81, 215.96. ESI-MS $[\text{M}+\text{H}]^+$ m/z calc. 784.22 for $\text{C}_{38}\text{H}_{46}\text{FNO}_9\text{S}$ found 785.1

4-((ethylthio)carbonothioyl)phenyl-(2-((9R,10S,11S,13S,16S,17R)-9-fluoro-11-hydroxy-10,13,16-trimethyl-3-oxo-17-(pentanoyloxy)-6,7,8,9,10,11,12,13,14,15, 16,17-dodecahydro-3H-cyclopenta[a]phenanthren-17-yl)-2-oxoethyl) succinate (Betamethasone-17-valerate-21-succinate-HBTA, IV)

Compound **IV** has been obtained following the same procedure reported for **I**, starting from **2a** (1g, 1.7 mmol) and ethyl 4-hydroxybenzodithioate (HBTA, 0.34 g, 1.7 mmol). The residue was purified by silica gel column chromatography (CHCl_3 /ethyl acetate, 9/1, v/v). The obtained compound **IV** was crystallized from n-hexane. Pink powder. Yield 0.81g, 63%. m.p. 103.0–104.5°C.

^1H NMR (DMSO- d_6) δ 8.01 (d, $J=8.6$, 2H), 7.28 (d, $J=10.2$, 1H), 7.24 (d, $J=8.6$, 2H), 6.24 (dd, $J = 10.1$, 1.8 Hz, 1H), 6.02 (s, 1H), 5.57 (d, $J=4.3$, 1H), 4.74 (d, $J=16.7$, 1H), 4.53 (d, $J=16.7$, 1H), 4.22 (m, 1H), 3.39 (q, $J=7.4$, 2H), 2.88 (t, $J=5.8$, 2H), 2.80 (t, $J=5.8$, 2H), 2.39 (m, 2H), 2.35 (m, 1H), 2.25 (m, 1H), 2.08 (m, 1H), 1.87-1.83 (m, 2H), 1.74 (d, $J=13.2$, 2H), 1.52 (m, overlapped, 2H), 1.50 (s, 3H), 1.38-1.36 (m, 1H), 1.35 (t, $d=7.4$, 3H), 1.27-1.22 (m, overlapped, 7H), 1.12-1.06 (m, 1H), 0.86-0.81 (m, overlapped, 6H). ^{13}C NMR (DMSO- d_6) δ 12.60, 14.03, 16.64, 19.98, 22.10, 23.40 (d, $^3J_{\text{C-F}} = 5.4$, C-18), 26.54, 28.02, 28.83, 29.36, 30.63, 31.63, 33.43 (d, $^2J_{\text{C-F}} = 19.2$, C-8), 34.15, 34.88, 36.67, 43.69, 46.64, 47.87, 48.18 (d, $^2J_{\text{C-F}} = 22.6$, C-10), 68.08, 70.50 (d,

$^2J_{C-F} = 35.3$, C-11), 93.89, 101.38 (d, $^1J_{C-F} = 175.8$, C-9), 122.52, 124.54, 128.28, 129.51, 142.44, 152.81, 154.48, 167.15, 170.80, 171.75, 174.32, 185.67, 198.79. ESI-MS $[M+H]^+$ m/z calc. 757.94 for $C_{38}H_{46}FNO_9S$ found 760.2

4-carbamothioylphenyl-(2-((6a*S*,6b*R*,7*S*,8a*S*,8b*S*,11a*R*)-6b-fluoro-7-hydroxy-6a,8a,10,10-tetramethyl-4-oxo-2,4,6a,6b,7,8,8a,8b,11a,12,12a,12b-dodecahydro-1*H*-naphtho[2',1':4,5]indeno[1,2-*d*][1,3]dioxol-8*b*-yl)-2-oxoethyl) succinate (Triamcinolone acetonide-21-succinate-TBZ, V)

To a solution of **2b** (1g, 1.9 mmol) in anhydrous tetrahydrofuran (30 mL), 4-hydroxythiobenzamide (TBZ, 0.29 g, 1.9 mmol) and DMAP (0.02 g, 0.19 mmol) were added. The reaction mixture was kept on ice bath stirring under nitrogen for 10 min and EDC (0.49 g, 2.85mmol) was then added. The mixture was stirred under nitrogen atmosphere at room temperature for 12 hours. The solvent was evaporated, and the residue was purified by silica gel column chromatography ($CHCl_3/MeOH$, 9/1, v/v). Compound **V** was crystallized from diethyl ether/n-hexane (1/1, v/v). Yellow powder. Yield 0.69g, 54%. m.p. 179.0–181.0 °C.

1H NMR ($DMSO-d_6$) δ 9.88 (bs, 1H, NH_2), 9.51 (bs, 1H, NH_2), 7.92 (d, $J = 8.8$, 2H), 7.28 (d, $J = 10.1$ Hz, 1H), 7.14 (d, $J = 8.8$, 2H), 6.23 (dd, $J = 10.1$, 1.8 Hz, 1H), 6.01 (s, 1H), 5.49 (d, $J = 3.9$ Hz, 1H), 5.21 (d, $J = 17.8$, 1H), 4.88 (d, $J = 5.1$, 1H), 4.82 (d, $J = 17.8$, 1H), 4.21 (m, 1H), 2.91 (t, $J = 5.8$, 2H), 2.85 (t, $J = 5.8$, 2H), 2.64 (m, 1H), 2.50-2.45 (m, overlapped, 2H), 2.34 (dd, $J = 13.5$, $J = 3.6$, 1H), 2.06 (d, $J = 13.5$, 1H), 1.96 (m, 1H), 1.83 (m, 1H), 1.73 (d, $J = 12.9$, 1H), 1.59 (m, 1H), 1.54 (m, 1H), 1.50 (s, 3H, CH_3), 1.37 (m, overlapped, 1H), 1.36 (s, 3H, CH_3), 1.16 (s, 3H, CH_3), 0.83 (s, 3H, CH_3). ^{13}C NMR ($DMSO-d_6$) δ 16.44, 22.99 (d, $^3J_{C-F} = 5.6$, C-18), 25.75, 26.47, 27.54, 28.68, 29.30, 30.88, 33.16 (d, $^2J_{C-F} = 19.5$, C-8), 33.60, 37.26, 43.00, 45.55, 48.11 (d, $^2J_{C-F} = 22.4$, C-10), 65.83, 67.93, 71.79 (d, $^2J_{C-F} = 38.3$, C-11), 81.87, 97.48, 100.03 (d, $^1J_{C-F} = 176.5$, C-9), 111.59, 121.43, 122.64, 125.17, 128.46, 129.87, 133.65, 136.70, 151.81, 153.29, 165.76, 170.45, 171.70, 186.35, 201.30, 203.49. ESI-MS $[M+H]^+$ m/z calcd 670.76 for $C_{35}H_{40}FNO_9S$; found 670.9

2-((6aS,6bR,7S,8aS,8bS,11aR)-6b-fluoro-7-hydroxy-6a,8a,10,10-tetramethyl-4-oxo-2,4,6a,6b,7,8,8a,8b,11a,12,12a,12b-dodecahydro-1H-naphtho-[2',1':4,5]-indeno[1,2-d][1,3]dioxol-8b-yl)-2-oxoethyl (4-isothiocyanatophenyl) succinate

(Triamcinolone acetonide-21-succinate-HPI, VI)

Compound **VI** has been obtained following the same procedure reported for **V**, starting from **2b** (1.0 g, 1.9 mmol) and 4-hydroxyphenyl isothiocyanate (HPI, 0.29 g, 1.9 mmol). The residue was purified by silica gel column chromatography (CHCl₃/ethyl acetate, 7/3, v/v). Compound **VI** was crystallized from n-hexane. White solid. Yield 0.66g, 52%. m.p. 206.0–207.0 °C.

¹H NMR (DMSO-d₆) δ 7.48 (d, J = 8.8, 2H), 7.26 (d, J = 10.1 Hz, 1H), 7.12 (d, J = 8.8, 2H), 6.21 (dd, J = 10.1, 1.8 Hz, 1H), 5.99 (s, 1H), 5.47 (d, J = 3.9 Hz, 1H), 5.16 (d, J = 17.8, 1H), 4.83 (d, J = 5.1, 1H), 4.77 (d, J = 17.8, 1H), 4.17 (m, 1H), 2.85 (t, J = 5.8, 2H), 2.81 (t, J = 5.8, 2H), 2.60 (m, 1H), 2.47-2.43 (m, overlapped, 2H), 2.30 (dd, J = 13.5, J = 3.6, 1H), 2.02 (d, J = 13.5, 1H), 1.90 (m, 1H), 1.78 (m, 1H), 1.68 (d, J = 12.9, 1H), 1.55 (m, 1H), 1.51 (m, 1H), 1.46 (s, 3H, CH₃), 1.33 (m, overlapped, 1H), 1.32 (s, 3H, CH₃), 1.12 (s, 3H, CH₃), 0.80 (s, 3H, CH₃). ¹³C NMR (DMSO-d₆) δ 16.50, 23.25 (d, ³J_{C-F} = 5.6, C-18), 25.79, 26.74, 27.93, 28.74, 29.25, 30.53, 32.85 (d, ²J_{C-F} = 19.5, C-8), 33.46, 36.41, 43.25, 45.61, 48.17 (d, ²J_{C-F} = 22.3, C-10), 67.80, 70.64 (d, ²J_{C-F} = 36.6, C-11), 81.56, 97.54, 101.44 (d, ¹J_{C-F} = 176.5, C-9), 111.33, 123.70, 124.69, 127.61, 127.97, 129.47, 134.18, 149.81, 152.89, 167.00, 170.84, 171.72, 185.61, 203.78. ESI-MS [M+H]⁺ m/z calcd 668.74 for C₃₅H₃₈FNO₉S; found 668.9

2-((6aS,6bR,7S,8aS,8bS,11aR)-6b-fluoro-7-hydroxy-6a,8a,10,10-tetramethyl-4-oxo-2,4,6a,6b,7,8,8a,8b,11a,12,12a,12b-dodecahydro-1H-naphtho-[2',1':4,5]-indeno[1,2-d][1,3]dioxol-8b-yl)-2-oxoethyl (4-(3-thioxo-3H-1,2-dithiol-5-yl)phenyl) succinate

(Triamcinolone acetonide-21-succinate-ADT, VII)

Compound **VII** has been obtained following the same procedure reported for **V**, starting from **2b** (1.0 g, 1.9 mmol) and 5-(p-hydroxyphenyl)-1,2-dithione-3-thione (ADT-OH, 0.43 g, 1.9 mmol). The obtained residue was purified by silica gel column chromatography (CH₂Cl₂/ethyl acetate, 8/2, v/v). Compound **VII** was crystallized from diethyl ether. Orange solid. Yield 0.83g, 59%. m.p. 222.0–224.0 °C.

¹H NMR (DMSO-d₆) δ 7.96 (d, J = 8.8, 2H), 7.81 (s, 1H), 7.28 (overlapped, 2H), 7.27 (overlapped, 1H), 6.22 (dd, J = 10.1, 1.8 Hz, 1H), 6.00 (s, 1H), 5.46 (d, J = 3.9 Hz, 1H), 5.18 (d, J=17.8, 1H), 4.85 (d, J=5.1, 1H), 4.79 (d, J=17.8, 1H), 4.18 (m, 1H), 2.89 (t, J=5.8, 2H), 2.83 (t, J=5.8, 2H), 2.60 (m, 1H), 2.47-2.43 (m, overlapped, 2H), 2.31 (dd, J=13.5, J=3.6, 1H), 2.03 (d, J=13.5, 1H), 1.92 (m, 1H), 1.80 (m, 1H), 1.70 (d, J=12.9, 1H), 1.55 (m, 1H), 1.52 (m, 1H), 1.47 (s, 3H, CH₃), 1.33 (m, overlapped, 1H), 1.32 (s, 3H, CH₃), 1.12 (s, 3H, CH₃), 0.81 (s, 3H, CH₃). ¹³C NMR (DMSO-d₆) δ 16.51, 23.25 (d, ³J_{C-F} = 5.6, C-18), 25.82, 26.76, 27.92, 28.76, 29.35, 30.54, 32.85 (d, ²J_{C-F} = 19.5, C-8), 33.48, 36.43, 43.27, 45.62, 48.20 (d, ²J_{C-F} = 22.3, C-10), 67.82, 70.67 (d, ²J_{C-F} = 36.6, C-11), 81.57, 97.55, 101.40 (d, ¹J_{C-F} = 176.5, C-9), 111.35, 123.43, 124.69, 129.11, 129.27, 129.48, 136.24, 152.88, 153.81, 167.01, 170.77, 171.75, 173.12, 185.61, 203.77, 215.92. ESI-MS [M+H]⁺ m/z calcd 743.89 for C₃₇H₃₉FO₉S₃; found 744.3

*4-((ethylthio)carbonothioyl)phenyl-(2-((6a*S*,6b*R*,7*S*,8a*S*,8b*S*,11a*R*)-6b-fluoro-7-hydroxy-6a,8a,10,10-tetramethyl-4-oxo-2,4,6a,6b,7,8,8a,8b,11a,12,12a,12b-dodecahydro-1*H*-naphtho[2',1':4,5]indeno[1,2-*d*][1,3]dioxol-8b-yl)-2-oxoethyl) succinate*

(Triamcinolone acetonide-21-succinate-HBTA, VIII)

Compound **VIII** has been obtained following the same procedure above reported for **V**, starting from **2b** (1.0 g, 1.9 mmol) and ethyl 4-hydroxybenzodithioate (HBTA, 0.38 g, 1.9 mmol). The residue was purified by silica gel column chromatography (ethyl acetate/n-hexane, 6/4, v/v). Compound **VIII** was crystallized from n-hexane. Pink solid. Yield 0.76 g, 56%. m.p. 179.0–180.0°C.

¹H NMR (DMSO-d₆) 8.00 (d, J = 8.8, 2H), 7.26 (d, J = 10.1 Hz, 1H), 7.22 (d, J = 8.8, 2H), 6.21 (dd, J = 10.1, 1.8 Hz, 1H), 5.99 (s, 1H), 5.46 (d, J = 3.9 Hz, 1H), 5.18 (d, J=17.8, 1H), 4.85 (d, J=5.1, 1H), 4.79 (d, J=17.8, 1H), 4.18 (m, 1H), 3.35 (q, J=7.4, 2H), 2.89 (t, J=5.8, 2H), 2.83 (t, J=5.8, 2H), 2.60 (m, 1H), 2.47-2.43 (m, overlapped, 2H), 2.31 (dd, J=13.5, J=3.6, 1H), 2.03 (d, J=13.5, 1H), 1.92 (m, 1H), 1.80 (m, 1H), 1.70 (d, J=12.9, 1H), 1.55 (m, 1H), 1.52 (m, 1H), 1.47 (s, 3H, CH₃), 1.33 (m, overlapped, 4H), 1.32 (s, 3H, CH₃), 1.13 (s, 3H, CH₃), 0.81 (s, 3H, CH₃). ¹³C NMR (DMSO-d₆) δ 12.57, 16.50, 23.26 (d, ³J_{C-F} = 5.6, C-18), 25.81, 26.76, 27.93, 28.74,

29.32, 30.53, 31.61, 32.86 (d, $^2J_{C-F} = 19.5$, C-8), 33.48, 36.42, 43.26, 45.62, 48.18 (d, $^2J_{C-F} = 22.3$, C-10), 67.81, 70.63 (d, $^2J_{C-F} = 36.6$, C-11), 81.57, 97.56, 101.33 (d, $^1J_{C-F} = 175.7$, C-9) 111.35, 122.44, 124.69, 128.30, 129.48, 142.39, 152.89, 154.41, 167.02, 170.73, 171.76, 185.61, 203.76, 227.26. ESI-MS $[M+H]^+$ m/z calcd 715.86 for $C_{37}H_{43}FO_9S_2$; found 716.2

5.4. Synthesis of compounds IX-XII

(2E,4E,6E,8E)-4-carbamothioylphenyl 9-(4-methoxy-2,3,6-trimethylphenyl)-3,7-dimethylnona-2,4,6,8-tetraenoate
(Acitretin-TBZ, IX)

To a solution of acitretin (1.0 g, 3.1 mmol) in anhydrous tetrahydrofuran (30 mL), 4-hydroxythiobenzamide (TBZ, 0.47 g, 3.1 mmol) and DMAP (0.04 g, 0.31 mmol) were added. The reaction mixture was kept on ice bath stirring under nitrogen for 10 min and EDC (0.88 g, 4.60 mmol) was then added. The mixture was stirred under nitrogen atmosphere at room temperature for 12 hours. The solvent was evaporated, and the residue was purified by silica gel column chromatography ($CHCl_3$ /ethyl acetate, 9/1, v/v). Compound IX was crystallized from diethyl ether. Yellow solid. Yield 0.70 g, 49%. m.p. 179.0–180.0 °C.

1H NMR ($CDCl_3$) δ 7.93 (d, $J=8.5$ Hz, 2H), 7.63 (s, 1H), 7.35–7.10 (m, 4H), 6.77 (d, $J=16.3$ Hz, 1H), 6.64 (s, 1H), 6.43 (d, $J=15.0$ Hz, 1H), 6.29 (t, $J=13.9$ Hz, 2H), 6.02 (s, 1H), 3.85 (s, 3H), 2.46 (s, 3H), 2.34 (s, 3H), 2.28 (s, 3H), 2.18 (s, 3H), 2.17 (s, 3H). ^{13}C NMR ($CDCl_3$) δ 201.72, 164.87, 156.37, 153.88, 140.46, 138.00, 136.30, 135.97, 135.03, 133.97, 132.30, 130.13, 129.71, 129.23, 128.36, 122.82, 121.82, 116.80, 110.01, 55.55, 21.45, 17.50, 14.21, 13.08, 11.87. ESI-MS $[M+H]^+$ m/z calc. 461.62 for $C_{28}H_{31}NO_3S$; found 462.21

(2E,4E,6E,8E)-4-isothiocyanatophenyl 9-(4-methoxy-2,3,6-trimethylphenyl)-3,7-dimethylnona-2,4,6,8-tetraenoate

(Acitretin-HPI, X)

Compound **X** has been obtained following the same procedure reported for **IX**, starting from acitretin (1.0 g, 3.1 mmol) and 4-hydroxyphenyl isothiocyanate (HPI, 0.46 g, 3.1 mmol). The residue was purified by silica gel column chromatography (CHCl₃/ n-hexane, 6/4, v/v). Compound **X** was crystallized from diethyl ether/n-hexane (1/1, v/v). Yellow solid. Yield 0.75 g, 53%. m.p. 187.0–188.0°C.

¹H NMR (CDCl₃) δ 7.21–7.10 (m, 2H), 7.10–6.98 (m, 3H), 6.66 (d, J=16.3 Hz, 1H), 6.54 (s, 1H), 6.38–6.10 (m, 3H), 5.90 (s, 1H), 3.75 (s, 3H), 2.35 (d, J=0.6 Hz, 3H), 2.24 (s, 3H), 2.17 (s, 3H), 2.07 (d, J=8.7 Hz, 6H). ¹³C NMR (CDCl₃) δ 164.94, 156.30, 149.54, 140.40, 137.99, 135.96, 135.64, 135.04, 133.96, 132.23, 130.12, 129.71, 129.20, 128.40, 126.65, 123.09, 122.82, 116.78, 110.00, 59.54, 55.54, 38.16, 31.26, 21.45, 17.49, 14.17, 13.07, 11.87. ESI-MS [M+H]⁺ m/z calc. 459.60 for C₂₈H₂₉NO₃S; found 482.18 [M+Na]⁺ and 498.15 [M+K]⁺

(2E,4E,6E,8E)-4-(3-thioxo-3H-1,2-dithiol-5-yl)phenyl 9-(4-methoxy-2,3,6-trimethylphenyl)-3,7-dimethylnona-2,4,6,8-tetraenoate

(Acitretin-ADT, XI)

Compound **XI** has been obtained following the same procedure reported for **IX**, starting from acitretin (1.0 g, 3.1 mmol) and 5-(*p*-hydroxyphenyl)-1,2-dithione-3-thione (ADT-OH, 0.70 g, 3.1 mmol). The obtained residue was purified by silica gel column chromatography (CHCl₃, 100%). Compound **XI** was crystallized from diethyl ether. Orange solid. Yield 1.19 g, 72%. m.p. 180.8–182.3 °C.

¹H NMR (CDCl₃) δ 7.71 (d, J=8.7 Hz, 2H), 7.44 (s, 1H), 7.35 – 7.27 (m, 3H), 6.76 (dd, J = 16.1, 8.7 Hz, 1H), 6.64 (s, 1H), 6.44 (d, J = 15.1 Hz, 1H), 6.29 (t, J = 13.8 Hz, 2H), 6.03 (s, 1H), 3.84 (d, J = 4.3 Hz, 3H), 2.47 (s, 3H), 2.34 (s, 3H), 2.28 (s, 3H), 2.18 (d, J = 5.8 Hz, 6H). ¹³C NMR (CDCl₃) δ 215.51, 172.03, 164.67, 156.84, 156.29, 153.97, 140.63, 137.96, 135.93, 134.93, 133.97, 132.49, 130.08, 129.68, 129.34, 128.81, 128.13, 123.14, 122.83, 116.53, 110.01, 55.55, 30.95, 21.45, 17.50, 14.24, 13.09, 11.87. ESI-MS [M+H]⁺ m/z calc. 534.75 for C₃₀H₃₀O₃S₃; found 534.14

(2E,4E,6E,8E)-4-((ethylthio)carbonothioyl)phenyl 9-(4-methoxy-2,3,6-trimethylphenyl)-3,7-dimethylnona-2,4,6,8-tetraenoate
(Acitretin-HBTA, XII)

Compound **XII** has been obtained following the same procedure above reported for **IX**, starting from acitretin (1.0 g, 3.1 mmol) and ethyl 4-hydroxybenzodithioate (HBTA, 0.62 g, 3.1 mmol). The residue was purified by silica gel column chromatography (CHCl₃, 100%). Compound **XII** was crystallized from n-hexane. Orange solid. Yield 0.74 g, 47%. m.p. 141.0–143.0°C.

¹H NMR (CDCl₃) δ 8.09 (d, J=8.4 Hz, 2H), 7.17 (t, J=13.1 Hz, 3H), 6.75 (t, J=12.4 Hz, 1H), 6.64 (s, 1H), 6.41 (t, J=18.9 Hz, 1H), 6.29 (dd, J=18.5, 9.6 Hz, 2H), 6.03 (s, 1H), 3.85 (s, 3H), 3.40 (dd, J=14.5, 7.2 Hz, 2H), 2.42 (d, J=30.8 Hz, 3H), 2.34 (s, 3H), 2.28 (s, 3H), 2.19 (s, 3H), 2.17 (s, 3H), 1.45 (t, J = 7.3 Hz, 3H). ¹³C NMR (CDCl₃) δ 164.72, 156.25, 154.31, 142.29, 140.42, 138.11, 135.97, 135.11, 133.97, 132.16, 130.16, 129.73, 129.43, 129.07, 128.14, 122.81, 121.54, 116.99, 114.92, 110.00, 55.55, 31.59, 21.45, 21.20, 17.50, 14.19, 13.07, 12.31, 11.87. ESI-MS [M+H]⁺ m/z calc. 506.72 for C₃₀H₃₄O₃S₂; found 506.19

5.5. Synthesis of compounds XIII-XVI

4-carbamothioylphenyl 6-((4,4-dimethylthiochroman-6-yl)ethynyl)nicotinate
(Tazarotene-TBZ, XIII)

To a solution of tazarotenic acid (1.0 g, 3.1 mmol) in anhydrous tetrahydrofuran (30 mL), 4-hydroxythiobenzamide (TBZ, 0.47 g, 3.1 mmol) and DMAP (0.04 g, 0.31 mmol) were added. The reaction mixture was kept on ice bath stirring under nitrogen for 10 min and EDC (0.88 g, 4.60 mmol) was then added. The mixture was stirred under nitrogen atmosphere at room temperature for 12 hours. The solvent was evaporated, and the residue was purified by silica gel column chromatography (CH₂Cl₂/MeOH, 9.5/0.5, v/v). Compound **XIII** was crystallized from diethyl ether. Light orange solid. Yield 0.60 g, 42%. m.p. 195.0–197.0 °C.

¹H NMR (DMSO-d₆) δ 9.95 (s, 1H), 9.58 (s, 1H), 9.26 (d, J=1.5 Hz, 1H), 8.50 (dd, J=8.2, 2.2 Hz, 1H), 8.01 (d, J=8.7 Hz, 2H), 7.86 (d, J=8.3 Hz, 1H), 7.70 (d, J=1.6 Hz,

1H), 7.41 (d, $J=8.7$ Hz, 2H), 7.33 (dd, $J=8.2, 1.6$ Hz, 1H), 7.16 (d, $J=8.2$ Hz, 1H), 3.15–3.00 (m, 2H), 2.00–1.85 (m, 2H), 1.32 (s, 6H). ^{13}C NMR (DMSO- d_6) δ 199.46, 163.42, 152.95, 151.53, 147.27, 143.02, 138.51, 137.91, 135.71, 130.71, 129.72, 129.31, 127.52, 127.17, 124.08, 121.82, 116.41, 93.37, 88.66, 36.93, 33.16, 30.07, 22.97. ESI-MS $[\text{M}+\text{H}]^+$ m/z calc. 458.60 for $\text{C}_{26}\text{H}_{22}\text{N}_2\text{O}_2\text{S}_2$; found 459.29

4-isothiocyanatophenyl 6-((4,4-dimethylthiochroman-6-yl)ethynyl)nicotinate
(Tazarotene-HPI, XIV)

Compound **XIV** has been obtained following the same procedure reported for **XIII**, starting from tazarotenic acid (1.0 g, 3.1 mmol) and 4-hydroxyphenyl isothiocyanate (HPI, 0.47 g, 3.1 mmol). The residue was purified by silica gel column chromatography ($\text{CH}_2\text{Cl}_2/\text{n-hexane}$, 9.5/0.5, v/v). Compound **XIV** was crystallized from n-hexane. Light yellow solid. Yield 0.79 g, 56%. m.p. 147.1–147.5°C.

^1H NMR (DMSO- d_6) δ 9.29 (dd, $J=2.2, 0.8$ Hz, 1H), 8.53 (dd, $J=8.2, 2.2$ Hz, 1H), 7.91 (dd, $J=8.2, 0.7$ Hz, 1H), 7.75 (d, $J=1.7$ Hz, 1H), 7.70–7.57 (m, 2H), 7.57–7.42 (m, 2H), 7.41–7.29 (m, 1H), 7.21 (d, $J=8.2$ Hz, 1H), 3.19–3.08 (m, 2H), 2.02–1.91 (m, 2H), 1.37 (s, 6H). ^{13}C NMR (DMSO- d_6) δ 163.41, 151.52, 149.76, 143.01, 138.50, 135.71, 134.30, 130.70, 129.71, 128.40, 127.77, 127.49, 127.16, 124.01, 116.41, 93.37, 88.66, 36.92, 33.15, 30.06, 22.97. ESI-MS $[\text{M}+\text{H}]^+$ m/z calc. 456.58 for $\text{C}_{26}\text{H}_{20}\text{N}_2\text{O}_2\text{S}_2$; found 457.20

4-(3-thioxo-3H-1,2-dithiol-5-yl)phenyl 6-((4,4-dimethylthiochroman-6-yl)ethynyl)nicotinate
(Tazarotene-ADT, XV)

Compound **XV** has been obtained following the same procedure reported for **XIII**, starting from tazarotenic acid (1.0 g, 3.1 mmol) and 5-(*p*-hydroxyphenyl)-1,2-dithione-3-thione (ADT-OH, 0.70 g, 3.1 mmol). The obtained residue was purified by silica gel column chromatography ($\text{CH}_2\text{Cl}_2/\text{n-hexane}$, 9.5/0.5, v/v). Compound **XV** was crystallized from diethyl ether. Orange solid. Yield 1.05 g, 64%. m.p. 187.0–189.0 °C.

^1H NMR (DMSO- d_6) δ 9.27 (d, $J=1.5$ Hz, 1H), 8.51 (dd, $J=8.2, 2.1$ Hz, 1H), 8.06 (d, $J=8.7$ Hz, 2H), 7.88 (s, 1H), 7.87 (d, $J=6.1$ Hz, 1H), 7.71 (d, $J=1.3$ Hz, 1H), 7.56 (d,

$J=8.7$ Hz, 2H), 7.33 (dd, $J=8.2$, 1.4 Hz, 1H), 7.16 (d, $J=8.2$ Hz, 1H), 3.13–3.04 (m, 2H), 1.95–1.88 (m, 2H), 1.32 (s, 6H). ^{13}C NMR (DMSO- d_6) δ 216.01, 173.13, 163.30, 153.76, 151.59, 147.31, 143.03, 138.57, 136.41, 135.73, 130.72, 129.73, 129.69, 129.25, 127.52, 127.17, 124.04, 123.70, 116.40, 93.41, 88.71, 36.93, 33.16, 30.07, 22.97. ESI-MS $[\text{M}+\text{H}]^+$ m/z calc. 531.73 for $\text{C}_{28}\text{H}_{21}\text{NO}_2\text{S}_4$; found 532.30

4-((ethylthio)carbonothioyl)phenyl 6-((4,4-dimethylthiochroman-6-yl)ethynyl)nicotinate

(Tazarotene-HBTA, XVI)

Compound **XVI** has been obtained following the same procedure reported for **XIII**, starting from acitretin (1.0 g, 3.1 mmol) and ethyl 4-hydroxybenzodithioate (HBTA, 0.62 g, 3.1 mmol). The residue was purified by silica gel column chromatography ($\text{CH}_2\text{Cl}_2/\text{n-hexane}$, 9.5/0.5, v/v). Compound **XII** was crystallized from n-hexane. Pink solid. Yield 1.05 g, 67%. m.p. 121.4–122.1°C.

^1H NMR (DMSO- d_6) δ 9.26 (s, 1H), 8.50 (d, $J=7.7$ Hz, 1H), 8.08 (d, $J=8.1$ Hz, 2H), 7.85 (d, $J=8.0$ Hz, 1H), 7.70 (s, 1H), 7.48 (d, $J=8.1$ Hz, 2H), 7.32 (d, $J=7.8$ Hz, 1H), 7.15 (d, $J=7.9$ Hz, 1H), 3.45–3.37 (m, 2H), 3.08 (t, 2H), 1.91 (t, 2H), 1.36 (t, $J=7.3$ Hz, 3H), 1.32 (s, 6H). ^{13}C NMR (DMSO- d_6) δ 163.22, 154.31, 151.56, 147.32, 143.01, 142.73, 138.54, 135.72, 130.71, 129.72, 128.41, 127.51, 127.17, 123.99, 122.68, 116.41, 93.42, 88.67, 36.92, 33.15, 31.70, 30.06, 22.98, 12.60. ESI-MS $[\text{M}+\text{H}]^+$ m/z calc. 503.70 for $\text{C}_{28}\text{H}_{25}\text{NO}_2\text{S}_3$; found 504.20

5.6. Molecular Modelling

Molecular modelling calculations were performed on High Performance Computing Cluster (HPCC) and molecular modelling graphics were carried out on a personal computer equipped with Intel(R) Core(TM) i7-4790 processor.

Compounds **II** and **VI** were built using the Small Molecule tool of Discovery Studio 2017 (Dassault Systèmes BIOVIA, San Diego). Atomic potentials and charges were assigned using the CHARMM force field [91]. The conformational space of the compounds was sampled using the random search algorithm Boltzmann Jump for the

random generation of a maximum of 400 conformations. By applying this method, each random perturbation is either accepted or rejected according to the Metropolis selection criterion with a ratio according to the Boltzmann distribution ($T = 300\text{K}$). An energy threshold value of 20 kcal/mol was used as selection criteria. The generated structures were then subjected to MM energy minimization until the maximum RMS derivative was less than 0.01 kcal/Å, using Conjugate Gradient [92] as minimization algorithm and the Generalized Born implicit solvent model with a solvent dielectric constant value of 80. Resulting conformers were ranked by their conformational energy. Conformers within 5 kcal/mol from the global minimum ($\Delta\text{EGM} \leq 5$ kcal/mol) were classified into families according to their values of root mean squared deviation (RMSD; heavy atoms). Pairwise RMSDs were calculated between all the conformers and the set of conformers characterized by a RMSD value < 3 Å were grouped in the same conformational family. The occurrence rate of each conformational family was calculated. The solvent accessible surface area (SASA) of the isothiocyanate carbon atom of the lowest energy conformer of each family was calculated and visually analysed. The calculated SASA values were compared to the maximum SASA value of the isothiocyanate carbon atom (i.e., 15.2 Å) and the rate of SASA decrease was accordingly calculated.

5.7. Pharmacological procedures

Amperometric determination of H₂S release

The H₂S-generating properties of the tested compounds have been evaluated by an amperometric approach, through an Apollo-4000 Free Radical Analyzer (WPI) detector and H₂S-selective mini-electrodes at room temperature as reported previously [93]. Briefly, a “PBS buffer 10×” was prepared (NaH₂PO₄·H₂O 1.28 g, Na₂HPO₄·12H₂O 5.97 g, and NaCl 43.88 g in 500 mL of H₂O) and stocked at 4 °C. Immediately before the experiments, the “PBS buffer 10×” was diluted in distilled water (1:10) to obtain the assay buffer (AB); pH was adjusted to 7.4. The H₂S-selective minielectrode was equilibrated in 10 mL of the AB, until the recovery of a stable baseline. Then, 100 μL of a dimethyl sulfoxide (DMSO) solution of the tested compounds was added (final concentration of the H₂S-donors 100 μM; final concentration of DMSO in the AB 1%).

The generation of H₂S was observed for 30 min. When required by the experimental protocol, 4 mM L-cysteine was added, before the H₂S-donors. The correct relationship between the amperometric currents (recorded in pA) and the corresponding concentrations of H₂S was determined by opportune calibration curves with increasing concentrations of NaHS (1, 3, 5, and 10 μM) at pH 4.0. The lower limit of reliable quantitative determination was 0.3 μM.

Tissues

The tissues were purchased from Episkin (Lyon, France) and are in vitro reconstructed human epidermis from normal human keratinocytes cultured on a collagen matrix at the air-liquid interface. The tissues are grown on a 0.5 cm² inert permeable polycarbonate filter in vertical direction, and then cultivated for 5 days in a supplemented, chemically defined medium at the air-liquid interface, in order to form a structured epithelium. Characterization and morphological analysis were performed, demonstrating that these tissues reproduce many of the characteristics of normal human epidermis. Immediately after delivery, tissues were removed from nutrient agar and transferred into 6-well plates containing the growth medium provided by the manufacturer under sterile airflow conditions. Before experiments, tissues were equilibrated overnight in an incubator at 37°C and 5% CO₂.

Treatment

Negative control: tissues were treated with 30 μL vehicle (DMSO 0.05%) for 48h.

Positive control: Tissues were topically treated with 30 μL of LPS 5μg/ml for 48h.

Tested compounds: tissues were treated with LPS 5μg/ml and with the tested compounds 1μM for 48h.

MTT assay

The Cell Proliferation dye 3-(4, 5-dimethylthiazolyl-2)-2, 5-diphenyltetrazolium bromide (MTT) is a colorimetric probe for the nonradioactive quantification of cellular proliferation, viability, and cytotoxicity. This colorimetric assay analyzes the number of viable cells by the cleavage of tetrazolium salts formazan by enzymes of the

endoplasmic reticulum. This bioreduction occurs in viable cells only and is related to NAD(P)H production through glycolysis. Therefore, the amount of formazan dye formed directly correlates to the number of metabolically active cells in the culture. The tissues are incubated with 0.3 mL MTT solution (1 mg/mL) for 3 h (± 15 min). The formazan crystals are extracted by adding to the apical surface of tissues 1 mL isopropanol for 2 h (± 15 min) at room temperature, avoiding light exposure, under agitation. The solutions were resuspended, and 200 μ L of extract transferred into a 96-well plate. In the same 96-well plate, 200 μ L isopropanol was loaded (8 wells) and used as blank: isopropanol OD was subtracted from each OD value recorded. Results were expressed as mean OD \pm mean error (SEM) and as the proportion of cell viability measured with the negative control.

Enzyme-Linked Immunosorbent Assay (ELISA) for TNF, IL-6 and IL1 beta measurement.

The quantification of TNF, IL-6 and IL1 beta has been performed by using ELISA sandwich assay (ThermoFisher) following the technical instructions. Briefly, after the treatment protocol, culture medium was collected in sterile tube and stored at -80 °C in 200 μ L aliquots. Before starting, all reagents and samples were thawed to reach room temperature before use and gently mixed. Standard curve was performed by using Reconstituted Human TNF or IL-6 or IL1 beta opportunely diluted (500, 250, 125, 62.5, 31.2, 15.6, and 0 pg/mL). 100 μ L tested samples or standard were added into the pre-coated wells and incubated at room temperature for 2h. Then, the solution was aspirated, and the wells washed 4 times with 1x wash buffer. 100 μ L Human TNF or IL-6 or IL1 beta biotin conjugate solution was added into each well and incubated at room temperature for 1h. Then, the solution was aspirated, and the wells washed 4 times with 1x wash buffer. 100 μ L 1X Streptavidin-HRP solution (previously prepared and immediately used) were added into each well and incubated for 30 minutes at room temperature. Then, the solution was aspirated, and the wells washed 4 times with 1x wash buffer. 100 μ L Stabilized Chromogen were added to each well and incubated for 30 minutes at room temperature in the dark. 100 μ L Stop Solution were added into each well and the absorbance was Read 450 nm. A curve fitting line software (GraphPad 6)

was used to generate the standard curve applying a four-parameter algorithm. Results were expressed in pg/mL.

Animals

Adult male Balb/c mice (20–30 g; 7–8 week-old), obtained from the animal house facilities at the Faculty of Medicine (University of São Paulo, Brazil), were used in the experiments in accordance with the Ethical Principles for Animal Research established by the ICB/USP Ethics Committees (n° 67/2017) for Animal Use in research, according to the National Council for Animal Experimentation Control (CONCEA) principles comprising with the Animal Welfare Act. According to the internal laboratory rules, euthanasia will be performed if severe distress related to the protocol developed during the experiment. Animals were group-housed in number of 4 and kept in a temperature-controlled room at 22°C with a 12/12-hour light/dark cycle and allowed free access to food (Nuvilab CR-1, Quimtia S/A, Brazil) and filtered water.

Test substances and therapeutic approach

For the preparation of the topical formulation containing the hybrid-H₂S donors, the compounds Triamcinolone acetonide-TBZ, Triamcinolone acetonide-HBTA and Triamcinolone acetonide were daily weighed and incorporated into the components (oily phase + surfactant or polar) prior to treatment in order to avoid destabilizing and to facilitate solubilization in the delivery system, based on the polar or apolar characteristic of the molecule under study. Imiquimod was obtained from Germed Farmacêutica Ltda (São Paulo). At the end of the experiments, all mice were euthanized with an overdose of isoflurane followed by cervical dislocation.

Mice were topically treated with either vehicle (65 mg/area of DLC) or corresponding volume of test agents (65 mg of DLC containing test agents 1 %) [79].

Psoriasis induction and experimental design

Male Balb/C mice with 6 to 7 weeks were used and psoriasis was induced by topical administration of imiquimod cream (IMQ) on mice dorsal skin for 5 consecutive days.

Four to six hours later, mice were topically treated in the dorsal skin with 65 mg of a nanodispersion (DLC) alone or DLC containing 1% Triamcinolone acetonide-HBTA, Triamcinolone acetonide-TBZ or Triamcinolone acetonide (Figure 16). The gravity of some Psoriasis Area Severity Index (PASI), skin thickness and itch behaviour were daily evaluated daily. After the 6th day of treatment, mice were euthanized and biological material (skin, blood, ears, spleen etc.) were collected and stored for further analysis [94].

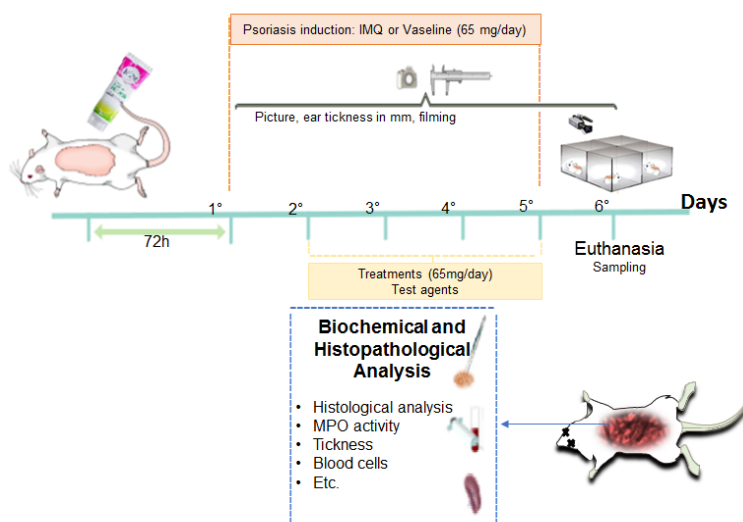


Figure 16. Schematic illustration of the experimental design and treatments. The dorsal skin was shaved and after 72 h, topical treatment with daily (single) doses of the naive skin formulations started. Once the chosen formulation was established, the psoriasis model was induced by imiquimod administration (IMQ) in the morning and in the afternoon (16-17 h) the formulation was administered alone or carrying the test agents (SAIDs-H₂S donors). After the study period, the animal was euthanized and the biological material (eg skin, blood, spleen) was removed.

Experimental groups

The table below shows the groups for evaluation:

Groups	Topical treatment	Dose	n
Sham	DLC from 2 nd day	65 mg/animal, daily	4
Psoriasis	DLC from 2 nd day	65 mg/animal, daily	4
Psoriasis	Triamcinolone acetonide-TBZ-DLC 1% from 2 nd day	65 mg/animal, daily	4
Psoriasis	Triamcinolone acetonide-HBTA-DLC 1% from 2 nd day	65 mg/animal, daily	4
Psoriasis	Triamcinolone acetonide 1% from 2 nd day	65 mg/animal, daily	4

Evaluation of the clinical index of psoriasis severity (PASI)

The degree of skin inflammation on the back of the animals was quantified via the scoring system, which was based on the clinical index of psoriasis area and severity (PASI - <http://pasi.corti.li/>), adopting a growing scale from 0-4, where 0 = no lesion; 1 = mild lesion; 2 = moderate; 3 = intense; 4 = very intense. Flushing and peeling were assessed independently. The analysis of acanthosis was represented by the increase in ear thickness, based on a daily measurement of ear thickness, made in triplicate with the aid of a digital caliper (Satarrett 799A) by trained investigators unaware to experimental protocols. The result was expressed in millimeters (mm)[83].

Quantification of spontaneous chronic itching

The animals were individually acclimatized for 2 days during 30 min in a transparent Perspex box (12 x 20 x 17 cm, Insight; Ribeirão Preto; SP) in a quiet room adapted for camcorder recording. Behavioural recording of the spontaneous pruritus of each animal was performed for 30 min by filming (Sony Handycam DCR-PJ6 camcorder) before the administration of the IMQ (- 60 min, day 1) and after 24h (day 2), 48h (day 3) 72h (day 4) and day 5, which corresponds to the 6th day after the first application of IMQ, which represents the acute and chronic phases of the disease. Episodes of itch attack behaviour was considered when the animal scratch his back with hind paw three or more times with rapid movements [79]. Results obtained over 30 min were numerically expressed as episodes/attacks of pruritus during the 30 min interval. The quantification of a pruritus was performed by trained investigators unaware to the study protocol.

Total quantification of splenocytes

After euthanasia of the animals, the spleen was quickly removed, weighed, and macerated in 5 ml of aseptic PBS medium to obtain the homogenate. From this homogenate, a volume of 10 μ L was obtained and added to the 190 μ L volume of crystal violet dye (0.2%) to count the total number of cells using the Neubauer chamber.

Cell culture

Human bronchial smooth muscle cells (BSMCs) were cultured in Medium 231 (Life technologies) supplemented with Smooth Muscle Growth Supplement (SMGS, Life Technologies) and 1% of 100 units/mL penicillin and 100 mg/mL streptomycin (Sigma Aldrich) in tissue culture flasks at 37°C in a humidified atmosphere and 5% CO₂. BSMCs were cultured up to about 90% confluence and 24 h before the experiment cells were seeded onto a 96-well black plate, clear bottom pre-coated with gelatin 1% (from porcine skin, Sigma Aldrich), at density of 72×10^3 per well. Cells were split 1:2 twice a week and used until passage 18. RBL-2H3 cells were purchased from ATCC (American Type Culture Collection, Manassas, VA, USA) and cultured in Minimum Essential Medium (MEM - Sigma-Aldrich) supplemented with 10% of Fetal Bovine Serum (FBS - Sigma-Aldrich) and 1% streptomycin/penicillin (Sigma-Aldrich) at 37°C in a humidified 5% CO₂ atmosphere.

Intracellular H₂S release

BSMCs were cultured up to about 90% confluence and 24 h before the experiment cells were seeded onto a 96 well clear bottom black plate at a density of 72×10^3 per well. After 24 h, the medium was replaced and cells were incubated for 30 min with a 100 µM solution of the fluorescent dye WSP-1 (Washington State Probe, 1,3'-methoxy-3-oxo-3H-spiro[isobenzofuran-1,9'-xanthen]-6'-yl 2-(pyridine-2-yl-disulfanyl benzoate) that is highly sensitive for H₂S detection [95, 96]. Then, the supernatant was removed and replaced with different solutions of the teste compounds dissolved in standard buffer (HEPES 20 mM; NaCl, 120 mM; KCl, 2 mM; CaCl₂·2H₂O, 2 mM; MgCl₂·6H₂O, 1 mM; glucose, 5 mM; and pH 7.4, at room temperature) at the concentration of 100 and 300 µM. The change in fluorescence (expressed as fluorescence index measured at $\lambda=465-515$ nm) was monitored every 5 min for 60 min, by means of a spectrofluorometer. On the bases of previous experiments [97, 98], diallyl disulfide (DADS, Sigma-Aldrich) 100 µM was used as slow H₂S-donor reference compound. Six different experiments (n=6) were performed, each carried out in three replicates. The results are expressed as mean±SEM.

β-hexosaminidase (β-HEX) release assay

The β-hexosaminidase (β-HEX) release was detected as a reliable indicator of mast cell degranulation. This assay was carried out on rat basophilic RBL-2H3 cell line. After reaching 80% confluence, RBL-2H3 cells were seeded into a 96-well plate at 37°C at the density of 72000 cells for well and incubated for 24h at 37°C in a humidified 5% CO₂ atmosphere to allow cell attachment. FcεRI-mediated degranulation: RBL-2H3 were sensitized with an overnight anti-dinitrophenylated-human serum albumin (DNP-HSA), IgE treatment (0.50 μg/mL), and subsequently, MEM was replaced with phenol-free DMEM supplemented with 1 mg/mL bovine serum albumin (BSA). Vehicle (DMSO 0.1%), cromolyn (1 mM) - a well-known mast cell stabilizer - and the tested compounds (100 and 300 μM) were incubated for 5 min at 37°C. Cells were then treated with DNP (10 ng/mL) to induce the degranulation. TRITON-X-100 0.1%, was used to cause exhaustive release of β-hexosaminidase (β-HEX) (data not shown). One hour later the degranulation stimuli (DNP), 50 μL of supernatants from each well were collected and added to 50 μL of p-nitrophenyl-N-acetyl-β-D-glucosaminide 1.4 mM in citrate buffer 0.2 M, pH 4.2. The enzymatic reaction was terminated after 1 h by adding 100 μL/well of Trizma solution 0.3 M pH 9.4. The release of β-HEX was measured at 405 nM in a multiplate reader (EnSpire, PerkinElmer, Milan, Italy).

Evaluation of the membrane hyperpolarizing effects on BSMCs

The membrane hyperpolarizing effects were evaluated on BSMCs by spectrofluorometric methods, as already described [96]. BSMCs were cultured up to about 90% confluence and 24 h before the experiment cells were seeded onto a 96-well black plate, clear bottom pre-coated with gelatin 1% (from porcine skin, Sigma Aldrich), at density of 72×10^3 per well. After 24 h to allow cell attachment, the medium was replaced, and cells were incubated for 1 h in the buffer standard (see above) containing the bisoxonol dye bis-(1,3-dibutylbarbituric acid) DiBac4(3) (Sigma Aldrich) 2.5 μM [96]. This membrane potential-sensitive dye DiBac4(3) allowed us to measure the cell membrane potential; in fact, this lipophilic and negatively-charged oxonol dye shuffles between cellular and extracellular fluids in a membrane potential-dependent manner (following the Nernst laws), thus allowing to assess changes in

membrane potential by means of spectrofluorometric recording. An increase of fluorescence, corresponding to an inward flow of the dye, reflects a membrane depolarization; in contrast, a decrease in fluorescence, due to an outward flow of the dye, is linked to membrane hyperpolarization. The spectrofluorometric recording is carried out at excitation and emission wavelengths of 488 and 520 nm, respectively (Multiwells reader, Enspire, PerkinElmer). NS1619 (Sigma-Aldrich) at the concentration of 10 μ M, was used as reference drug since it evokes membrane hyperpolarizing effects with highest potency and efficacy. After the assessment of baseline fluorescence, the tested compounds were added, and the trends of fluorescence was followed for 40 min. The relative fluorescence decrease, linked to hyperpolarizing effects, was recorded every 2.5 min, and was calculated as:

$$(F_t - F_0)/F_0$$

where F_0 is the basal fluorescence before the addition of the tested compounds, and F_t is the fluorescence at time t after their administration. The value corresponding to the maximum hyperpolarizing effect were expressed as % AUC of that induced by NS1619 10 μ M.

Statistical analysis

Data are expressed as arithmetic mean \pm SEM. Statistical analysis of data was carried out using Software GraphPad Prism v5.01. The results were analysed using one-way ANOVA, followed by the Bonferroni's multiple comparison test. Statistical P values less than 0.05 were taken as significant. For the experiments on tissue viability and quantification of cytokine levels, the number of replicates does not allow now to report the significance data and therefore these are only preliminary data.

6. Results and Discussion

Triamcinolone acetonide, Betamethasone 17-valerate, Acitretin and Tazarotenic acid hybrid derivatives have been tested at the Department of Pharmacy – University of Pisa, by the research group of Professor Vincenzo Calderone, and at Department of Pharmacology – University of San Paolo in Brazil, by research group of Professor Marcelo Muscarà. In addition, a study of molecular modelling has been performed by Professor Caterina Fattorusso at the Department of Pharmacy – University of Naples Federico II.

At the present, only findings about steroidal anti-inflammatory H₂S-releasing hybrids are available due to the reduction in activity related to COVID-19, and the difficulties and costs behind working with animals for screening assays. However, the studies on retinoids derivatives are ongoing.

The compounds **I-VIII** have been evaluated *in vitro* for their H₂S releasing properties via amperometric assay by the research group of Professor Vincenzo Calderone. Moreover, the same research group have performed experiments on tissue viability and determination of cytokine levels, because of involvement of proinflammatory mediators at different stages of the disease [18].

Different H₂S releasing properties for the two glucocorticoid molecular hybrids with the isothiocyanate moiety have been investigated by Professor Caterina Fattorusso through computer aided Structure-Activity Relationship studies demonstrating that the steric accessibility of the isothiocyanate moiety is crucial for this effect.

Following, *in vivo* screening on two of Triamcinolone acetonide hybrid derivatives have been performed by research group of Professor Marcelo Muscarà. The comparative effects of topical administration of Triamcinolone acetonide-HBTA and Triamcinolone acetonide-TBZ vs Triamcinolone acetonide have been investigated in a mouse model of psoriasis. Compounds have been evaluated for their antipsoriatic activity and the obtained scientific evidence have been: Psoriasis Area Severity Index (PASI), as degree of skin inflammation on the back of the animals; skin thickness, based on a daily measurement of ear thickness; itch behaviour; quantification of splenocytes.

Finally, since glucocorticoids represent the first-line treatment of inflammation in asthmatic patients [99-101] and H₂S has been described to exert positive effect on this

disease, because of the interest of Genetic s.p.a. towards respiratory diseases, H₂S-releasing glucocorticoids have been also tested for their anti-asthmatic properties by research group of Professor Vincenzo Calderone. In particular, synthesized compounds have been evaluated for the potential H₂S-releasing profile in the cytosol of bronchial smooth muscle cells (BSMCs), for inhibitory effect on mast cell degranulation and for the ability to induce cell membrane hyperpolarization in BSMCs.

6.1. Amperometric evaluation of H₂S releasing properties

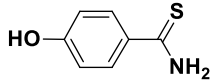
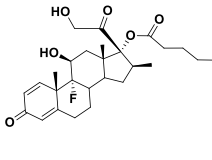
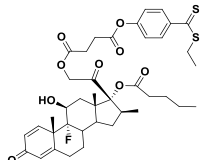
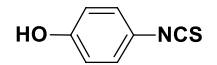
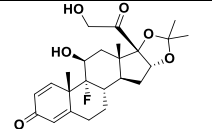
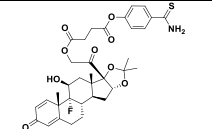
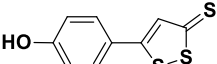
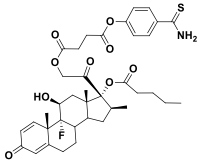
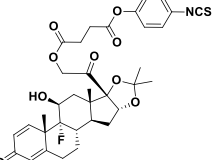
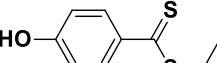
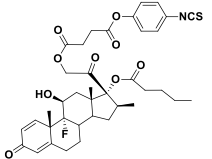
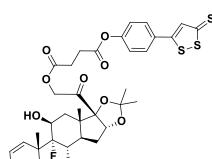
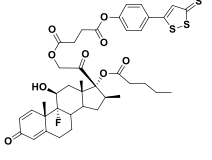
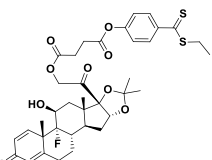
The H₂S-release of the H₂S-donor moieties and the novel synthesized hybrid molecules were investigated in vitro by an amperometric assay in the absence of biological substrates. This approach allows to obtain a peculiar description of the H₂S-releasing process thanks to a real-time assessment of the H₂S release. In Table 3 are reported the data of the highest amount of H₂S reached in the recording time of 30 min (C_{max}) from the tested compounds 100 μM in the different experimental conditions (in the absence (– L-Cys) or in the presence (+ L-Cys) of an excess of L-cysteine (4 mM) that was added to mimic the endogenous presence of free thiols). Generally, in the absence of L-Cys very low H₂S release has been recorded for all the tested compounds, confirming the H₂S-releasing feature showed by other H₂S-donors described in the literature [102,103]. In the absence of L-Cys, the H₂S generation from the hybrid drugs was almost negligible, while the H₂S-donor moieties showed low but clear release of H₂S. The presence of an excess of L-Cys (4 mM) increased the H₂S generation from almost all the tested molecules. Comparing the results obtained for the two different series of derivatives, we evidenced that when TBZ was used as H₂S-donor the amount of produced gasotransmitter was equivalent (2.0 ± 0.3 vs 1.9 ± 0.4 for **I** and **V**, respectively). Generally, with all the other H₂S-donor moieties we noticed a better releasing profile in the series of the hybrids obtained from Triamcinolone acetonide and the best result was obtained with compound **VI** with a value of 2.8 ± 0.6 μM. Taken together, these data indicate that, in the presence of organic thiols (L-Cys), most of the tested compounds behaved as H₂S donors, albeit with different features in the quantitative aspects that can be related to their chemical structures.

The differences evidenced between the two series of hybrids have been investigated by computer aided structure activity relationship studies that suggest how the less flexible acetal substituent of positions 16 and 17 in triamcinolone acetonide, in comparison to the more flexible alkyl chain of betamethasone 17-valerate, influences the interactions of L-Cys with the H₂S donor moieties.

The L-Cys mediated effects caused progressive and time-related “slow” H₂S releasing profiles from almost all the compounds. The graphics showing the H₂S-kinetic release for each compound incubated in the presence or in the absence of L-Cys are reported in Figure 17.

Noteworthy, the pharmacological effect of H₂S-releasing molecules is not directly related only with the quantity of the H₂S donation because, even small, a low but long-lasting H₂S generation can exert beneficial effects. This has been reported for slow H₂S-donors, such as isothiocyanates and some aryl-thioamides and other H₂S-donors [104, 105]. In particular, the effects of H₂S-releasing molecules on inflammatory response are clearly modulated by the rate of the H₂S release [106].

Table 3. H₂S-releasing rate: values of C_{max} of H₂S-release obtained with H₂S-donors, with parent drugs and with hybrids **I-VIII** (100 μM), recorded in the absence (-L-Cys) or in the presence (+L-Cys) of an excess of L-Cysteine (4 mM). Data are expressed as means ± SEM.

Compd.	Structure	H ₂ S release (μM)		Compd.	Structure	H ₂ S release (μM)		Compd.	Structure	H ₂ S release (μM)	
		+L-Cys	--L-Cys			+L-Cys	--L-Cys			+L-Cys	--L-Cys
TBZ		1,6 ± 0,3	0.3 ± 0.1	Betametasone 17-valerate		-	-	IV		0.9 ± 0.2	< 0.1
HPI		1,6 ± 0,2	0.9 ± 0.3	Triamcinolone acetonide		-	-	V		1.9 ± 0.4	< 0.1
ADT-OH		1,8 ± 0,5	1,0 ± 0,3	I		2,0 ± 0,3	< 0.1	VI		2,8 ± 0,6	< 0.1
HBTA		3.5 ± 0.6	0.8 ± 0.3	II		0,4 ± 0,1	< 0.1	VII		0.5 ± 0.2	< 0.1
				III		0,3 ± 0,1	< 0.1	VIII		1.6 ± 0.3	< 0.1

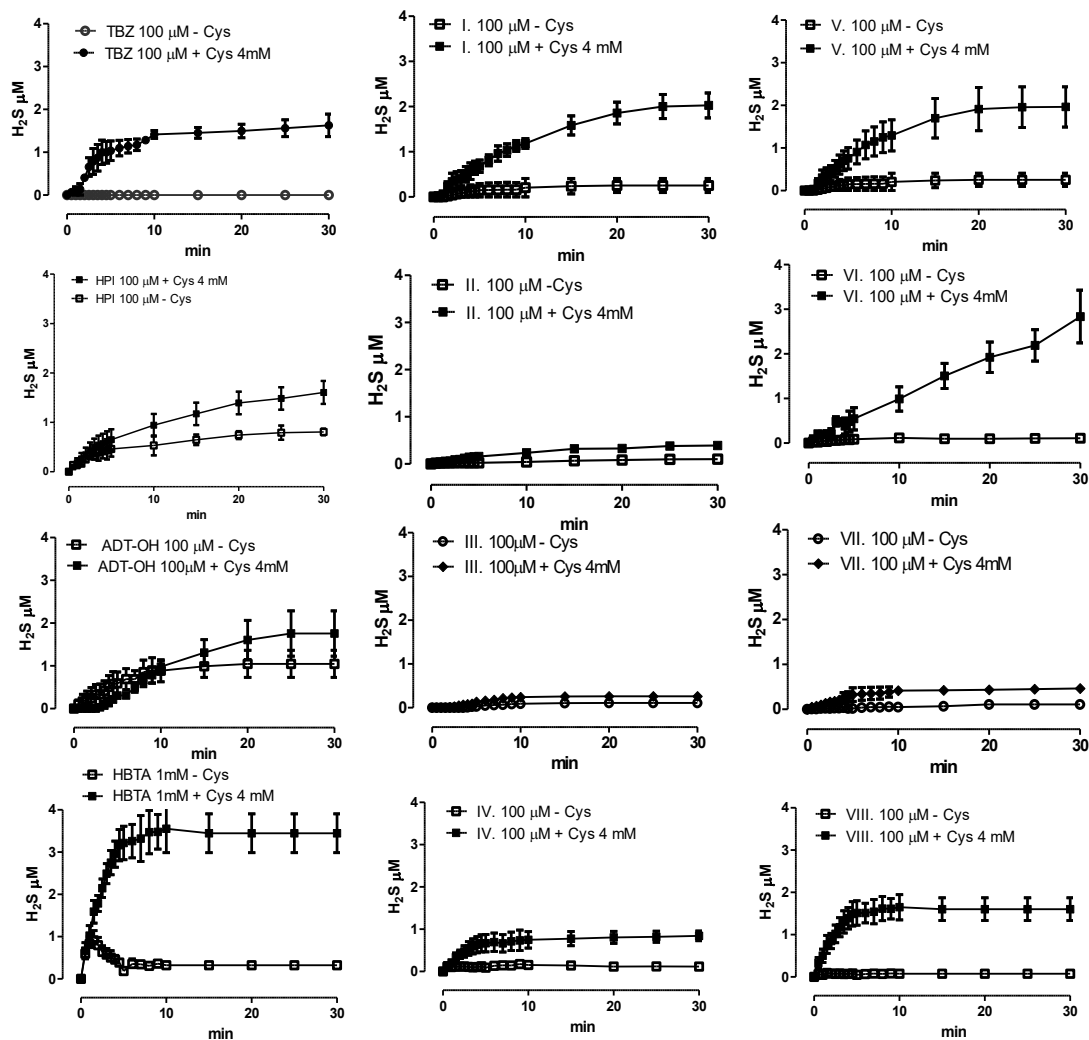


Figure 17. The figure shows the H₂S-kinetic release obtained through the amperometric assay in the presence and in the absence of L-Cys of the “free” H₂S-donor moieties (TBZ, HPI, ADT-OH and HBTA), of the Betamethasone 17 valerate H₂S-donor hybrids (I, II, III, IV) and of the Triamcinolone acetonide H₂S-donor hybrids (V, VI, VII, VIII).

6.2. Computer Aided Structure-Activity Relationship Studies

According to the multistep mechanism proposed by Lin et Al. [107], the carbon atom of the isothiocyanate group undergoes two subsequent nucleophilic attacks upon reaction with L-Cys, the first by the sulphur atom and the second by the nitrogen atom, to finally release H₂S. Thus, we hypothesized that the steric accessibility of the isothiocyanate moiety could be responsible for the different H₂S releasing properties observed for the two hybrids **II** and **VI**, characterized by the presence of the Triamcinolone acetonide and Betamethasone 17-valerate moiety, respectively.

To investigate this issue, **II** and **VI** were firstly subjected to an in depth conformational analysis based on a stochastic search algorithm. This led to the identification of the most probable (i.e., higher occurrence rate) energetically allowed (within 5 kcal/mol from the global minimum conformer) conformational families of each compound (see Experimental section for details). Compound **II** showed six possible orientations of the isothiocyanate group with respect to the glucocorticoid moiety (family i-vi; Table 4), while compound **VI** resulted in fifteen families corresponding to as many orientations of the isothiocyanate group with respect to the glucocorticoid moiety (family i-xv; Table 5). Thus, the steric hindrance caused by the presence of the bulky and flexible valerate chain at position 17 limited the conformational freedom of the isothiocyanate group of **II** with respect to that of **VI**, which presented the smaller and more rigid 16,17-cyclic acetal substituents.

Table 4. Compound **II** conformational families within 5 kcal/mol from the global minimum energy conformer (GM). ΔE_{GM} values (kcal/mol), occurrence rates, and SASA decrease values of the isothiocyanate carbon atom.

Family	ΔE_{GM}^a (kcal/mol)	Occurrence Rate (%)	SASA decrease (%)
i	0.00-4.21	15	38
ii	2.17-4.72	39	27
iii	3.02-4.38	8	4
iv	3.03-4.40	15	37
v	3.20-4.56	19	4
vi	4.42	4	4

^aThe values reported refer to the lowest and the highest energy conformers of the family.

Table 5. Compound VI conformational families within 5 kcal/mol from the global minimum energy conformer (GM). ΔE_{GM} values (kcal/mol), occurrence rates, and SASA decrease values of the isothiocyanate carbon atom.

Family	ΔE_{GM}^a (kcal/mol)	Occurrence Rate (%)	SASA decrease (%)
i	0.00-1.02	2	36
ii	0.72-4.91	9	7
iii	0.75-4.85	10	14
iv	0.97-3.62	10	22
v	1.17	1	5
vi	1.58	1	5
vii	1.78-4.25	10	4
viii	1.87-4.62	6	5
ix	1.94-4.55	11	3
x	2.56-4.83	9	4
xi	2.99-4.40	2	2
xii	3.07-4.68	7	0
xiii	3.07-4.80	6	40
xiv	3.16-4.99	10	4
xv	4.15-4.94	6	3

^aThe values reported refer to the lowest and the highest energy conformers of the family.

Then, we calculated the solvent accessible surface area (SASA) of the isothiocyanate carbon atom in the energetically allowed conformational families of compounds II and VI. The resulting SASA values were compared with the maximum SASA value calculated for the isothiocyanate carbon atom (full accessibility; Figure 18) and accordingly reported as SASA decrease percentage (Table 4 and Table 5).

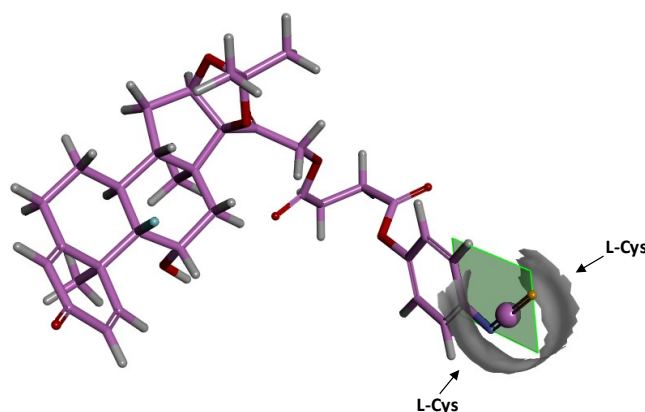


Figure 18. Compound VI lowest energy conformer of the conformational family xii characterized by the highest calculated solvent accessible surface area (SASA) of the isothiocyanate carbon atom (15.2 \AA^2). The SASA is shown as grey surface. The plane of the isothiocyanate group is displayed and coloured in green. The isothiocyanate carbon atom is evidenced as ball. The compound is coloured by atom type (C: pink, O: red, N: blue, S: yellow and H: white). Black arrows indicate the putative L-Cys approach from both sides of the double bond plane.

A SASA decrease higher than 25% corresponded to conformational families characterized by the steric inaccessibility of the isothiocyanate carbon from at least one side of the double bond (Figure 19A). The most populated conformational family of compound **II** (i.e., family ii; occurrence rate: 39%) presented a reduced steric accessibility of the isothiocyanate carbon (i.e., SASA decrease = 27%; Figure 19A) while that of **VI** presented only 3% of SASA decrease (i.e., family ix; occurrence rate: 11%; Figure 19B).

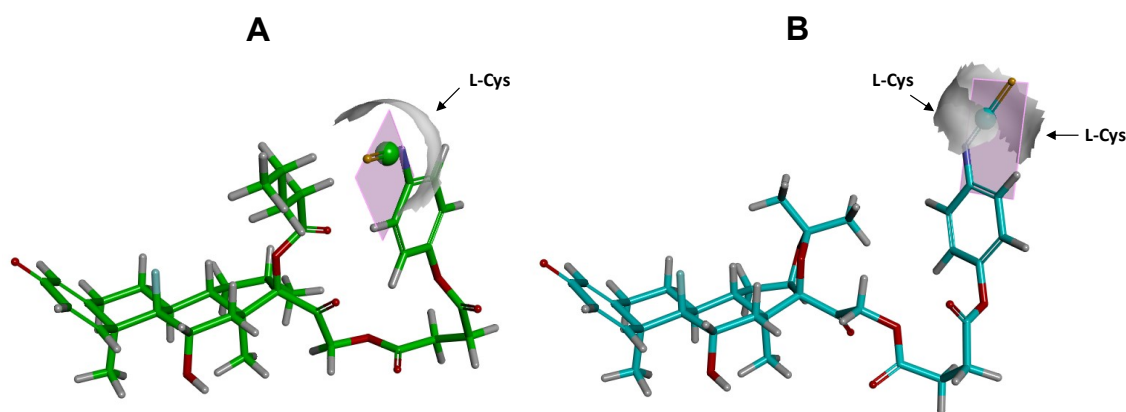


Figure 19. Lowest energy conformers of the most populated conformational families of compound **II** (green, A; SASA decrease = 27%) and **VI** (cyan, B; SASA decrease = 3%). The calculated solvent accessible surface area (SASA) of the isothiocyanate carbon atom is shown as grey transparent surface. The plane of the isothiocyanate group is displayed and coloured in pink. The isothiocyanate carbon atom is evidenced as ball. The compounds are coloured by atom type (O: red, N: blue, S: yellow and H: white). The putative L-Cys approach from one side (A) or both sides (B) of the double bond plane is indicated by a black arrow.

This trend is confirmed considering all the conformers within 5 kcal/mol from GM. Indeed, compound **II** presented 69% of conformers within 5 kcal/mol from GM with a SASA decrease > 25 % (Table 4). On the contrary, compound **VI** showed 92 % of the conformers within 5 kcal/mol from GM with a SASA decrease for the isothiocyanate carbon atom < 25% (Table 5).

The above results indicate that the substituents at positions 16 and 17 affect both the conformational behaviour and the steric accessibility of the H₂S donor moiety, likely affecting its ability to react with L-Cys. Accordingly, the less hindered hybrids obtained from Triamcinolone acetonide (i.e., **VI-VIII**) resulted to be able to release a greater

amount of H₂S with respect their corresponding hybrids obtained from Betamethasone 17-valerate (i.e., **II-IV**) (Table 3).

On the other hand, the higher ability to release H₂S of compound **VI** with respect to the “free” H₂S donor HPI could be explained considering that H₂S formation rate is dependent on the nature of the substituent bound to the isothiocyanate group and an electron-donating group, such as the hydroxyl group, increases the electronic density on the isothiocyanate group thus reducing its reactivity [107, 108].

6.3. Tissue viability

Tissue viability was measured with the MTT assay. Tissues were topically treated with LPS 5µg/mL and with the tested compounds 1µM for 48h. In addition, tissues were treated with 30 µL vehicle (DMSO 0.05%) for 48h for negative control, while with 30 µL of LPS 5µg/mL for 48h for positive control. Results are reported in Table 6 and graphically summarized in Figure 20.

Table 6. Values of tissue viability on in vitro reconstructed human epidermis.

	Viability value (mean OD ± SEM)
Vehicle 0,05%	100,00 ±5,19
LPS 5µg/µL	87,52 ±1,30
LPS 5µg/mL + BMV 1µM	76,55 ±2,20
LPS 5µg/mL + I 1µM	95,78 ±5,40
LPS 5µg/mL + II 1µM	84,63 ±7,58
LPS 5µg/mL + III 1µM	83,07 ±3,38
LPS 5µg/mL + IV 1µM	83,25 ±4,16
LPS 5µg/mL + TAA 1µM	98,25 ±3,58
LPS 5µg/mL + V 1µM	90,24 ±3,17
LPS 5µg/mL + VI 1µM	112,03 ±1,23
LPS 5µg/mL + VII 1µM	101,57 ±4,68
LPS 5µg/mL + VIII 1µM	103,33 ±4,27
LPS 5µg/mL + TBZ 1µM	81,58 ±9,00
LPS 5µg/mL + HPI 1µM	82,14 ±4,32
LPS 5µg/mL + ADT 1µM	99,07 ±4,35
LPS 5µg/mL + HBTA 1µM	94,85 ±4,09

The evidence suggests that LPS caused a slight reduction in viability of about 13%. Although all compounds did not show significant toxicity since the viability was always greater than 50%. Betamethasone 17-valerate and its derivatives, with the only exception of the TBZ hybrid (95,78±5,40), did not show an excellent cytoprotective activity, in fact the viability values are comparable to those obtained with LPS. On the other hand, Triamcinolone acetonide and its derivatives proved to have a cytoprotective activity, although not significance. Furthermore, the derivative with HPI moiety showed greater cytoprotective activity in comparison to either Triamcinolone acetonide and HPI moiety tested alone.

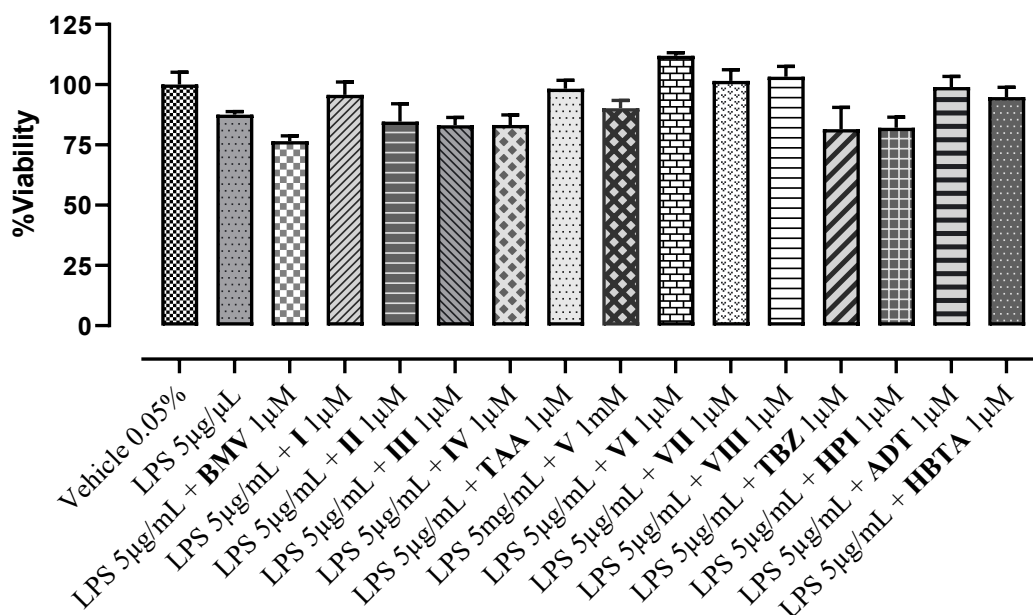


Figure 20. Tissue viability.

6.4. Determination of cytokine levels

Psoriasis is an immune-mediated inflammatory skin disease and due to the involvement of proinflammatory mediators at different stages of the disease [18], the anti-inflammatory activity of the compounds was evaluated. $TNF\alpha$, IL-6 and IL-1 beta are the most involved cytokines in the pro-inflammatory response following LPS treatment. The quantification of $TNF\alpha$, IL-6 and IL-1 beta has been performed by using ELISA

sandwich assay, with a culture medium collected in sterile tube and stored at – 80 °C in 200 µL aliquots.

LPS promoted the production of TNF α , a not very significant response on the release of IL-6, and a massive production of IL-1 beta (Table 7). The results of ELISA assay are reported in Table 7.

Table 7. Results of enzyme-Linked Immunosorbent Assay (ELISA) for TNF α , IL-6 and IL-1 beta measurement.

	TNF α (pg/mL)	IL-6 (pg/mL)	IL-1beta (pg/mL)
Vehicle 0,05%	8,33±0,28	2,70±0,17	10,27±0,14
LPS 5µg/µl	10,60±0,83	3,12±0,25	17,76±2,78
LPS 5µg/ml + BMV 1µM	10,85±0,20	2,97±0,40	14,51±0,11
LPS 5µg/ml + I 1µM	9,66±0,27	2,11±0,16	15,37±1,64
LPS 5µg/ml + II 1µM	9,42±0,90	2,54±0,08	15,58±1,25
LPS 5µg/ml + III 1µM	10,21±1,52	3,45±0,23	17,88±0,93
LPS 5µg/ml + IV 1µM	11,73±2,44	3,22±0,33	17,26±1,65
LPS 5µg/ml + TAA 1µM	8,11±0,74	2,59±0,57	11,44±0,31
LPS 5µg/ml + V 1µM	6,82±0,31	1,62±0,14	11,34±0,32
LPS 5µg/ml + VI 1µM	7,16±0,83	1,45±0,09	11,42±0,37
LPS 5µg/ml + VII 1µM	7,33±0,70	2,44±0,04	13,56±1,05
LPS 5µg/ml + VIII 1µM	8,10±0,31	2,97±0,12	11,05±0,61
LPS 5µg/ml + TBZ 1µM	8,31±1,08	2,08±0,15	11,91±0,57
LPS 5µg/ml + HPI 1µM	6,67±0,20	2,01±0,07	11,67±0,46
LPS 5µg/ml + ADT 1µM	7,61±0,61	1,73±0,27	12,20±0,37
LPS 5µg/ml + HBTA 1µM	8,80±1,43	1,70±0,37	11,67±0,30

As shown in Figure 21, Betamethasone 17-valerate and its derivatives were not effective in decreasing TNF α levels, while Triamcinolone acetonide and its derivatives limited TNF α production and resulted to be the most promising compounds. Triamcinolone acetonide-HPI (VI) and Triamcinolone acetonide-TBZ (V) were the most active with TNF α values of 7,16±0,83 pg/mL and 6,82±0,31 pg/mL, respectively. However, the HPI moiety promoted a greater anti-inflammatory response when incubated alone (6,67±0,20 pg/mL), whereas the TBZ moiety (8,31±1,08 pg/mL) was less active than the hybrid compound Triamcinolone acetonide-TBZ (V).

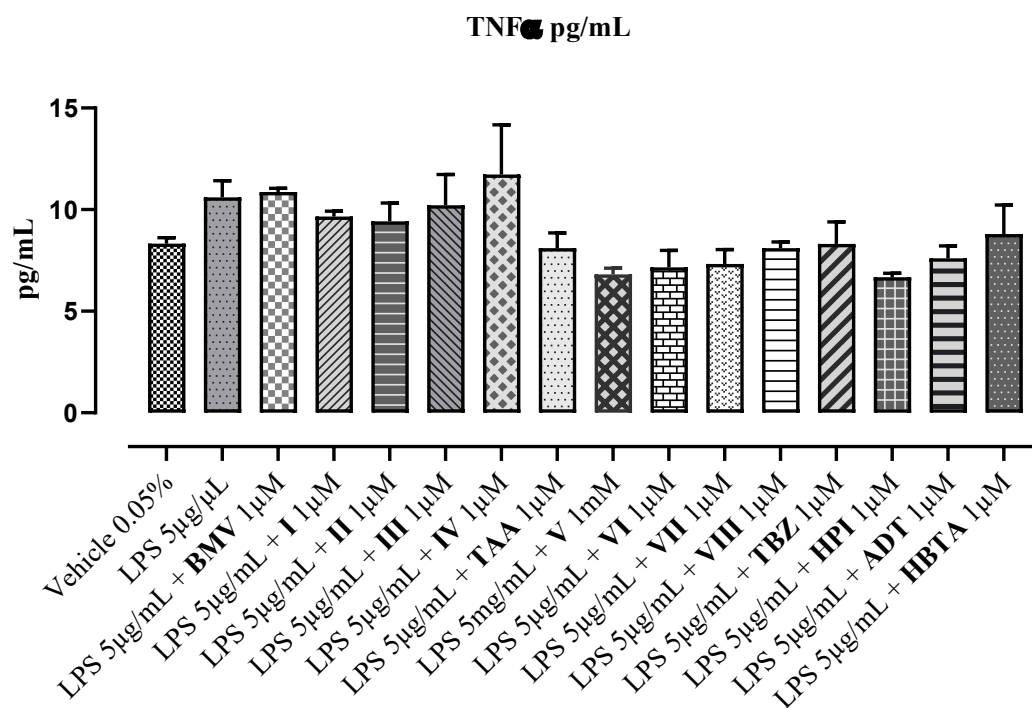


Figure 21. ELISA sandwich assay: TNF α levels and effect of compounds I-VIII.

Figure 22 shows a slightly higher LPS value in producing IL-6 than the control. However, the anti-inflammatory activity of some compounds is appreciable.

Among Betamethasone 17-valerate derivatives, the hybrid with TBZ moiety (**I**) was the most active ($2,11 \pm 0,16$ pg/mL), while for the Triamcinolone acetonide series we found again the TBZ and HPI hybrids (compounds **V** and **VI**) as the most active compounds ($1,62 \pm 0,14$ pg/mL and $1,45 \pm 0,09$, respectively). Moreover, the H₂S-donor moieties exerted an appreciable anti-inflammatory activity, comparable to the most active hybrid derivatives.

As shown in Figure 23, Betamethasone 17-valerate and its derivatives showed a moderate effect on the IL-1 beta production. In line with the other results, Triamcinolone acetonide and its hybrid derivatives were instead the most promising as they showed a substantial reduction of IL-1 beta production. In this case, it was not possible to identify the "best" compound, as all data are comparable. To confirm the above results, also in this case the H₂S-donor moieties showed an anti-inflammatory effect almost similar to the Triamcinolone acetonide hybrid derivatives.

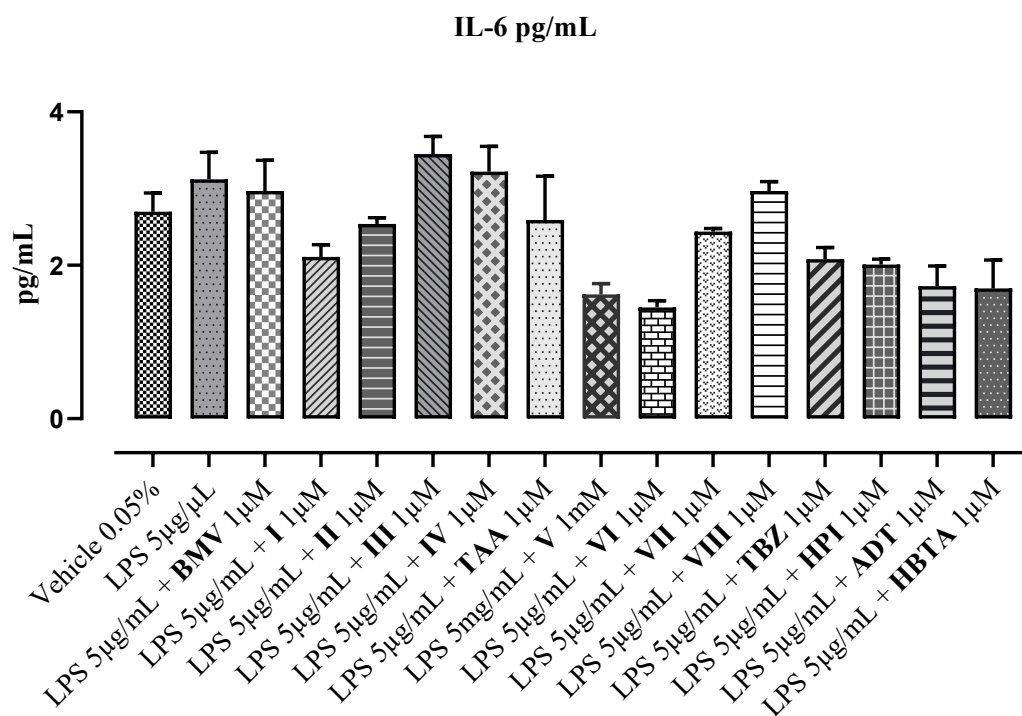


Figure 22. ELISA sandwich assay: IL-6 levels and effect of compounds I-VIII.

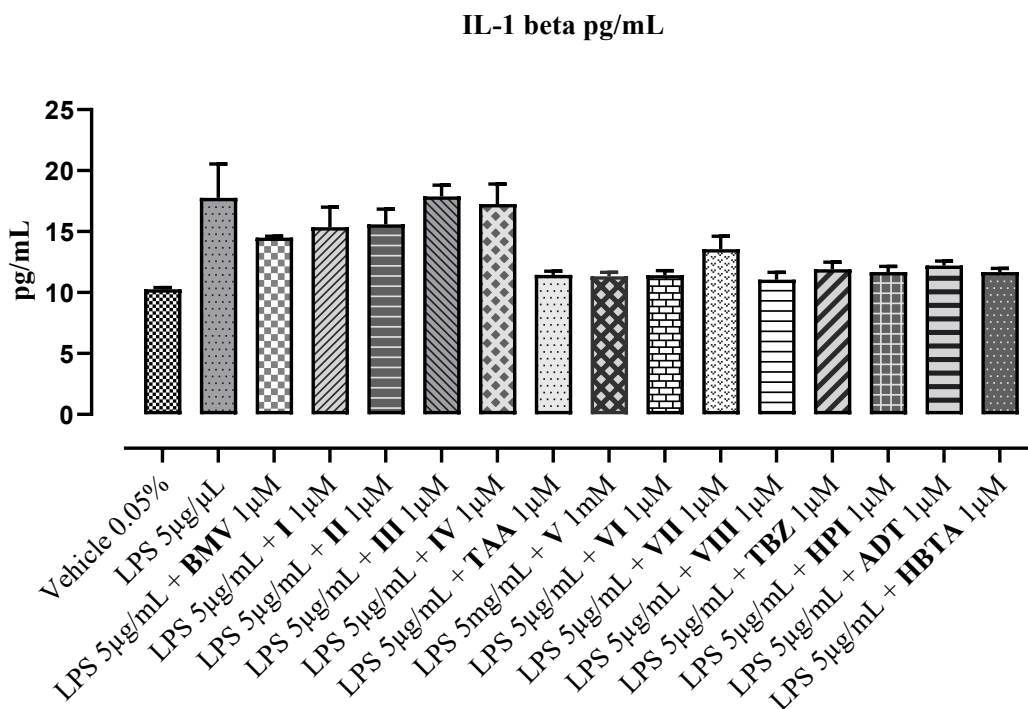


Figure 23. ELISA sandwich assay: IL-1 beta levels and effect of compounds I-VIII.

6.5. PASI score and skin thickness

Daily application of IMQ (65 mg) resulted in a significant and time-dependent increase of erythema, skin scaling and skin thickness ($P < 0.05$ - $P < 0.001$), compared to the control group (vaseline), as shown in Figure 24 (A-F). The co-treatment with 1% Triamcinolone acetonide-TBZ (V) and Triamcinolone acetonide-HBTA (VIII) nanodispersion, applied once a day, significantly ($P < 0.01$) reduced erythema and desquamation or acanthosis (ears thickness), as analyzed as area under the curve (AUC). Likewise, 1% Triamcinolone acetonide-HBTA (VIII) and Triamcinolone acetonide, but not Triamcinolone acetonide-TBZ (V) nanodispersion treatment, applied once a day, evoked a significant reduction ($P < 0.01$) of skin scaling (Figure 24 B, E).

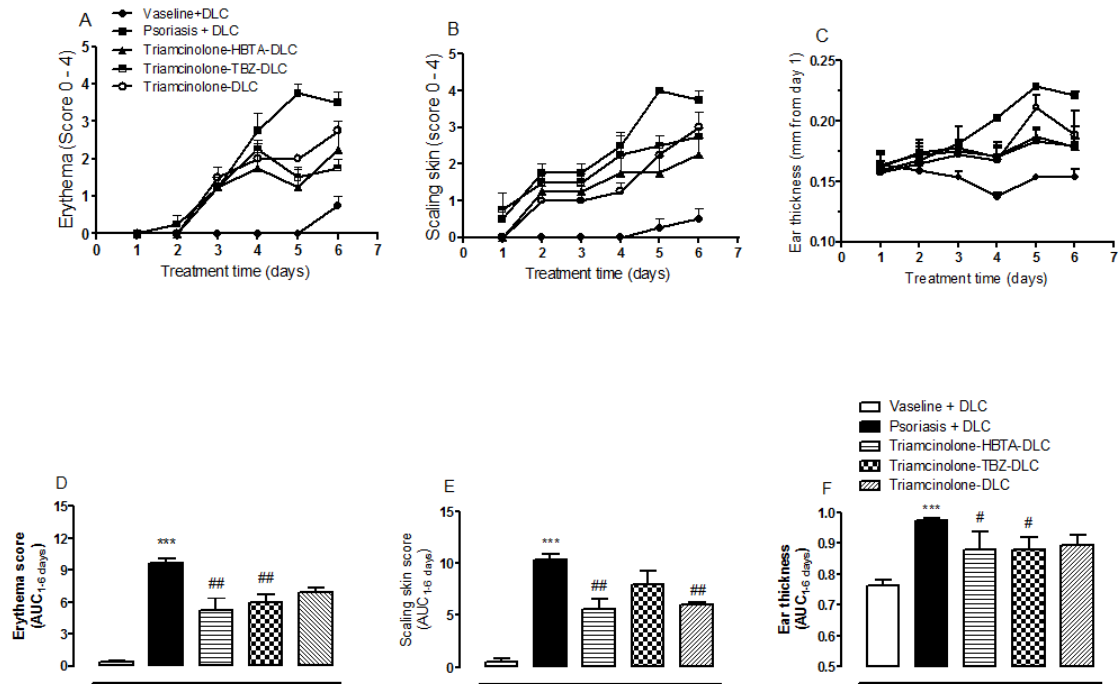


Figure 24. Topical application effect of DLC formulation containing triamcinolone in the PASI score. The clinical signs (erythema, scales and ear thickness) were evaluated once a day, for 6 days, considering the scores ranging from 0-4 (0 = nothing; 1 = slight; 2 = moderate; 3 intense; 4 = very intense). Panels A, B and C indicate the temporal evolution of the erythema, scales, and ear thickness scores, respectively. The bars in the graphs D, E and F show the area under curve (AUC) values corresponding to the respective absolute values of scores obtained in panels A, B and C. *** $P < 0.001$ vs. Control (vaseline) and # $P < 0.05$ -## $P < 0.01$ vs. psoriasis for $n = 4$ /group. Stats were performed via one-way ANOVA followed by Bonferroni's multiple comparison test.

In the last day of evaluation (6th), Figure 25A-C shows that treatment with 1% Triamcinolone acetonide-TBZ (V) and Triamcinolone acetonide-HBTA (VIII) nanodispersion, rather than Triamcinolone acetonide itself, was able to reduce most of psoriasis scores ($P < 0.05$ - $P < 0.001$).

However, daily treatment with 1% Triamcinolone acetonide-TBZ (V) and triamcinolone acetonide-HBTA (VIII) nanodispersion were slightly more effective to reduce PASI score than Triamcinolone acetonide.

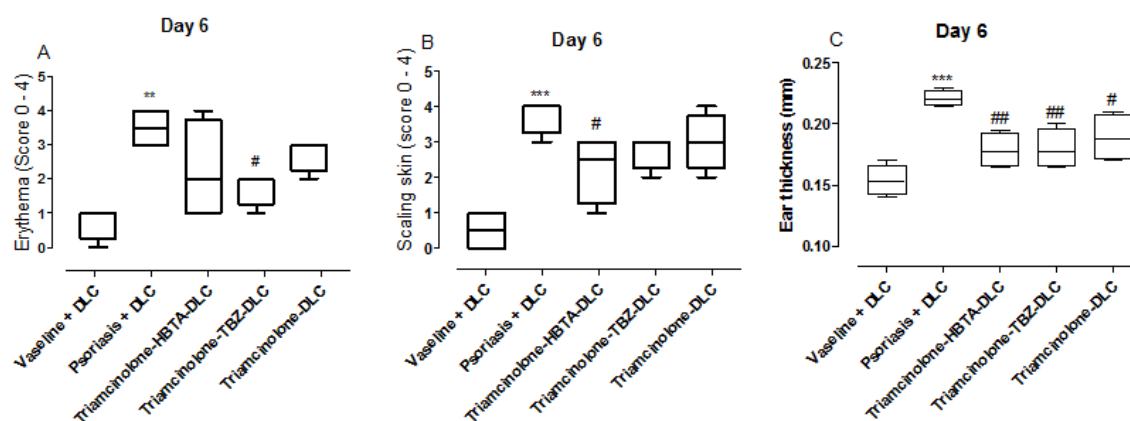


Figure 25. DLC formulation containing triamcinolone-HBTA and TBZ ameliorates PASI score in a murine model of psoriasis. The clinical signs (erythema, scales and ear thickness) were evaluated once a day, for 6 days, considering the scores ranging from 0-4 (0 = nothing; 1 = slight; 2 = moderate; 3 intense; 4 = very intense). Panels A, B and C indicate the evolution of the erythema, scales, and ear thickness scores, respectively, in the last day of analysis (6th day). *** $P < 0.001$ vs. Control (vaseline) and # $P < 0.05$ - ## $P < 0.01$ vs. psoriasis for $n = 4$ /group. Stats were performed via one-way ANOVA followed by Bonferroni's multiple comparison test.

6.6. Itch behaviour

The induction of experimental psoriasis with IMQ promoted increase in itching behaviour. Topical treatment of the animals with 65 mg nanodispersion containing the Triamcinolone acetonide-TBZ (V), Triamcinolone acetonide-HBTA (VIII) or corresponding Triamcinolone acetonide molecule reference, at 1%, when applied once a day, did not affect pruritus behaviour in mice with psoriasis (Figure 26). In particular, treatment with Triamcinolone acetonide-HBTA (VIII) or Triamcinolone acetonide (but not Triamcinolone acetonide-TBZ, V) significantly reduces total bouts of scratching.

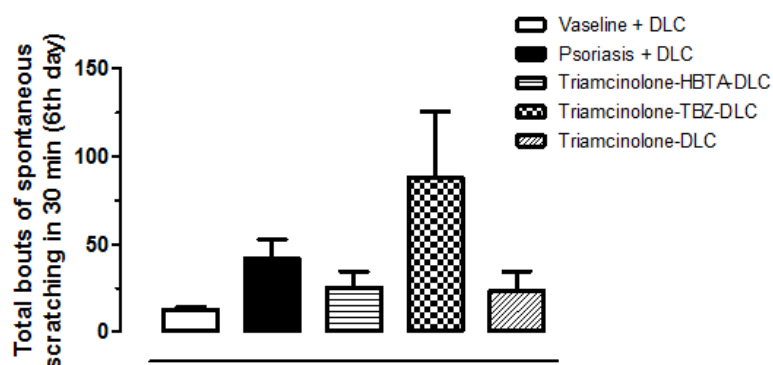


Figure 26. Episodes of spontaneous scratching bouts over 30 minutes in the last day experiment (6th).

6.7. Quantification of splenocytes

Mice with experimental psoriasis exhibited a significant increase in splenocytes number when compared to control (vaseline). When applied once daily, the topical treatment of animals with 65 mg nanodispersion (DLC) containing 1% Triamcinolone acetonide-HBTA (VIII), but not Triamcinolone acetonide-TBZ hybrid molecule (V) or Triamcinolone acetonide alone, significantly reduced the total number of splenocytes in mice with psoriasis (Figure 27).

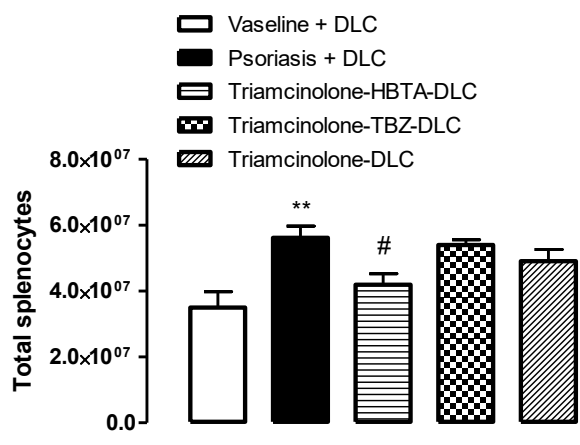


Figure 27. Effect of DLC containing Triamcinolone acetonide and its tested hybrids on the total number of splenocytes. Bars indicate the total number of splenocytes in different animal groups on day 6. **P < 0.01 vs. Control (vaseline) and #P < 0.05 vs. psoriasis for n = 4/group. Stats were performed via one-way ANOVA followed by Bonferroni's multiple comparison test.

6.8. In vitro studies of H₂S-releasing glucocorticoids anti-asthmatic properties

Intracellular H₂S release in BSMC

The amperometric assay aims at defining the profile of potential H₂S release compounds, showing that many of sulfur compounds may be considered as “smart” donors: they are H₂S-releasing molecules in biological environments as the intracellular compartment where they can react with endogenous organic thiols, but they are relatively stable in water and do not release H₂S. However, the amperometric assay was performed only in buffered aqueous solution in the presence and in the absence of L-Cys. Therefore, considering the interest of Genetic s.p.a. towards respiratory diseases, H₂S-releasing glucocorticoids have been also tested in a fluorometric assay using bronchial smooth muscle cells (BSMCs), without the addition of exogenous thiols, for demonstrating that these compounds are able to release H₂S if added to biological substrates. The intracellular H₂S release was detected using the dye WSP-1, which selectively and irreversibly reacts with H₂S. BSMCs have been chosen because they represent an *in vitro* reliable model for the evaluation of the activity of the bronchial muscle. Spectrofluorometric recordings showed that the addition of the vehicle caused a slight increase of fluorescence index (FI), probably due to endogenous production of H₂S. In contrast, the addition of DADS (diallyl disulfide, reference H₂S-donor) to BSMCs preloaded with the fluorescent dye WSP-1 led to a significant increase of fluorescence (FI, fluorescence index), indicating a clear significant formation of H₂S (P < 0.01 vs vehicle).

Results obtained with “free” H₂S-donors are reported for comparison both in Figures 28 and 29: the addition of ADT-OH 100 μM and 300 μM and TBZ 100 μM to WSP1-preloaded BSMCs led to a slight and not significant increase of FI. Increasing concentration of TBZ (300 μM), led to a significant increase in FI even higher if compared to the reference compound DADS. HPI showed a massive increase in H₂S intracellular donation when incubated 100 μM and 300 μM.

The intracellular H₂S release profiles following the incubation of Betamethasone 17-valerate hybrids are reported in Figure 28. Compound **I** 100 μM and 300 μM promoted a mild but significant H₂S release; compound **II** 100 μM and 300 μM when incubated

into BSMCs led to appreciable H₂S intracellular release, while **III** 100 and 300 μM did not cause any significant increase of fluorescence.

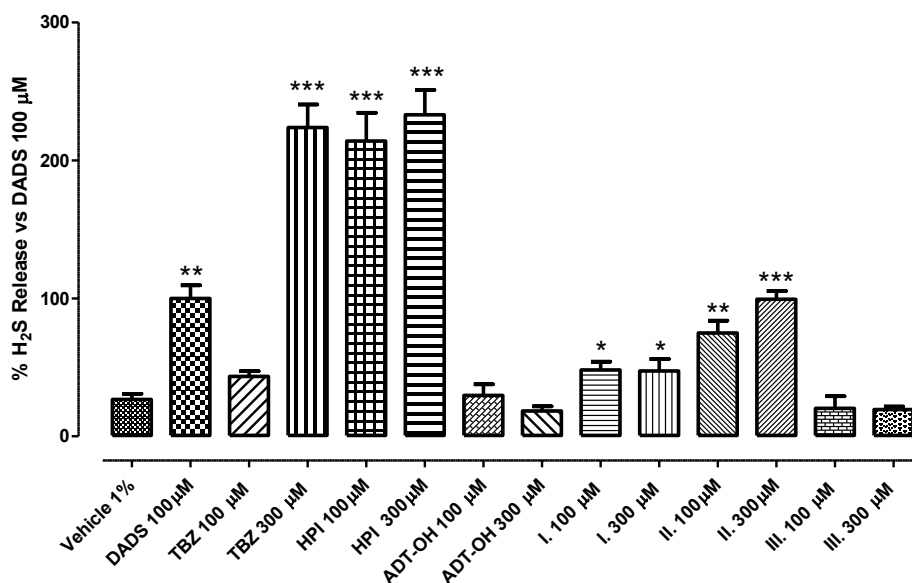


Figure 28. Cumulative H₂S formation (expressed as area under the curve of the WSP-1 fluorescence in the recording time) produced by the incubation of vehicle or different concentrations of the tested compounds: DADS (100 μM), “free” H₂S-donors and compounds **I-III**. Data were expressed as mean ± SEM setting DADS H₂S release as 100%. Three different experiments were carried out, each in triplicate. One-way ANOVA post-test Bonferroni has been applied to calculate the significance level. (* P < 0.05; ** P < 0.01; *** P < 0.001).

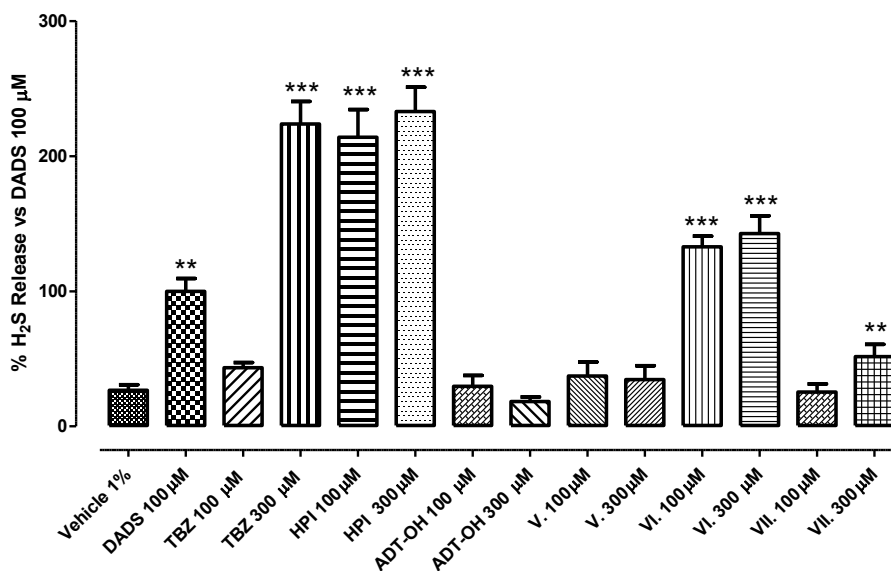


Figure 29. Cumulative H₂S formation (expressed as area under the curve of the WSP-1 fluorescence in the recording time) produced by the incubation of vehicle or different concentrations of the tested compounds: DADS (100 μM), “free” H₂S-donors and compounds **V-VII**. Data were expressed as mean ± SEM setting DADS H₂S release as 100%. Three different experiments were carried out, each in triplicate. One-way ANOVA post-test Bonferroni has been applied to calculate the significance level. (** P < 0.01; *** P < 0.001).

Figure 29 shows the results about the intracellular H₂S release after the incubation of Triamcinolone acetonide hybrids. The incubation of compounds **V** 100 μM and 300 μM and compound **VII** 100 μM did not cause any significant increase of fluorescence, while **VII** 300 μM promoted only a mild increase in fluorescence index. The incubation of **VI** 100 and 300 μM both evoked a significant increase in the intracellular level of H₂S, even higher if compared to DADS.

Generally, the addition of the moieties to the native corticosteroid drugs led to different H₂S-profiles. In particular, the moieties TBZ and HPI, except for ADT-OH which was not able to release H₂S into the cytosol of BSMCs, led to a massive H₂S release. The corresponding corticosteroid derivatives, both Betamethasone 17-valerate and Triamcinolone acetonide ones, showed a weaker H₂S-donor profile. This is probably due to the different lipophilicity/solubility which influence the capacity of the compounds to enter the cells and exert the H₂S donation.

Looking at the results obtained on the intracellular H₂S-releasing rate, the “best” compounds resulted to be the HPI-derivatives. Indeed, both the single moiety HPI and the compounds **II** and **VI** showed the most promising H₂S donating profiles since they are able enter the cells, react with the endogenous thiols (mainly L-Cys and glutathione) and lead to appreciable H₂S increasing levels. Isothiocyanates represent a promising H₂S-donor moiety, as shown in our previous works, and the specific mechanism leading to H₂S release in the presence of L-Cys has been described by Lin and colleagues [107, 108]. Such a mechanism is driven by a nucleophilic attack by the cysteine thiol group on the isothiocyanate moiety central carbon, leading to an ITC-cysteine adduct, facilitating the release of H₂S. It has been confirmed through the computational SAR study that steric accessibility to the isothiocyanate moiety is crucial for H₂S release as we demonstrated for the different H₂S releasing properties observed for the two hybrids **II** and **VI**.

Unfortunately, the moiety HBTA and the corresponding hybrid drugs **IV** and **VIII** have not been fluorometrically tested due to an unexpected reaction with the probe. Indeed, the compounds are intrinsically coloured, and this feature probably interferes with the dye WSP-1 (data not showed). For these molecules therefore the available rate of H₂S release is only that recorded through amperometric evaluation: HBTA demonstrated an impressive capability to produce H₂S in the presence of L-Cys (3.5 μM ±0.6); when this

moiety was bonded with Betamethasone 17-valerate (compound **IV**) or with Triamcinolone acetonide (compound **VIII**) the data obtained were of $0.9\mu\text{M} \pm 0.2$ and $1.6\mu\text{M} \pm 0.3$, respectively. Once again, these results confirmed that less flexible acetalic chain of compound **VIII** allowed a higher H_2S release in comparison to the most flexible chain of compound **IV**.

Inhibition of mast cell degranulation

$\text{Fc}\epsilon\text{RI}$ -receptor activation triggers mast cell degranulation by promoting a tyrosine kinase cascade and interestingly Marino et al [109] showed that H_2S releasing compounds reduce degranulation of RBL-2H3 induced by the incubation of antigens by targeting proteins downstream of the $\text{Fc}\epsilon\text{RI}$ pathway.

Accordingly, we next investigated the inhibitory effects of HPI and of its hybrid compounds **II** and **VI** and the relative native drugs (Betamethasone 17-valerate and Triamcinolone acetonide) in an antigen-mediated mast cell degranulation assay. These compounds have been selected considering their clear and satisfactory ability to donate H_2S inside the cells.

The addition of the antigen DNP-HSA to pre-sensitized RBL-2H3 cells caused a significant degranulation highlighted as β -hexosaminidase release confirming the activation of $\text{Fc}\epsilon\text{RI}$ pathway (Figures 30 and 31). Cromolyn has been chosen as reference compound whose inhibitory effect on mast cell degranulation is well documented in the literature, being a clinically used drug for the treatment of allergic asthma [110]. Indeed, cromolyn stabilizes the mast cell membrane, preventing their degranulation following the antigen-antibody bond and the consequent release of histamine. In DNP-HAS activate RBL-2H3 cells, cromolyn significantly inhibited β -hexosaminidase release by 20%. The treatment with HPI 100 μM and 300 μM promoted a remarkable and impressive inhibition of the RBL-2H3 degranulation induced by DNP-HSA, reducing β -hexosaminidase release by about 75%.

In contrast, Betamethasone 17-valerate (Figure 30) and Triamcinolone acetonide (Figure 31) exhibit only a mild and not significant inhibitory activity on the degranulation induced DNP-HSA if incubated 300 μM . The effect of long-lasting treatment with corticosteroid on mast cell degranulation is related to post-transcriptional

mechanism leading to reduction of the expression of FcεRI on the surface of mast cell membrane as reported by Yamaguchi and colleagues [111]. In the model used in this paper, corticosteroids are incubated 5 min before the antigenic stimulus, probably not enough to promote those intracellular modifications responsible for the pharmacological activity of corticosteroid drugs.

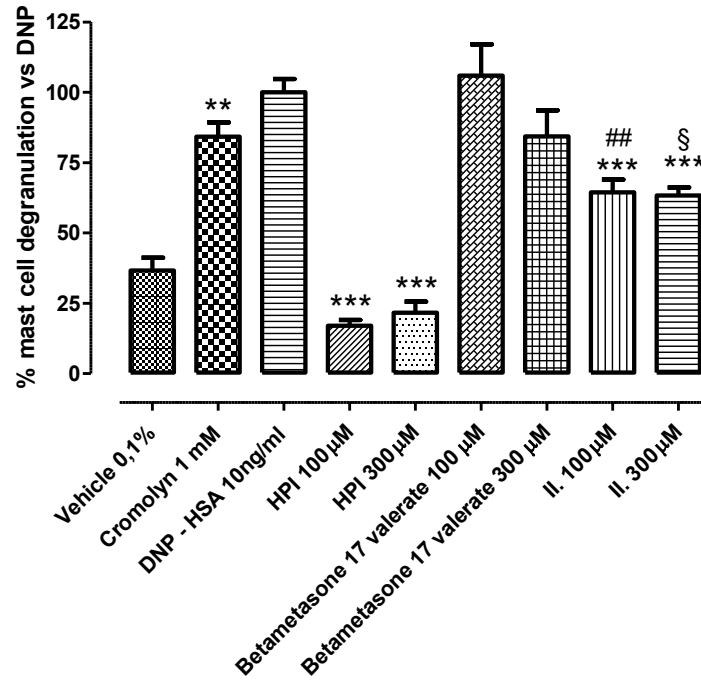


Figure 30. Effect on RBL-2H3 degranulation. Cells were sensitized with DNP-IgE and after 24h incubated for 5 min with the tested compounds, cromolyn (1 mM) or the vehicle (DMSO 0.1%). Cell degranulation was induced by DNP. Triton-X-100 was added, to elicit cell lysis and exhaustive release of β -HEX (data not shown). The release of β -HEX was measured at 405nm. One-way ANOVA plus Bonferroni has been used as statistical analysis. * indicates significant differences vs DNP-HSA setted as 100% (** = $P < 0.01$; *** = $P < 0.001$); § indicates significant differences vs Betametasone 17-valerate 300 μ M (§ = $P < 0.01$); # indicates significant differences vs Betametasone 17-valerate 100 μ M (## = $P < 0.01$).

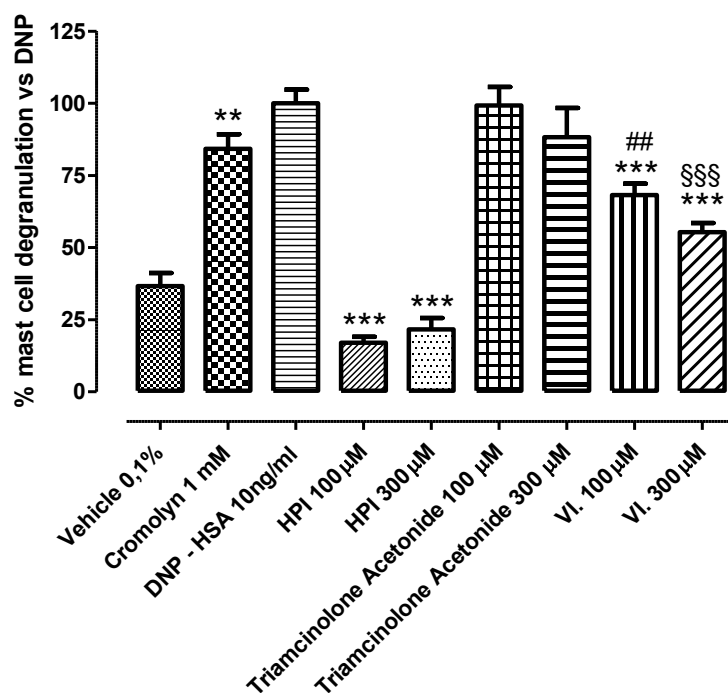


Figure 31. Effect on RBL-2H3 degranulation. Cells were sensitized with DNP-IgE and after 24h incubated for 5 min with the tested compounds, cromolyn (1 mM) or the vehicle (DMSO 0.1%). Cell degranulation was induced by DNP. Triton-X-100 was added, to elicit cell lysis and exhaustive release of β -HEX (data not shown). The release of β -HEX was measured at 405nm. One-way ANOVA plus Bonferroni has been used as statistical analysis. * indicates significant differences vs DNP-HSA setted as 100% (** = $P < 0.01$; *** = $P < 0.001$); § indicates significant differences vs Triamcinolone acetonide 300 μ M (§§§= $P < 0.001$); # indicates significant differences vs Triamcinolone acetonide 100 μ M (## = $P < 0.01$).

Contrarily, the hybrid compounds **II** (Figure 30) and **VI** (Figure 31) of 100 and 300 μ M showed a significant inhibitory effect on mast cell degranulation, resulting to reduce β -hexosaminidase release more efficiently than the corresponding native drugs.

These results suggest that the molecules able to release H_2S (HPI and compounds **II** and **VI**), reduce the activation of Fc ϵ RI receptor directly and rapidly acting on the molecular target, rather than involving intracellular modifications. Merging the H_2S -donor moiety to the corticosteroid drugs could lead to a double time-dependent pharmacodynamic activity: H_2S could promote a fast inhibition of mast cell degranulation since its target it is the already expressed Fc ϵ RI receptor, while the native corticosteroid drug could reduce the expression of the receptor contributing to the lately beneficial effect for the treatment of allergic pathologies.

Bronchial smooth muscle cell membrane hyperpolarizing effect

The relaxant activity of H₂S is mediated by different mechanisms but the activation of bronchial ATP-sensitive potassium (K_{ATP}) channels seems to play a relevant role.

In this view, it was interesting to evaluate the effects of the moiety HPI and of hybrids **II** and **VI** on the membrane potential of cultured BSMCs taking 1,3-dihydro-1-[2-hydroxy-5-(trifluoromethyl)phenyl]-5-(trifluoromethyl)-2H-benzimidazole-2-one (NS1619), a well-known potassium channel activator, as reference hyperpolarizing agent [112]. HPI showed a significant hyperpolarizing effect compared to vehicle but assisting to lower values if compared to the NS1619-induced hyperpolarizing effect. Interestingly, both the hybrid compounds **II** and **VI** tested at 100 and 300 μM caused a significant and massive membrane hyperpolarization of BSMCs (Figure 32) by 4-fold higher compared to NS1619 when incubated at the maximal concentration.

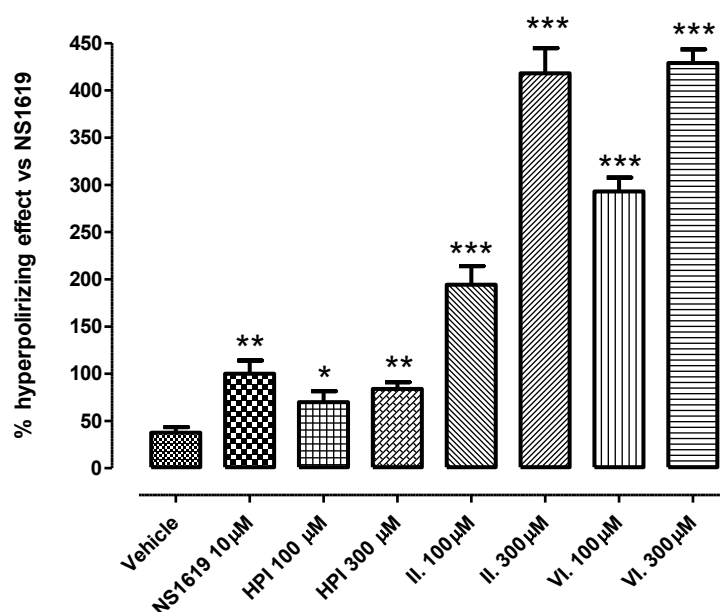


Figure 32. Hyperpolarizing effect of the tested compounds on BSMCs membrane. The graph shows the hyperpolarizing effect of the tested compounds on cell membrane of BSMCs; effects are expressed as % of the hyperpolarization evoked by the reference compound NS1619. Data are expressed as mean ± SEM. Six different experiments were performed each in six replicates. One-way ANOVA post-test Bonferroni has been applied to calculate the significance level (* P < 0.05, ** P < 0.01, *** P < 0.001).

Looking at the results of the intracellular donation of H₂S, the HPI moiety resulted to be a stronger H₂S-donor if compared to the corresponding H₂S-hybrid glucocorticoids. Surprisingly, the results about the hyperpolarizing efficacy followed an opposite trend since the hybrid molecules exerted a more efficient effect. The hypothesis which may explain this marked difference between the hyperpolarizing effect of HPI and both the hybrid derivatives could be addressed to the direct airway relaxant activity of some glucocorticoids. Indeed, Nabishah and colleagues [113] reported that rats treated with either dexamethasone or cortisone for 7 days showed a reduced contractile response of isolated bronchial smooth muscle preparations to acetylcholine. Another research investigated the effect of glucocorticoids changes in intracellular Ca²⁺ concentration in airway smooth muscle cells and demonstrated that 24 h-pretreatment with dexamethasone reduced the subsequent calcium-mobilizing response to bradykinin [114]. Furthermore, Schramm and Grunstein [115] demonstrated that methylprednisolone increases rabbit airway smooth muscle relaxation by potentiating the electrogenic Na⁺/K⁺ ATPase pump.

The tested H₂S-donor hybrid molecules, being made up by the H₂S-donor portion which is able to open different classes of potassium channels and by the “native” corticosteroid drug, may promote a marked hyperpolarizing effect because of these different mechanisms of action.

7. Conclusion

Hybridization of different molecules is a widely exploited strategy in medicinal chemistry and this approach has been reported as an effective strategy in the development of compounds able to modulate multiple targets [116, 117]. My PhD project has focused on novel H₂S-releasing molecular hybrids, containing active pharmacological compounds in psoriasis treatment and H₂S donors. These hybrids have been developed for merging the beneficial effect of H₂S to pharmacological effect of the starting drug.

Bearing in mind the importance of these combined molecules, H₂S-releasing hybrid corticosteroids and retinoids have been synthesized and characterized. The first ones have been tested for their antipsoriatic activity, while the pharmacological evaluation of retinoid derivatives is ongoing.

Triamcinolone acetonide and Betamethasone 17-valerate hybrid derivatives have been evaluated for their ability to release H₂S via amperometric assay, and for their cytoprotective and anti-inflammatory activity through preliminary assay on tissue viability and quantification of cytokine levels. The amperometric assay without biological substrates has evaluated in the absence or in the presence of L-cysteine that was added to mimic the endogenous presence of free thiols. In the absence of L-Cys, the H₂S generation from the hybrid drugs was almost negligible, while the H₂S-donor moieties showed low but clear release of H₂S. In the presence of an organic thiols (L-Cys), most of the tested compounds showed a progressive and time-related slow H₂S releasing profiles. Compounds **I** and **V** produced an amount of gasotransmitter quite equivalent. Triamcinolone acetonide hybrids resulted to be able to release a greater amount of H₂S than Betamethasone 17-valerate hybrids, and compound **VI** gave the best H₂S-releasing profile. These different ability of H₂S release are related to their chemical structures. In fact, the differences evidenced between the two series of hybrids have been investigated by computer aided structure activity relations studies on compounds **II** and **VI** that allow to demonstrate that the less flexible acetal substituent of positions 16 and 17 in Triamcinolone acetonide in comparison to the more flexible and bulky alkyl chain of Betamethasone 17-valerate limited the conformational freedom of the H₂S-releasing group and influenced the interactions of L-Cys with H₂S donor

moiety. On the other hand, the higher ability to release H₂S of compound **VI** than the “free” H₂S donor HPI could be explained considering that H₂S formation rate is dependent on the nature of the substituent bound to the isothiocyanate group and an electron-donating group, such as the hydroxyl group, increases the electronic density on the isothiocyanate group thus reducing its reactivity.

Furthermore, *in vitro* assays have confirmed the superior efficacy of Triamcinolone acetonide hybrid derivatives (**V-VIII**). The MTT assay demonstrated all compounds did not show significant toxicity since the viability was always greater than 50%, but Betamethasone 17-valerate hybrid derivatives did not have an excellent cytoprotective activity except for that with TBZ moiety, while Triamcinolone acetonide derivatives proved to have a cytoprotective activity although not significant, and the hybrid with HPI moiety showed greater cytoprotective activity. The anti-inflammatory activity of the compounds was further evaluated with the cytokine level assays, which showed that compounds **I-IV** were not effective in decreasing TNF α , IL-6 and IL-1 beta levels, except for compound **I** that slightly limited the production of IL-6, although LPS promoted a not very significant response on the release of IL-6. On the other hand, Triamcinolone acetonide derivatives proved to be more effective in limiting the cytokine levels. Compounds **V** and **VI** were the most active in reducing TNF α and IL-6 production, while all Triamcinolone acetonide hybrids (**V-VIII**) showed a comparable and substantial reduction of IL-1 beta production. In addition, H₂S-donor moieties anyway showed an anti-inflammatory effect quite similar to the Triamcinolone acetonide hybrid derivatives. However, these represent only preliminary data, because the replicates number of experiments on tissue viability and quantification of cytokine levels does not allow now to report the significance.

In vivo studies of derivatives **V-VIII** were subsequently performed, investigating the comparative effects of topical administration vs Triamcinolone acetonide in a mouse model of IMQ-induced psoriasis. At the present results are available only for compounds **V** and **VIII**.

The topical treatment with the nanostructured delivery system containing either the hybrids **V** and **VIII** reduced the inflammatory disease index scores (PASI) in comparison to Triamcinolone acetonide or to the untreated group. This beneficial effect

was more marked when the Triamcinolone acetonide-HBTA (**VIII**) was tested. Even in itching behaviour the compound **VIII** resulted active in reducing total bouts of scratching but was not superior to Triamcinolone acetonide alone. Moreover, this hybrid also significantly reduced the total number of splenocytes in mice with psoriasis. Thus, in comparison to Triamcinolone acetonide, the tested hybrids **V** and **VIII** showed only a small and, in some cases, not significant improvement. This not significant additive or synergistic efficacy of synthesized hybrids has been addressed to the already very high efficacy of glucocorticoids at the very low dose adopted. H₂S donors, instead, need higher dosage to ensure their full pharmacological effect. Therefore, both compounds **V** and **VIII**, at the applied dose, did not show superiority of enhanced efficacy when compared to Triamcinolone acetonide in a murine model of psoriasis. It is worthwhile mentioning that the compound doses were calculated with basis on clinical approach. In conclusion we can assert that corticosteroids are so potent and efficient drugs and are generally administered in a dosage that does not fit with the one required by H₂S donors. Therefore, the addition of a unique H₂S-releasing moiety, as done in these hybrids, do not allow to evidence specific pharmacological differences.

Finally, due to the interest of Genetic s.p.a. towards respiratory diseases and the well-known anti-inflammatory pharmacological effect of glucocorticoids in the treatment of asthma in addition to the positive effect of H₂S on the respiratory tract, H₂S-releasing glucocorticoids have been also tested for their anti-asthmatic properties. Synthesized compounds have been evaluated for the potential H₂S-releasing profile in the cytosol of bronchial smooth muscle cells (BSMCs), for inhibitory effect on mast cell degranulation and for the ability to induce cell membrane hyperpolarization in BSMCs. A fluorometric assay has been performed using bronchial smooth muscle cells (BSMCs), without the addition of exogenous thiols for demonstrating that these compounds are able to release H₂S if added to biological substrates. Although all the compounds showed appreciable H₂S-releasing properties in the presence biological substrates, some differences regarding the amount of the generation of H₂S emerged. The most active compounds resulted to be the HPI-derivatives. The reason should be addressed to the different spatial conformation as shown in molecular modelling study. Asthma symptoms are often related to a massive mast cell degranulation, leading to the increase of pro-inflammatory mediators which contribute to the hypercontractility of

bronchial smooth muscles. Interestingly, the two HPI hybrid molecules **II** and **VI** promoted significant reduction of mast cell degranulation and hyperpolarization of BSMCs in *in vitro* models, which can be viewed as an enrichment of the pharmacological activity of the native drugs.

The idea of preparing H₂S-corticosteroid hybrids to be employed in the treatment of respiratory tract diseases such as asthma can be considered an interesting therapeutic strategy. Indeed, adding the H₂S releasing moiety provides further pharmacological effects to native drugs and more importantly could prevent those side effect linked to long-lasting treatment with corticosteroid drugs.

The effects described using *in vitro* models should be further strengthen by *in vivo* models, but these preliminary data may already pave the way for exploiting the hybridization process with H₂S-donor moieties for increasing the pharmacological activity of already employed drugs or counteracting specific side effects.

References

1. Ni X, Lai Y. Keratinocyte: A trigger or an executor of psoriasis? *J Leukoc Biol.* 2020;108(2):485-491.
2. Benhadou F, Mintoff D, Del Marmol V. Psoriasis: Keratinocytes or Immune Cells - Which Is the Trigger? *Dermatology.* 2019;235(2):91-100.
3. Parisi R, Symmons DP, Griffiths CE, Ashcroft DM; Identification and Management of Psoriasis and Associated Comorbidity (IMPACT) project team. Global epidemiology of psoriasis: a systematic review of incidence and prevalence. *J Invest Dermatol.* 2013;133(2):377-385.
4. Saraceno R, Mannheimer R, Chimenti S. Regional distribution of psoriasis in Italy. *J Eur Acad Dermatol Venereol.* 2008;22(3):324-329.
5. Icen M, Crowson CS, McEvoy MT, Dann FJ, Gabriel SE, Maradit Kremers H. Trends in incidence of adult-onset psoriasis over three decades: a population-based study. *J Am Acad Dermatol.* 2009;60(3):394-401.
6. Tollefson MM, Crowson CS, McEvoy MT, Maradit Kremers H. Incidence of psoriasis in children: a population-based study. *J Am Acad Dermatol.* 2010;62(6):979-987.
7. Griffiths CE, Barker JN. Pathogenesis and clinical features of psoriasis. *Lancet.* 2007;370(9583):263-271.
8. Rendon A, Schäkel K. Psoriasis Pathogenesis and Treatment. *Int J Mol Sci.* 2019;20(6):1475.
9. Menter A, Gottlieb A, Feldman SR, Van Voorhees AS, Leonardi CL, Gordon KB, Lebwohl M, Koo JY, Elmets CA, Korman NJ, Beutner KR, Bhushan R. Guidelines of care for the management of psoriasis and psoriatic arthritis: Section 1. Overview of psoriasis and guidelines of care for the treatment of psoriasis with biologics. *J Am Acad Dermatol.* 2008;58(5):826-850.
10. Di Meglio P, Villanova F, Nestle FO. Psoriasis. *Cold Spring Harb Perspect Med.* 2014;4(8):a015354.
11. Langley RG, Krueger GG, Griffiths CE. Psoriasis: epidemiology, clinical features, and quality of life. *Ann Rheum Dis.* 2005;64 Suppl 2(Suppl 2):ii18-ii25.
12. Kurd SK, Troxel AB, Crits-Christoph P, Gelfand JM. The risk of depression, anxiety, and suicidality in patients with psoriasis: a population-based cohort study. *Arch Dermatol.* 2010;146(8):891-895.

13. Samarasekera EJ, Neilson JM, Warren RB, Parnham J, Smith CH. Incidence of cardiovascular disease in individuals with psoriasis: a systematic review and meta-analysis. *J Invest Dermatol.* 2013;133(10):2340-2346.
14. Takeshita J, Grewal S, Langan SM, Mehta NN, Ogdie A, Van Voorhees AS, Gelfand JM. Psoriasis and comorbid diseases: Implications for management. *J Am Acad Dermatol.* 2017;76(3):393-403.
15. Kirby B, Fortune DG, Bhushan M, Chalmers RJ, Griffiths CE. The Salford Psoriasis Index: an holistic measure of psoriasis severity. *Br J Dermatol.* 2000;142(4):728-732.
16. Oliveira Mde F, Rocha Bde O, Duarte GV. Psoriasis: classical and emerging comorbidities. *An Bras Dermatol.* 2015;90(1):9-20.
17. Chandran V, Raychaudhuri SP. Geoepidemiology and environmental factors of psoriasis and psoriatic arthritis. *J Autoimmun.* 2010;34(3):J314-J321.
18. Harden JL, Krueger JG, Bowcock AM. The immunogenetics of Psoriasis: A comprehensive review. *J Autoimmun.* 2015;64:66-73.
19. Menter A, Griffiths CE. Current and future management of psoriasis. *Lancet.* 2007;370(9583):272-284.
20. Sevilla LM, Pérez P. Roles of the Glucocorticoid and Mineralocorticoid Receptors in Skin Pathophysiology. *Int J Mol Sci.* 2018;19(7):1906. Published 2018 Jun 29.
21. Greb JE, Goldminz AM, Elder JT, Lebwohl MG, Gladman DD, Wu JJ, Mehta NN, Finlay AY, Gottlieb AB. Psoriasis. *Nat Rev Dis Primers.* 2016;2:16082.
22. Hu Y, Chen Z, Gong Y, Shi Y. A Review of Switching Biologic Agents in the Treatment of Moderate-to-Severe Plaque Psoriasis. *Clin Drug Investig.* 2018;38(3):191-199.
23. Torsekar R, Gautam MM. Topical Therapies in Psoriasis. *Indian Dermatol Online J.* 2017;8(4):235-245.
24. Vakirlis E, Kastanis A, Ioannides D. Calcipotriol/betamethasone dipropionate in the treatment of psoriasis vulgaris. *Ther Clin Risk Manag.* 2008;4(1):141-148.
25. Uva L, Miguel D, Pinheiro C, et al. Mechanisms of action of topical corticosteroids in psoriasis. *Int J Endocrinol.* 2012;2012:561018.
26. McGill A, Frank A, Emmett N, Turnbull DM, Birch-Machin MA, Reynolds NJ. The anti-psoriatic drug anthralin accumulates in keratinocyte mitochondria, dissipates mitochondrial membrane potential, and induces apoptosis through a pathway dependent on respiratory competent mitochondria. *FASEB J.* 2005;19(8):1012-1014.
27. Roeder A, Schaller M, Schäfer-Korting M, Korting HC. Tazarotene: therapeutic strategies in the treatment of psoriasis, acne and photoaging. *Skin Pharmacol Physiol.* 2004;17(3):111-8.

28. Heath MS, Sahni DR, Curry ZA, Feldman SR. Pharmacokinetics of tazarotene and acitretin in psoriasis. *Expert Opin Drug Metab Toxicol.* 2018;14(9):919-927.
29. Bikle DD. Vitamin D and the skin. *J Bone Miner Metab.* 2010;28(2):117-130.
30. Wang C, Lin A. Efficacy of topical calcineurin inhibitors in psoriasis. *J Cutan Med Surg.* 2014;18(1):8-14.
31. Reynolds NJ, Al-Daraji WI. Calcineurin inhibitors and sirolimus: mechanisms of action and applications in dermatology. *Clin Exp Dermatol.* 2002;27(7):555-561.
32. Rahman M, Alam K, Ahmad MZ, Gupta G, Afzal M, Akhter S, Kazmi I, Jyoti, Ahmad FJ, Anwar F. Classical to current approach for treatment of psoriasis: a review. *Endocr Metab Immune Disord Drug Targets.* 2012;12(3):287-302.
33. Lee CS, Li K. A review of acitretin for the treatment of psoriasis. *Expert Opin Drug Saf.* 2009;8(6):769-79.
34. Reich K, Thaci D, Mrowietz U, Kamps A, Neureither M, Luger T. Efficacy and safety of fumaric acid esters in the long-term treatment of psoriasis--a retrospective study (FUTURE). *J Dtsch Dermatol Ges.* 2009;7(7):603-611.
35. Treumer F, Zhu K, Gläser R, Mrowietz U. Dimethylfumarate is a potent inducer of apoptosis in human T cells. *J Invest Dermatol.* 2003;121(6):1383-1388.
36. Keating GM. Apremilast: A Review in Psoriasis and Psoriatic Arthritis. *Drugs.* 2017;77(4):459-472.
37. Pasut G. Pegylation of biological molecules and potential benefits: pharmacological properties of certolizumab pegol. *BioDrugs.* 2014;28 Suppl 1:S15-S23.
38. Papp KA, Blauvelt A, Bukhalo M, et al. Risankizumab versus Ustekinumab for Moderate-to-Severe Plaque Psoriasis. *N Engl J Med.* 2017;376(16):1551-1560.
39. Blauvelt A, Papp KA, Griffiths CE, Randazzo B, Wasfi Y, Shen YK, Li S, Kimball AB. Efficacy and safety of guselkumab, an anti-interleukin-23 monoclonal antibody, compared with adalimumab for the continuous treatment of patients with moderate to severe psoriasis: Results from the phase III, double-blinded, placebo- and active comparator-controlled VOYAGE 1 trial. *J Am Acad Dermatol.* 2017;76(3):405-417.
40. Gordon KB, Duffin KC, Bissonnette R, Prinz JC, Wasfi Y, Li S, Shen YK, Szapary P, Randazzo B, Reich K. A Phase 2 Trial of Guselkumab versus Adalimumab for Plaque Psoriasis. *N Engl J Med.* 2015;373(2):136-44.
41. AbuHilal M, Walsh S, Shear N. The Role of IL-17 in the Pathogenesis of Psoriasis and Update on IL-17 Inhibitors for the Treatment of Plaque Psoriasis. *J Cutan Med Surg.* 2016;20(6):509-516.

42. Reiffenstein RJ, Hulbert WC, Roth SH. Toxicology of hydrogen sulfide. *Annu Rev Pharmacol Toxicol.* 1992;32:109-134.
43. Abe K, Kimura H. The possible role of hydrogen sulfide as an endogenous neuromodulator. *J Neurosci.* 1996;16(3):1066-1071.
44. Szabó C. Hydrogen sulphide and its therapeutic potential. *Nat Rev Drug Discov.* 2007;6(11):917-935.
45. Wang R. Two's company, three's a crowd: can H₂S be the third endogenous gaseous transmitter?. *FASEB J.* 2002;16(13):1792-1798.
46. Caliendo G, Cirino G, Santagada V, Wallace JL. Synthesis and biological effects of hydrogen sulfide (H₂S): development of H₂S-releasing drugs as pharmaceuticals. *J Med Chem.* 2010;53(17):6275-6286.
47. Doeller JE, Isbell TS, Benavides G, Koenitzer J, Patel H, Patel RP, Lancaster JR Jr, Darley-Usmar VM, Kraus DW. Polarographic measurement of hydrogen sulfide production and consumption by mammalian tissues. *Anal Biochem.* 2005;341(1):40-51.
48. Kolluru GK, Shen X, Bir SC, Kevil CG. Hydrogen sulfide chemical biology: pathophysiological roles and detection. *Nitric Oxide.* 2013;35:5-20.
49. Searcy DG, Lee SH. Sulfur reduction by human erythrocytes. *J Exp Zool.* 1998;282(3):310-322.
50. Benavides GA, Squadrito GL, Mills RW, Patel HD, Isbell TS, Patel RP, Darley-Usmar VM, Doeller JE, Kraus DW. Hydrogen sulfide mediates the vasoactivity of garlic. *Proc Natl Acad Sci USA.* 2007;104(46):17977-82.
51. Cao X, Ding L, Xie ZZ, Yang Y, Whiteman M, Moore PK, Bian JS. A Review of Hydrogen Sulfide Synthesis, Metabolism, and Measurement: Is Modulation of Hydrogen Sulfide a Novel Therapeutic for Cancer? *Antioxid Redox Signal.* 2019;31(1):1-38.
52. Coavoy-Sánchez SA, Costa SKP, Muscará MN. Hydrogen sulfide and dermatological diseases. *Br J Pharmacol.* 2020;177(4):857-865.
53. Chen X, Jhee KH, Kruger WD. Production of the neuromodulator H₂S by cystathionine beta-synthase via the condensation of cysteine and homocysteine. *J Biol Chem.* 2004;279(50):52082-52086.
54. Singh S, Padovani D, Leslie RA, Chiku T, Banerjee R. Relative contributions of cystathionine beta-synthase and gamma-cystathionase to H₂S biogenesis via alternative trans-sulfuration reactions. *J Biol Chem.* 2009;284(33):22457-22466.
55. Aitken SM, Kirsch JF. The enzymology of cystathionine biosynthesis: strategies for the control of substrate and reaction specificity. *Arch Biochem Biophys.* 2005;433(1):166-175.

56. Chiku T, Padovani D, Zhu W, Singh S, Vitvitsky V, Banerjee R. H₂S biogenesis by human cystathionine gamma-lyase leads to the novel sulfur metabolites lanthionine and homolanthionine and is responsive to the grade of hyperhomocysteinemia. *J Biol Chem.* 2009;284(17):11601-11612.
57. Nagahara N, Yoshii T, Abe Y, Matsumura T. Thioredoxin-dependent enzymatic activation of mercaptopyruvate sulfurtransferase. An intersubunit disulfide bond serves as a redox switch for activation. *J Biol Chem.* 2007;282(3):1561-1569.
58. Shibuya N, Koike S, Tanaka M, Ishigami-Yuasa M, Kimura Y, Ogasawara Y, Fukui K, Nagahara N, Kimura H. A novel pathway for the production of hydrogen sulfide from D-cysteine in mammalian cells. *Nat Commun.* 2013;4:1366.
59. Ishigami M, Hiraki K, Umemura K, Ogasawara Y, Ishii K, Kimura H. A source of hydrogen sulfide and a mechanism of its release in the brain. *Antioxid Redox Signal.* 2009;11(2):205-214.
60. Kimura H, Shibuya N, Kimura Y. Hydrogen sulfide is a signaling molecule and a cytoprotectant. *Antioxid Redox Signal.* 2012;17(1):45-57.
61. Whiteman M, Le Trionnaire S, Chopra M, Fox B, Whatmore J. Emerging role of hydrogen sulfide in health and disease: critical appraisal of biomarkers and pharmacological tools. *Clin Sci (Lond).* 2011;121(11):459-488.
62. Yonezawa D, Sekiguchi F, Miyamoto M, Taniguchi E, Honjo M, Masuko T, Nishikawa H, Kawabata A. A protective role of hydrogen sulfide against oxidative stress in rat gastric mucosal epithelium. *Toxicology.* 2007;241(1-2):11-8.
63. Zhong G, Chen F, Cheng Y, Tang C, Du J. The role of hydrogen sulfide generation in the pathogenesis of hypertension in rats induced by inhibition of nitric oxide synthase. *J Hypertens.* 2003;21(10):1879-1885.
64. Bhatia M, Sidhapuriwala J, Moochhala SM, Moore PK. Hydrogen sulphide is a mediator of carrageenan-induced hindpaw oedema in the rat. *Br J Pharmacol.* 2005;145(2):141-144.
65. Mok YY, Atan MS, Yoke Ping C, Zhong Jing W, Bhatia M, Moochhala S, Moore PK. Role of hydrogen sulphide in haemorrhagic shock in the rat: protective effect of inhibitors of hydrogen sulphide biosynthesis. *Br J Pharmacol.* 2004;143(7):881-9.
66. Kawabata A, Ishiki T, Nagasawa K, Yoshida S, Maeda Y, Takahashi T, Sekiguchi F, Wada T, Ichida S, Nishikawa H. Hydrogen sulfide as a novel nociceptive messenger. *Pain.* 2007;132(1-2):74-81.
67. Fiorucci S, Distrutti E, Cirino G, Wallace JL. The emerging roles of hydrogen sulfide in the gastrointestinal tract and liver. *Gastroenterology.* 2006;131(1):259-271.

68. Laggner H, Hermann M, Esterbauer H, Muellner MK, Exner M, Gmeiner BM, Kapiotis S. The novel gaseous vasorelaxant hydrogen sulfide inhibits angiotensin-converting enzyme activity of endothelial cells. *J Hypertens*. 2007;25(10):2100-4.
69. Sekiguchi F, Sekimoto T, Ogura A, Kawabata A. Endogenous Hydrogen Sulfide Enhances Cell Proliferation of Human Gastric Cancer AGS Cells. *Biol Pharm Bull*. 2016;39(5):887-890.
70. Yang G, Wu L, Wang R. Pro-apoptotic effect of endogenous H₂S on human aorta smooth muscle cells. *FASEB J*. 2006;20(3):553-555.
71. Zanardo RC, Brancalone V, Distrutti E, Fiorucci S, Cirino G, Wallace JL. Hydrogen sulfide is an endogenous modulator of leukocyte-mediated inflammation. *FASEB J*. 2006;20(12):2118-2120.
72. Li L, Bhatia M, Moore PK. Hydrogen sulphide--a novel mediator of inflammation?. *Curr Opin Pharmacol*. 2006;6(2):125-129.
73. Xiao Q, Ying J, Xiang L, Zhang C. The biologic effect of hydrogen sulfide and its function in various diseases. *Medicine (Baltimore)*. 2018;97(44):e13065.
74. Wang R. Physiological implications of hydrogen sulfide: a whiff exploration that blossomed. *Physiol Rev*. 2012;92(2):791-896.
75. Kutz JL, Greaney JL, Santhanam L, Alexander LM. Evidence for a functional vasodilatory role for hydrogen sulphide in the human cutaneous microvasculature. *J Physiol*. 2015;593(9):2121-2129.
76. Xie X, Dai H, Zhuang B, Chai L, Xie Y, Li Y. Exogenous hydrogen sulfide promotes cell proliferation and differentiation by modulating autophagy in human keratinocytes. *Biochem Biophys Res Commun*. 2016;472(3):437-443.
77. Gobbi G, Ricci F, Malinverno C, Carubbi C, Pambianco M, Panfilis Gd, Vitale M, Mirandola P. Hydrogen sulfide impairs keratinocyte cell growth and adhesion inhibiting mitogen-activated protein kinase signaling. *Lab Invest*. 2009;89(9):994-1006.
78. Lee E, Kim HJ, Lee M, Jin SH, Hong SH, Ahn S, Kim SO, Shin DW, Lee ST, Noh M. Cystathionine metabolic enzymes play a role in the inflammation resolution of human keratinocytes in response to sub-cytotoxic formaldehyde exposure. *Toxicol Appl Pharmacol*. 2016;310:185-194.
79. Rodrigues L, Ekundi-Valentim E, Florenzano J, Cerqueira AR, Soares AG, Schmidt TP, Santos KT, Teixeira SA, Ribela MT, Rodrigues SF, de Carvalho MH, De Nucci G, Wood M, Whiteman M, Muscará MN, Costa SK. Protective effects of exogenous and endogenous

- hydrogen sulfide in mast cell-mediated pruritus and cutaneous acute inflammation in mice. *Pharmacol Res.* 2017;115:255-266.
80. Coavoy-Sánchez SA, Rodrigues L, Teixeira SA, Soares AG, Torregrossa R, Wood ME, Whiteman M, Costa SKP, Muscará MN. Hydrogen sulfide donors alleviate itch secondary to the activation of type-2 protease activated receptors (PAR-2) in mice. *Pharmacol Res.* 2016;113(Pt A):686-694.
 81. Merighi S, Gessi S, Varani K, Fazzi D, Borea PA. Hydrogen sulfide modulates the release of nitric oxide and VEGF in human keratinocytes. *Pharmacol Res.* 2012;66(5):428-436.
 82. Mirandola P, Gobbi G, Micheloni C, Vaccarezza M, Di Marcantonio D, Ruscitti F, de Panfilis G, Vitale M. Hydrogen sulfide inhibits IL-8 expression in human keratinocytes via MAP kinase signaling. *Lab Invest.* 2011;91(8):1188-94.
 83. Alshorafa AK, Guo Q, Zeng F, Chen M, Tan G, Tang Z, Yin R. Psoriasis is associated with low serum levels of hydrogen sulfide, a potential anti-inflammatory molecule. *Tohoku J Exp Med.* 2012;228(4):325-32.
 84. Wang XL, Tian B, Huang Y, Peng XY, Chen LH, Li JC, Liu T. Hydrogen sulfide-induced itch requires activation of Cav3.2 T-type calcium channel in mice. *Sci Rep.* 2015;5:16768.
 85. Yang C, Yang Z, Zhang M, Dong Q, Wang X, Lan A, Zeng F, Chen P, Wang C, Feng J. Hydrogen sulfide protects against chemical hypoxia-induced cytotoxicity and inflammation in HaCaT cells through inhibition of ROS/NF- κ B/COX-2 pathway. *PLoS One.* 2011;6(7):e21971.
 86. Yang CT, Zhao Y, Xian M, Li JH, Dong Q, Bai HB, Xu JD, Zhang MF. A novel controllable hydrogen sulfide-releasing molecule protects human skin keratinocytes against methylglyoxal-induced injury and dysfunction. *Cell Physiol Biochem.* 2014;34(4):1304-17.
 87. Powell CR, Dillon KM, Matson JB. A review of hydrogen sulfide (H₂S) donors: Chemistry and potential therapeutic applications. *Biochem Pharmacol.* 2018;149:110-123.
 88. Song ZJ, Ying Ng M, Lee ZW, Dai W, Hagen T, Moore PK, Huang D, Deng LW, Tan CH. Hydrogen sulfide donors in research and drug development. *Med. Chem. Commun.* 2014;5,557.
 89. Wallace GCJL, Caliendo G, Sparatore A, Santagada V, Fiorucci S. Derivatives of 4- or 5-aminosalicylic acid. Patent WO2006125293. 2006.
 90. Ercolano G, De Cicco P, Frecentese F, Saccone I, Corvino A, **Giordano F**, Magli E, Fiorino F, Severino B, Calderone V, Citi V, Cirino G, Ianaro A. Anti-metastatic Properties of Naproxen-HBTA in a Murine Model of Cutaneous Melanoma. *Front Pharmacol.* 2019;10:66.

91. Vanommeslaeghe K, Hatcher E, Acharya C, Kundu S, Zhong S, Shim J, Darian E, Guvench O, Lopes P, Vorobyov I, Mackerell AD Jr. CHARMM general force field: A force field for drug-like molecules compatible with the CHARMM all-atom additive biological force fields. *J Comput Chem.* 2010;31(4):671-90.
92. Fletcher R. Unconstrained optimization. In *Practical Methods of Optimization*. John Wiley&Sons 61. 1981; 408-408.
93. Lucarini E, Micheli L, Trallori E, Citi V, Martelli A, Testai L, De Nicola GR, Iori R, Calderone V, Ghelardini C, Di Cesare Mannelli L. Effect of glucoraphanin and sulforaphane against chemotherapy-induced neuropathic pain: Kv7 potassium channels modulation by H₂S release in vivo. *Phytother Res.* 2018;32(11):2226-2234.
94. van der Fits L, Mourits S, Voerman JS, Kant M, Boon L, Laman JD, Cornelissen F, Mus AM, Florencia E, Prens EP, Lubberts E. Imiquimod-induced psoriasis-like skin inflammation in mice is mediated via the IL-23/IL-17 axis. *J Immunol.* 2009;182(9):5836-45.
95. Peng B, Chen W, Liu C, Rosser EW, Pacheco A, Zhao Y, Aguilar HC, Xian M. Fluorescent probes based on nucleophilic substitution-cyclization for hydrogen sulfide detection and bioimaging. *Chemistry.* 2014;20(4):1010-6.
96. Martelli A, Citi V, Calderone V. Vascular Effects of H₂S-Donors: Fluorimetric Detection of H₂S Generation and Ion Channel Activation in Human Aortic Smooth Muscle Cells. *Methods Mol Biol.* 2019;2007:79-87.
97. Barresi E, Nesi G, Citi V, Piragine E, Piano I, Taliani S, Da Settimo F, Rapposelli S, Testai L, Breschi MC, Gargini C, Calderone V, Martelli A. Iminothioethers as Hydrogen Sulfide Donors: From the Gasotransmitter Release to the Vascular Effects. *J Med Chem.* 2017;60(17):7512-7523.
98. Citi V, Piragine E, Pagnotta E, Ugolini L, Di Cesare Mannelli L, Testai L, Ghelardini C, Lazzeri L, Calderone V, Martelli A. Anticancer properties of erucin, an H₂S-releasing isothiocyanate, on human pancreatic adenocarcinoma cells (AsPC-1). *Phytother Res.* 2019;33(3):845-855.
99. Boardman C, Chachi L, Gavrila A, Keenan CR, Perry MM, Xia YC, Meurs H, Sharma P. Mechanisms of glucocorticoid action and insensitivity in airways disease. *Pulm Pharmacol Ther.* 2014;29(2):129-43.
100. O'Byrne P, Fabbri LM, Pavord ID, Papi A, Petruzzelli S, Lange P. Asthma progression and mortality: the role of inhaled corticosteroids. *Eur Respir J.* 2019;54(1):1900491.

101. Alangari AA. Corticosteroids in the treatment of acute asthma. *Ann Thorac Med.* 2014;9(4):187-92.
102. Citi V, Corvino A, Fiorino F, Frecentese F, Magli E, Perissutti E, Santagada V, Brogi S, Flori L, Gorica E, Testai L, Martelli A, Calderone V, Caliendo G, Severino B. Structure-activity relationships study of isothiocyanates for H₂S releasing properties: 3-Pyridyl-isothiocyanate as a new promising cardioprotective agent. *J Adv Res.* 2020;27:41-53.
103. Martelli A, Testai L, Citi V, Marino A, Bellagambi FG, Ghimenti S, Breschi MC, Calderone V. Pharmacological characterization of the vascular effects of aryl isothiocyanates: is hydrogen sulfide the real player? *Vascul Pharmacol.* 2014;60(1):32-41.
104. Martelli A, Testai L, Citi V, Marino A, Pugliesi I, Barresi E, Nesi G, Rapposelli S, Taliani S, Da Settimo F, Breschi MC, Calderone V. Arylthioamides as H₂S Donors: l-Cysteine-Activated Releasing Properties and Vascular Effects in Vitro and in Vivo. *ACS Med Chem Lett.* 2013;4(10):904-8.
105. Citi V, Martelli A, Bucci M, Piragine E, Testai L, Vellecco V, Cirino G, Calderone V. Searching for novel hydrogen sulfide donors: The vascular effects of two thiourea derivatives. *Pharmacol Res.* 2020;159:105039.
106. Zhang L, Wang Y, Li Y, Li L, Xu S, Feng X, Liu S. Hydrogen Sulfide (H₂S)-Releasing Compounds: Therapeutic Potential in Cardiovascular Diseases. *Front Pharmacol.* 2018;9:1066.
107. Lin Y, Yang X, Lu Y, Liang D, Huang D. Isothiocyanates as H₂S Donors Triggered by Cysteine: Reaction Mechanism and Structure and Activity Relationship. *Org Lett.* 2019;21(15):5977-5980.
108. Citi V, Martelli A, Testai L, Marino A, Breschi MC, Calderone V. Hydrogen sulfide releasing capacity of natural isothiocyanates: is it a reliable explanation for the multiple biological effects of Brassicaceae? *Planta Med.* 2014;80(8-9):610-3.
109. Marino A, Martelli A, Citi V, Fu M, Wang R, Calderone V, Levi R. The novel H₂S donor 4-carboxy-phenyl isothiocyanate inhibits mast cell degranulation and renin release by decreasing intracellular calcium. *Br J Pharmacol.* 2016;173(22):3222-3234.
110. Netzer NC, Küpper T, Voss HW, Eliasson AH. The actual role of sodium cromoglycate in the treatment of asthma--a critical review. *Sleep Breath.* 2012;16(4):1027-1032.
111. Yamaguchi M, Hirai K, Komiya A, Miyamasu M, Furumoto Y, Teshima R, Ohta K, Morita Y, Galli SJ, Ra C, Yamamoto K. Regulation of mouse mast cell surface Fc epsilon RI expression by dexamethasone. *Int Immunol.* 2001;13(7):843-51.

112. Wrzosek A. The potassium channel opener NS1619 modulates calcium homeostasis in muscle cells by inhibiting SERCA. *Cell Calcium*. 2014;56(1):14-24.
113. Nabishah BM, Morat PB, Khalid BA, Kadir BA. Effect of acetylcholine and morphine on bronchial smooth muscle contraction and its modulation by steroid hormones. *Clin Exp Pharmacol Physiol*. 1990;17(12):841-847.
114. Tanaka H, Watanabe K, Tamaru N, Yoshida M. Arachidonic acid metabolites and glucocorticoid regulatory mechanism in cultured porcine tracheal smooth muscle cells. *Lung*. 1995;173(6):347-361.
115. Schramm CM, Grunstein MM. Corticosteroid modulation of Na(+)-K+ pump-mediated relaxation in maturing airway smooth muscle. *Br J Pharmacol*. 1996;119(5):807-812.
116. Ivasiv V, Albertini C, Gonçalves AE, Rossi M, Bolognesi ML. Molecular Hybridization as a Tool for Designing Multitarget Drug Candidates for Complex Diseases. *Curr Top Med Chem*. 2019;19(19):1694-1711.
117. Gontijo VS, Viegas FPD, Ortiz CJC, de Freitas Silva M, Damasio CM, Rosa MC, Campos TG, Couto DS, Tranches Dias KS, Viegas C. Molecular Hybridization as a Tool in the Design of Multi-target Directed Drug Candidates for Neurodegenerative Diseases. *Curr Neuropharmacol*. 2020;18(5):348-407.

Unit 2

Chapter 1

Intramolecular contacts to stabilize secondary structure

1. Introduction

1.1. Protein-protein interactions mediated by α -helices and β -strands

Protein-protein interactions (PPIs) are involved in many cellular processes such as gene expression, proliferation, intracellular communication, and apoptosis [1]. The ability to control and modulate PPIs is important to develop greater understanding of system biology, establish novel approaches for medical diagnostic of health and disease and develop new molecular therapeutics. Constrained peptides provide an interesting approach to design peptidomimetics targeting PPIs [2-4]. The stabilization of α -helices or β -strands can be acted by covalent or non-covalent constraints, for example lactam, disulfide and metal-mediated bridges or electrostatic interactions between side chains at selected positions. An approach for the stabilization of α -helical conformations in peptides is based on the side-chain cross-linking of i and $i+4$ or i and $i+7$ side chains lying on the same face of the helix. The cross-linking may involve lactam, thioether, triazole, C-C bond bridges, as well as metal-mediated chelation [5]. Another approach is based on the stabilization of the conformation by controlled π - π or cation- π interactions. The cross-link should result in a stabilized helical conformation in the peptide and improved stability of the peptide toward proteolysis [5].

β -Strand conformations can be stabilized by interactions between hydrophobic residues, disulfide bridges or salt bridges (for example, a salt-bridge formed between Glu and Lys residues) and π - π or cation- π interactions. β -strand conformations have been successfully stabilized by interaction of one Lys from one β -strand and two Trp residues from the other β -strand (sandwich motif via cation- π interaction) [6]. The dipeptide D-Pro-L-Pro in the turn has proved to be an extremely useful template in β -mimetic design because it stabilizes the β -strand structure [7]. Based on this consideration, several studies have been carried out with the aim of creating intermolecular contacts to stabilize the secondary structure of peptides.

My research has been focused on synthesizing BMP2 sequences. Bone morphogenic protein BMP2 is a cytokine from the TGF β family (transforming growth factor beta) and plays a key role in bone morphogenesis [8]. The research group of Prof. Dr. Chiara Cabrele focused its attention on the development of peptides as BMP2mimetics. They

already synthesized linear peptides reproducing some BMP2 sequences, involving two β -strands: β 3 and β 7, stabilized by Lys-Trp cation- π interaction. My attention was instead focused on the synthesis of a region characterized by three β -strands (β 3, β 7 and β 8) stabilized by Lys-Trp sandwich. Moreover, I studied the stabilization of α -helices by cation- π interaction by mean of peptide sequences ad hoc synthesized containing a KW half-zipper motif. Synthetic procedures and characterization of the above described peptides are successively reported.

1.2. Phosphorylated and non-phosphorylated Id3 protein

Inhibitors of DNA binding and cell differentiation (Id) proteins belong to the family of helix-loop-helix (HLH) transcription factors (Figure 1). The Id proteins (Id1-4) are cell-cycle regulators that play a key role during development, in cancer and vascular disorders [9]. They negatively regulate the gene expression and are characterized by a conserved HLH domain that folds into a parallel four-helix bundle upon self- or hetero-association with a basic-HLH transcription factor. Since dysregulated Id-protein expression has been associated with tumor growth, vascularization, invasiveness, metastasis, chemoresistance and stemness, as well as with various development defects and diseases, the Id proteins represent interesting therapeutic targets, and the synthetic Id-protein inhibitors would be very useful tools to understand the biology of these proteins [10].

My attention has been focused on Id3 protein that is involved in different biological processes, such as in controlling cell cycle, proliferation, differentiation and apoptosis. Id3 is involved in the DNA repair process, interacting with MDC1. Lee et al. [11] demonstrated that phosphorylation of Ser65 within the HLH domain of Id3 is important for modulating the interactions between MDC1 and Id3. In fact, when DNA double-strand breaks (DSBs) are generated, the DNA damage response (DDR) system activates an ATM protein kinase that induces phosphorylation of Id3 on Ser65 which is followed by a glutamine residue. This suggests that phosphorylated-Id3 protein may be localized to the site of DNA damage and that phosphorylated Ser65 of Id3 is necessary for interaction with MDC1.

In order to investigate the effect of phosphorylation on the helix-2 of Id3, I synthesized unphosphorylated and phosphorylated forms of this helix. The synthesis of peptides Id3(63-81) and pSer65-Id3(63-81) had already been previously attempted by mean of an automatic peptide synthesizer, but it proved to be a difficult peptide sequence. Thus, we decided to perform this sequence by batch manual synthesis and monitoring the synthetic procedures in two steps of peptide elongation in order to check the quality of the growing peptide chain.

	Helix-1	Loop	Helix-2
Id1 (66-106)	LYDMNGCYSRLKELVP	TLPQNRKVS	KVEILQHVIDYIRDLDQ
Id2 (36-76)	LYNMNDCYSKELKELVP	SIPQNKKVS	KMEILQHVIDYILDLDQ
Id3 (41-81)	LDDMNH CYSRLRELVP	GVPRGT QLS	QVEILQRVIDYILDLDQ
Id4 (65-105)	QCDMND CYSRLRRLVP	TIPPNKKVS	KVEILQHVIDYILDLDQ

Figure 1. Primary structure of the HLH domain of human Id1-4; the sequence of Id3(63-81) is in bold.

2. Experimental Part

2.1. Materials and methods

Materials

Chemical reagents and solvents used for the peptide syntheses were of peptide-synthesis grade; solvents used for HPLC and spectroscopy were of HPLC or spectroscopy grade. Nova PEG Rink Amide resin (loading 0.37 mmol/g) was purchased by Novabiochem (Merck Millipore, Germany). Fmoc-Rink-amide MBHS resin (loading 0.57 mmol/g) was purchased by Iris Biotech (Germany). Fmoc-L-Gln(Trt)-OH, Fmoc-L-Leu-OH, Fmoc-L-Asp(tBu)-OH, Fmoc-L-Ile-OH, Fmoc-L-Tyr(tBu)-OH, Fmoc-L-Val-OH, Fmoc-L-Glu(tBu)-OH, Fmoc-L-Ser(tBu)-OH, Fmoc-L-Lys(Boc)-OH, Fmoc-L-Ala-OH, Fmoc-L-Trp(Boc)-OH, Fmoc-L-Pro-OH, Fmoc-L-Asn(Trt)-OH were purchased by Iris Biotech (Germany). Fmoc-L-Arg(Pbf)-OH, Fmoc-L-Ser(PO-(OBzl)OH)-OH, Fmoc-L-Met(O)-OH, Fmoc-D-Pro-OH were purchased by Novabiochem (Merck Millipore, Germany). 2-(1H-benzotriazole-1-yl)-1,1,3,3-tetramethyluronium hexafluorophosphate (HBTU) and N-hydroxybenzotriazole (HOBt) were purchased by Biosolve (The Netherlands). N,N-diisopropylethylamine (DIPEA), piperidine (PIP), N-methyl-2-pyrrolidinone (NMP), dichloromethane (DCM) and diethyl ether (Et₂O) were purchased by Iris Biotech (Germany). 2,2,2-Trifluoroethanol (TFE), 1,2-ethanedithiol (EDT) and thioanisole (TIA) were purchased by Fluka. Acetic anhydride, triisopropylsilane (TIS), acetonitrile (ACN, for HPLC, gradient grade, ≥99.9%) and N,N-dimethylformamide (DMF) were purchased by Sigma-Aldrich (Germany). Trifluoroacetic acid (TFA, HPLC grade, 99.5+%) was purchased by Alfa Aesar.

Methods

The solid-phase peptide syntheses of peptides A1-8 and B1-2 were carried out on an automatic peptide synthesizer (Syro, Biotage). The solid-phase peptide syntheses of peptides Id3(63-81) and pSer65-Id3(63-81) were carried out manually. The analytical and semipreparative HPLC equipment was a Thermo Fisher Scientific Dionex (model UltiMate 3000). The analytical column was from Thermo Fisher Scientific (Synchronis

C18 column, 100 Å, 5 µm, 250 × 4.6 mm), the semipreparative column was from Macherey Nagel (NUCLEOSIL® C-18, 250x10 mm, 5µm). MALDI-TOF mass spectra were recorded on an Autoflex mass spectrometer from Bruker Daltonics using α-cyano-4-hydroxycinnamic acid as matrix. The UV measurements were carried out on an Agilent Cary 60 UV-Vis spectrophotometer. The circular dichroism (CD) measurements were recorded on an Applied Photophysics Chirscan-plus CD spectrometer (United Kingdom).

2.2. Peptide synthesis

Scaffolds for secondary structure using non-covalent cation π-interaction

The peptides A1-8 and B1-2 (Table 1) were assembled on an automatic peptide synthesizer by using Fmoc-Rink-amide MBHS resin and Fmoc chemistry.

Table 1. Sequence of the peptides A1-8 and B1-2.

<i>Name/Label</i>	<i>Sequence</i>
A1	Ac-KRQAW <u>E</u> QKRS <u>A</u> WESK-NH ₂
A2	Ac-K <u>A</u> QAW <u>E</u> QK <u>A</u> SAWESK-NH ₂
A3	Ac- <u>A</u> RQAW <u>E</u> Q <u>A</u> RS <u>A</u> WES <u>A</u> -NH ₂
A4	Ac-KRQ <u>A</u> <u>A</u> <u>E</u> QKRS <u>A</u> <u>A</u> ESK-NH ₂
A5	Ac-WRQ <u>A</u> KEQWRS <u>A</u> KE <u>S</u> W-NH ₂
A6	Ac-W <u>A</u> Q <u>A</u> KEQW <u>A</u> SAKESW-NH ₂
A7	Ac-WRQ <u>A</u> <u>A</u> <u>E</u> QWRS <u>A</u> <u>A</u> ESW-NH ₂
A8	Ac- <u>A</u> RQ <u>A</u> KEQ <u>A</u> RS <u>A</u> KE <u>S</u> <u>A</u> -NH ₂
B1	Ac-WIVA <u>p</u> PSULY <u>L</u> <u>Pp</u> VVLKN-NH ₂
B2	Ac-WIVA <u>p</u> PS <u>K</u> <u>L</u> <u>L</u> <u>Pp</u> VWL <u>W</u> N-NH ₂

p = D-Pro
U = Met(O)

The side-chain protecting groups were tBu (E, Y, S), Pbf (R), Trt (Q, N) and Boc (K, W). The Fmoc deprotection was carried out with 25% piperidine in DMF/NMP (70:30, v/v) for 3 min and 12.5% piperidine in DMF/NMP (70:30, v/v) for 12 min. The double couplings were realized with the mixture Fmoc-AA-OH/HOBt/HBTU/DIPEA (4:4:4:8 equiv.) for 40 min. N-terminal acetylation was performed manually with 10 equiv. acetic anhydride and 10 equiv. DIPEA in DMF for 30 min. In the end the peptides were cleaved from the resin with TFA/TIS/H₂O/EDT/TIA (90:3:1:3:3; V_{tot}=1 mL) for about 3 h, precipitated by ice-cold diethyl ether, recovered by centrifugation at 4°C for 5 min, and washed three times with ice-cold diethyl ether. The crude peptides were purified by semipreparative HPLC.

Synthetic Id3 helix

The peptides Id3(63-81) and pSer65-Id3(63-81) (Table 2) were assembled manually by using Nova PEG Rink Amide resin and Fmoc chemistry.

Table 2. Sequence of synthetic Id3 helix.

<i>Name/Label</i>	<i>Sequence</i>
Id3(63-81)	H-QLSQVEILQRVIDYILDLQ-NH ₂
pSer65-Id3(63-81)	H-QLS ^P QVEILQRVIDYILDLQ-NH ₂

S^P = Phosphorylated Serine

The side-chain protecting groups were tBu (D, E, Y, S), Pbf (R), Trt (Q) and OBzl (S^P). The Fmoc deprotection was carried out with 20% piperidine in DMF/NMP (80:20 v/v), for 5 min, repeating Fmoc deprotection twice. Each amino acid was coupled through double couplings. Peptide elongations till V11 and till Q4 were respectively realized using 5 eq Fmoc-AA-OH, 5 eq HOBt (0.45 M in DMF/NMP 80:20 v/v), 4.8 eq HBTU (0.45 M in DMF/NMP 80:20 v/v) and 10 eq DIPEA (1.2 M in NMP) and the mixture was shaken for 40 min, and 6 eq Fmoc-AA-OH, 6 eq HOBt (0.45 M in DMF/NMP 80:20 v/v), 5.8 eq HBTU (0.45 M in DMF/NMP 80:20 v/v) and 12 eq DIPEA (1.2 M in NMP) and the mixture was shaken for 1 h. After splitting of peptide resin in two parts,

peptide elongation with S3 or phospho-S3 was accomplished using 4 eq Fmoc-AA-OH, 4 eq HOBt (0.45 M in DMF/NMP 80:20 v/v), 3.8 eq HBTU (0.45 M in DMF/NMP 80:20 v/v) and 8 eq DIPEA (1.2 M in NMP) and the mixtures were shaken for 1 h. Lastly, peptide elongation till Q1 was completed using 6 eq Fmoc-AA-OH, 6 eq HOBt (0.45 M in DMF/NMP 80:20 v/v), 5.8 eq HBTU (0.45 M in DMF/NMP 80:20 v/v) and 12 eq DIPEA (1.2 M in NMP) and the mixture was shaken for 1 h. In the end the peptides were cleaved from the resin with TFA/TIS/H₂O/EDT/TIA (90:3:1:3:3; V_{tot}=1 mL) for about 3 h, precipitated by ice-cold diethyl ether, recovered by centrifugation at 4°C for 5 min, and washed three times with ice-cold diethyl ether. During the synthesis a small-scale TFA cleavage was performed in two steps of peptide elongation (till V11 and till Q4) in order to check the quality of the peptide chain by HPLC and MS: resin was treated with TFA/TIS/H₂O/EDT/TIA (90:3:1:3:3; V_{tot}=100μL) for about 3 h, followed by precipitation, centrifugation and washing with ice-cold diethyl ether.

3. Results and Discussion

3.1. Analytical characterization of the peptides

The purity and the identification of desired peptides were evaluated by analytical HPLC and MALDI-TOF-MS (Table 3 and Figures 2 and 3). The samples were prepared dissolving 0.2 mg of peptide in 150 μ L of ACN/0.1%TFA in H₂O (40% and 60%, respectively) for the Id3 helix peptides, because of their poor water solubility, and 0.2 mg of peptide in 150 μ L of ACN/0.1%TFA in H₂O (25% and 75%, respectively) for peptides A1-8 and B1-2.

Table 3. Analytical characterization of the peptides.

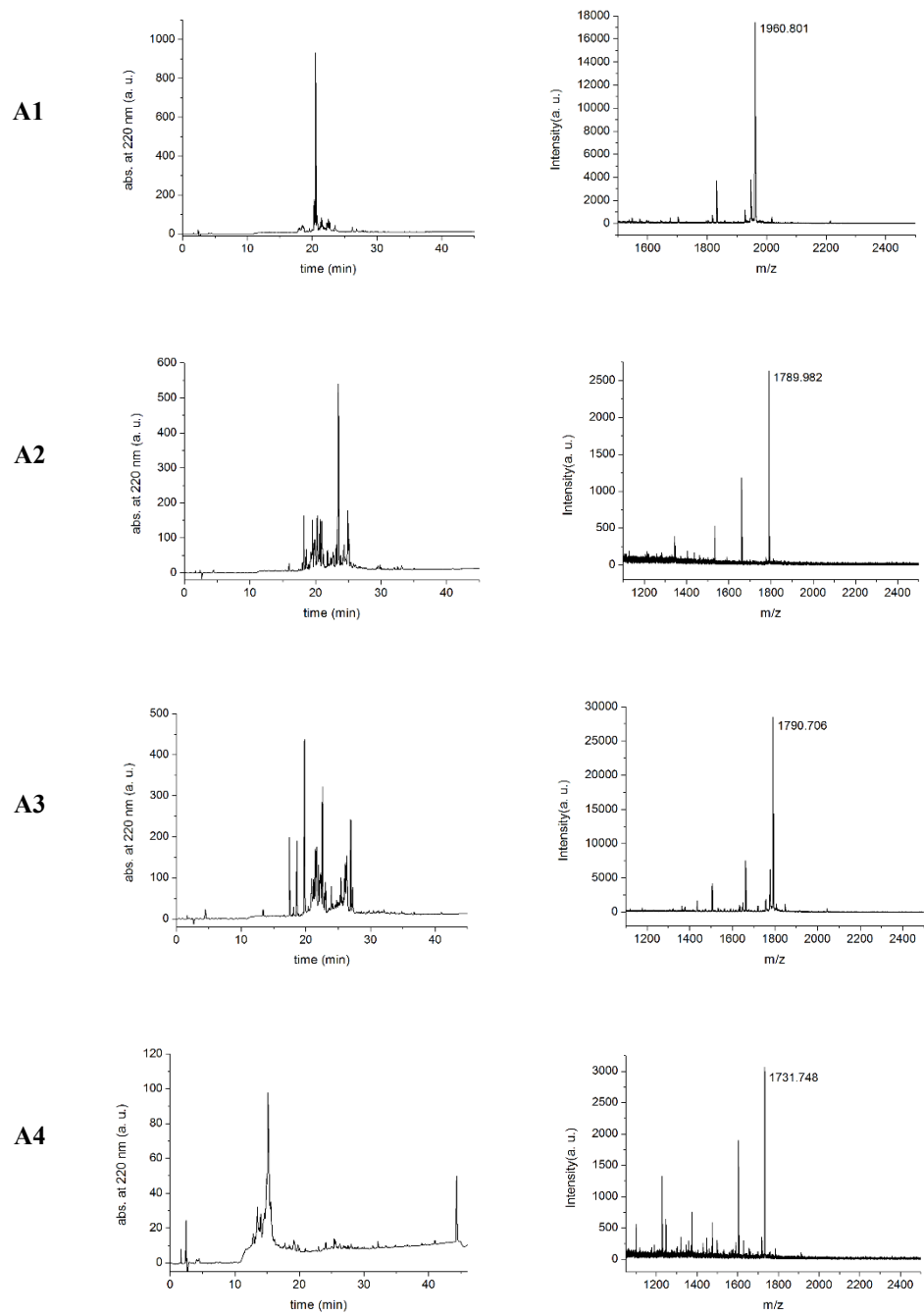
Peptide label	$M_{\text{theor.}}^{\text{a}}$ (Da)	$(M+H)^+_{\text{found}}^{\text{b}}$ (Da)	t_{R}^{c} (min)
A1	1959.17	1960.80	20.5
A2	1788.96	1789.98	23.5
A3	1787.89	1790.71	19.7
A4	1728.91	1731.75	15.1
A5	2017.21	2018.98	24.3
A6	1846.99	1848.74	26.9
A7	1903.02	1904.54	29.3
A8	1671.82	1673.06	16.5
B1	2094.56	2095.84	33.1
B2	2185.65	2187.05	35.7
Id3(63-81)	2285.64	2286.99	39.6
pSer65-Id3(63-81)	2365.62	2365.03	40.9

a. Monoisotopic/Average

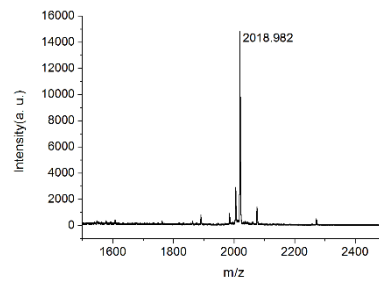
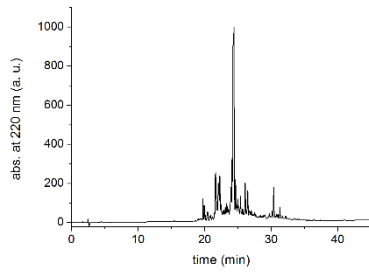
b. Measured by MALDI-TOF-MS (negative mode measurement for pSer65-Id3(63-81))

c. HPLC gradient: 3% B for 8 min, 3-60% in 35 min, with A = 0.06% TFA in water and B = 0.05% TFA in acetonitrile

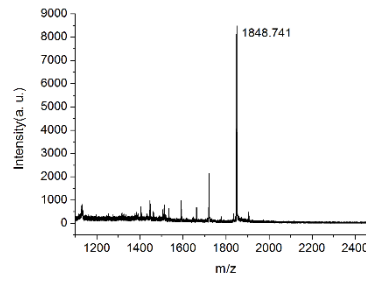
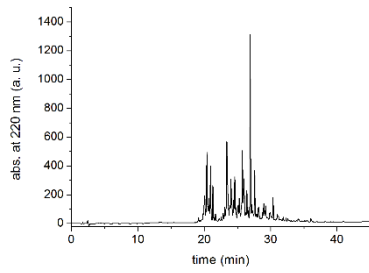
Figure 2. Analytical HPLC profiles and MALDI-TOF-MS of the peptides A1-8 and B1-2.



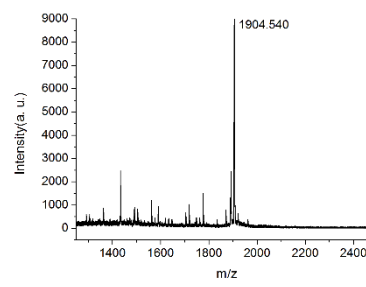
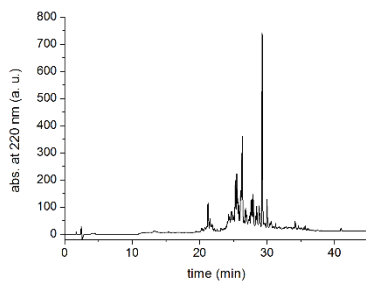
A5



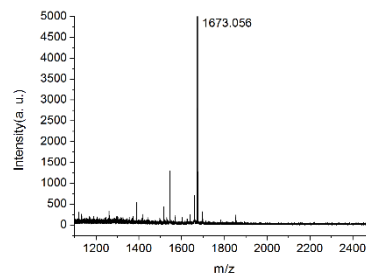
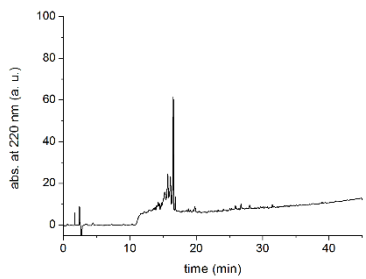
A6



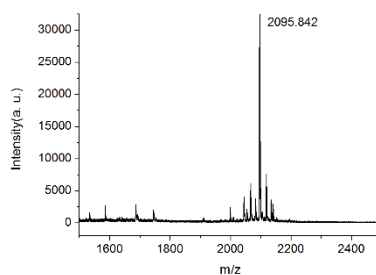
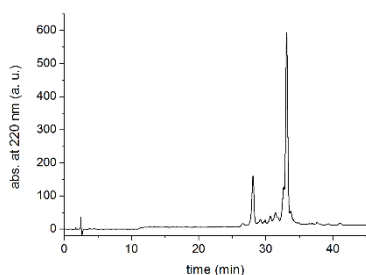
A7



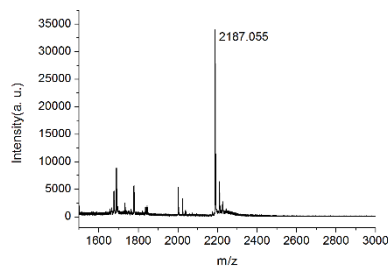
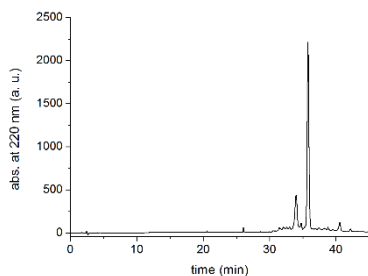
A8



B1



B2



Several difficulties arose during peptide purifications by semipreparative HPLC, probably due to their structural features. Best results have been obtained with purification of A1 and A5 peptides in the series A1-8: A1 and A5 differ each other only in the type of half-zipper: $(KW)_2K$ in A1 and $(WK)_2W$ in A5. On the other hand, the Ala-rich sequences obtained in other peptides by replacing W, K or R with the neutral, small, and helix-prone Ala residue gave complex mixtures, indicating that the sequence assembly was difficult. Probably, the helix propensity of Ala favoured the building of secondary structure during the peptide synthesis, thus lowering the yields of the coupling and deprotection steps.

The peptides B1 and B2 (mimetics of three β -strands of BMP2) were obtained with satisfying homogeneity (one more polar impurity was present, based on the HPLC chromatograms).

Only A1, A5, B1 and B2 were analyzed by CD spectroscopy.

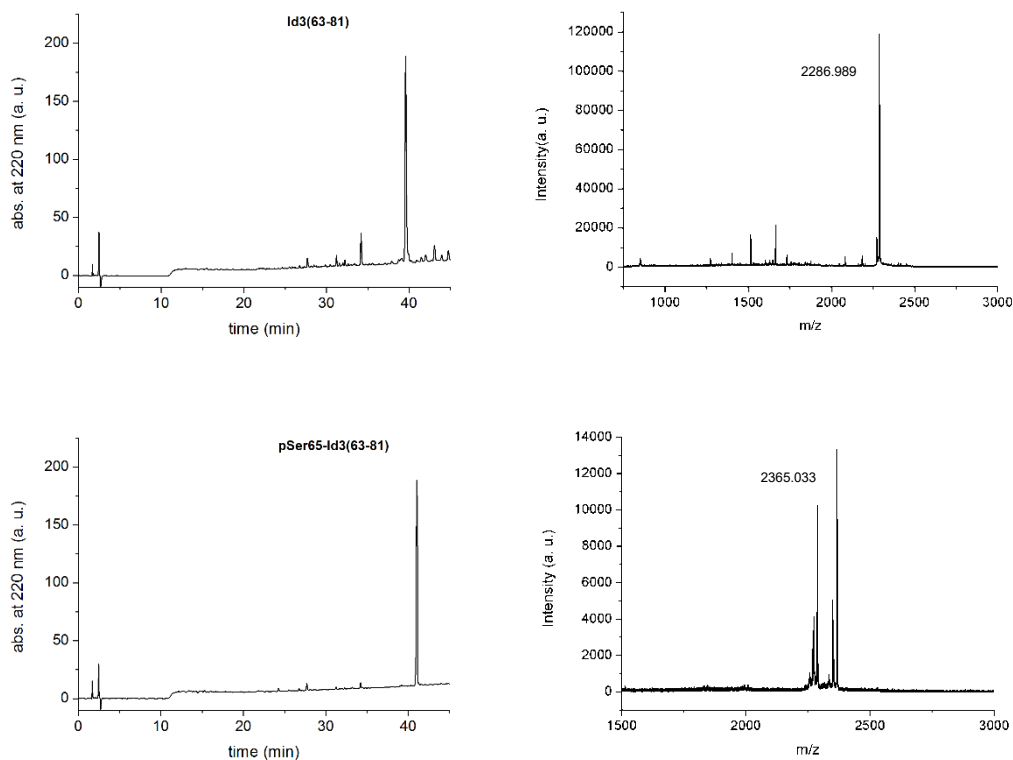


Figure 3. Analytical HPLC profiles and MALDI-TOF-MS of Id3 helix peptides.

Peptides Id3(63-81) and pSer65-Id3(63-81) were poorly soluble and this led to problems in the analysis of their secondary structures that we addressed to peptide aggregation. Phosphorylated peptide was, indeed, less soluble than the non-phosphorylated one.

3.2. CD spectroscopy

The conformation of synthesized peptides has been investigated by circular dichroism (CD) spectroscopy.

The samples of peptides A1, A5, B1 and B2 were prepared dissolving 0.2 mg of peptide in 200 μ L of phosphate buffer 0.2 M pH=6.9 (stock solution). 50 μ L of stock solution were diluted with 400 μ L of phosphate buffer or 30% of TFE in phosphate buffer or 30% of MeOH in phosphate buffer (Figure 4). The samples of peptides Id3(63-81) and

pSer65-Id3(63-81) were prepared dissolving 0.2 mg of peptide in 250 μL of 15% TFE in phosphate buffer 50 mM, pH=7 (stock solution). 64.3 μL of stock solution were diluted with 385.7 μL of 15% TFE in phosphate buffer (Figure 5). The concentrations of the samples were measured by UV spectroscopy.

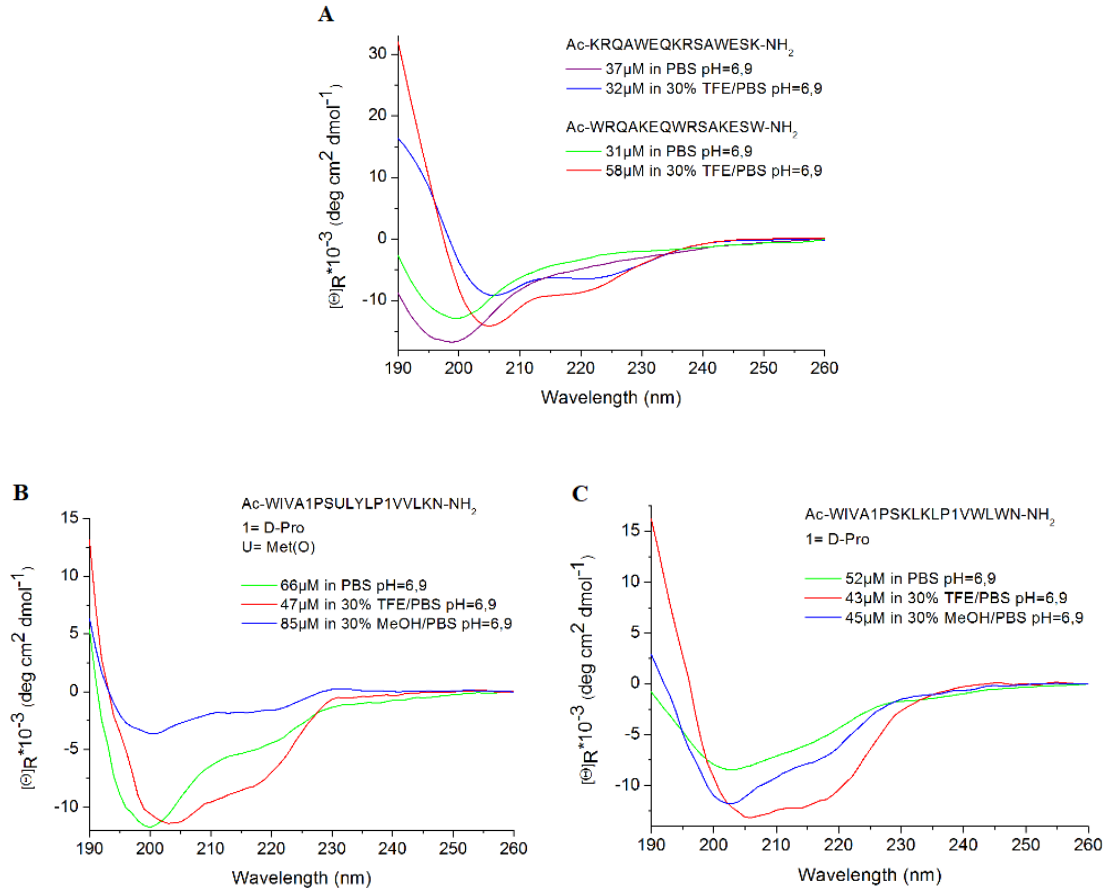


Figure 4. **A)** CD spectra of peptide A1 in phosphate buffer pH=6.9 (purple line) and in the presence of 30% of TFE (blue line) compared with peptide A5 in phosphate buffer pH=6.9 (green line) and in the presence of 30% of TFE (red line); **B)** CD spectra of peptide B1 in phosphate buffer pH=6.9 (green line), in the presence of 30% of TFE (red line) and in the presence of 30% of MeOH (blue line); **C)** CD spectra of peptide B2 in phosphate buffer pH=6.9 (green line), in the presence of 30% of TFE (red line) and in the presence of 30% of MeOH (blue line).

As shown in Figure 4a, A1 and A5 were mostly flexible in phosphate buffer, but could adopt a helical conformation in the presence of 30% TFE, which is known to stabilize secondary structures. A2 was more helical than A1, indicating that the half-zipper $(\text{WK})_2\text{W}$ is more efficient than $(\text{KW})_2\text{K}$.

In the case of the two BMP2 mimetics, it should be said that B1 does not contain the Lys-Trp sandwich motif like B2 (K8, K10, W15, W17). Accordingly, the CD spectrum of B2 indicates the presence of a more ordered structure in comparison to that of B1, which shows an intensive minimum at 200 nm. Also in the presence of organic solvent, B2 proved to be more structured than B1. Future NMR measurements will elucidate the conformation of the two peptides at the residue level.

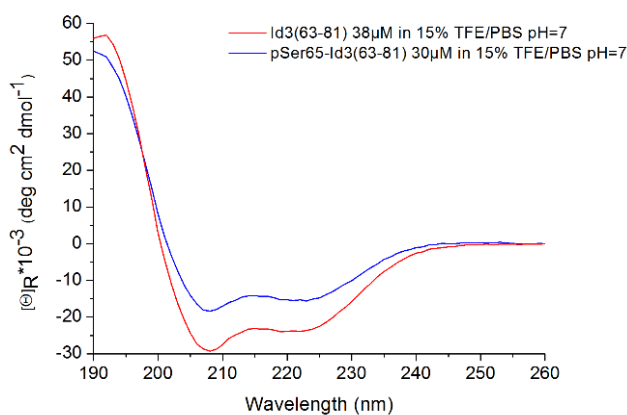


Figure 5. CD spectra of peptides Id3(63-81) (red line) and pSer65-Id3(63-81) (blue line) in 15% TFE in phosphate buffer pH=7.

In the Figure 5, the CD curves suggest the presence of α -helix (two minima at 208 nm and 222 nm, and a maximum below 195 nm). Moreover, peptide Id3(63-81) (red line) is more helical than pSer65-Id3(63-81) one (blue line), suggesting a positive effect of the negative phosphate group on the formation of the helix. This might explain the modulation of PPIs of the Id3 protein with its partners, including MDC1.

Chapter 2
Synthesis of FRET-active substrates
of bacterial serine protease HtrA

1. Introduction

The serine protease high temperature requirement A (HtrA) is secreted by gastric pathogen *Helicobacter pylori* (*H. pylori*) during infection and cleaves gastric epithelial cell surface proteins to decrease the epithelial integrity and barrier function [12]. It targets the cell adhesion protein and tumor suppressor E-cadherin that is responsible of maintaining intact intercellular adhesions between epithelial cells. Loss of E-cadherin function results in loss of epithelial architecture and gastric cancer development. Thus, HtrA cleaves E-cadherin in specific sites during bacterial infection and the data highlight the important role of HtrA in bacterial pathogenesis [12].

During my experience at University of Salzburg I carried out the synthesis and the characterization of fluorogenic peptides to investigate the activity of proteases by FRET (fluorescence or Forster resonance energy transfer) measurements. With this study on the fluorogenic peptides, I have contributed to a recent publication on the peer-reviewed journal Scientific Reports [12].

In this paper, a novel FRET peptide assay was carried out to determinate the activity of *H.pylori* HtrA. Moreover, due to the involvement of Zn^{++} in directly blocking the activity of serine proteases and to its contribution in potentiating moderate serine protease inhibitors by chelating the inhibitor to the histidine and serine of the catalytic triad in the active center, in this study it has been proved that Zn^{++} and Cu^{++} can block HtrA activity and hence, it was assumed that Zn^{++} or Cu^{++} could function as co-inhibitors of HtrA proteases [12]. The Zn^{++} and Cu^{++} mediated inhibitor activity has been monitored by *in vitro* cleavage experiments using casein or E-cadherin as substrates and in the FRET-peptide assay.

In this chapter, the synthetic procedures and the physicochemical characterization of four FRET-peptides (Table 4) as substrates of bacterial serine protease HtrA are reported. One of them was selected and further tested to determinate the activity of *H.pylori* HtrA in the FRET peptide assay.

2. Experimental Part

2.1. Materials and methods

Materials

Chemical reagents and solvents for the peptide synthesis were of peptide-synthesis grade. The natural Fmoc-protected amino acids, Fmoc-3-nitro-tyrosine, Rink-amide MBHA resin (loading 0.57 mmol/g), N,N-dimethylformamide (DMF), N-methyl-2-pyrrolidone (NMP), dichloromethane (DCM), diethylether, and N,N-diisopropylethylamine (DIPEA) were purchased from Iris Biotech (Marktredwitz, Germany). 2-(1H-benzotriazole-1-yl)-1,1,3,3-tetramethyluronium hexafluorophosphate (HBTU), N-hydroxybenzotriazole (HOBT), piperidine, and trifluoroacetic acid (TFA) were purchased from Biosolve (Valkenswaard, The Netherlands). Acetonitrile (ACN), triisopropylsilane (TIS), 1,2-ethanedithiol (EDT), thioanisole (TIA), and 2-(Boc-amino)-benzoic acid (2-Boc-Abz-OH) were purchased from Sigma-Aldrich (Vienna, Austria). HPLC-grade TFA was from Alfa-Aesar (Karlsruhe, Germany). α -Cyano-4-hydroxycinnamic acid (CHCA) was purchased from Acros Organics (Vienna, Austria). Trypsin was purchased from AppliChem (Darmstadt, Germany).

Methods

The solid-phase peptide synthesis was performed manually by using Fmoc-chemistry. HPLC analysis was carried out on a Dionex UltiMate 3000 system from Thermo Fisher Scientific (Germering, Germany), equipped with a Synchronis C-18 column (100 Å, 5 μ m, 250x4.6 mm, Thermo Fisher Scientific), and a diode-array detector set at 220 nm. The binary elution system consisted of (A) 0.06% (v/v) TFA in water, and (B) 0.05% (v/v) TFA in ACN (flow rate: 1.5 ml/min). The following gradient was used: 3% B for 8 min, 3-60% B over 35 min. MALDI-TOF mass spectra were recorded on an Autoflex mass spectrometer (Bruker Daltonics, Bremen, Germany) by using CHCA as matrix. For the determination of the peptide concentration in 50 mM sodium phosphate buffer (pH 7.3), the UV spectrum was recorded on an Agilent Cary 60 UV-Vis spectrophotometer (the buffer was used as blank). The absorbance of the 3-nitro-

tyrosine residue at 381 nm and a molar extinction coefficient of $2200 \text{ M}^{-1} \text{ cm}^{-1}$ were used to calculate the peptide concentration. To prove the intramolecular fluorescence quenching, fluorescence measurements of the peptide in absence and presence of trypsin or HpHtrA were performed on an Agilent Cary Eclipse fluorescence spectrophotometer.

FRET peptide assay

Quantification of HpHtrA activity was performed using a peptide labeled with a fluorophore (2-Abz) and a quencher (3-nitro-tyrosine). The measurements were performed in a black, flat bottom 96-well plate (Nunc, Thermo Scientific, Schwerte, Germany) at 37°C . $5 \mu\text{M}$ of the peptide were incubated with 250 nM HpHtrA, 125 nM trypsin in 50 mM HEPES buffer (pH 7.4). Where indicated, increasing concentrations of ZnCl_2 or CuCl_2 were added. Cleavage of the peptide leads to increasing fluorescence, which was measured in a plate reader (Infinite® 200 PRO, TECAN, Groedig, Austria) with a filter setting of $320 \text{ nm}/425 \text{ nm}$ (Ex/Em). Statistical analysis was performed with GraphPad Prism software (Vers. 8.0.2). One-way ANOVA was used to statistically compare changes of fluorescence between samples treated with HpHtrA wt or HpHtrA S₂₂₁A with samples treated with trypsin or with samples treated with increasing concentrations of ZnCl_2 or CuCl_2 or untreated control. Three independent experiments containing three technical replicates were analyzed for every sample. Significance was indicated as non-significant (ns) > 0.05 , * for $p < 0.05$, ** for $p < 0.01$, *** for $p < 0.001$, and **** for $p < 0.0001$.

2.2. Peptide synthesis and analysis

The solid-phase peptide synthesis was performed manually by using Fmoc-chemistry. Fmoc deprotection was carried out with 25% piperidine in DMF/NMP (80:20, v/v) for 3 min, and 12.5% piperidine in DMF/NMP (80:20, v/v) for 12 min. The double couplings (2x45 min) were accomplished with the mixture Fmoc-AA-OH/HOBt/HBTU/DIPEA (5:5:4.8:10 equiv.). 2-Boc-Abz-OH was coupled with the same protocol. Afterwards, the peptidyl-resin was treated with 25% piperidine in DMF/NMP (80:20, v/v) (2x12 min) to deacylate the 3-nitro-tyrosine side chain. The peptide was simultaneously

cleaved from the resin and deprotected by using the mixture TFA/H₂O/TIA/EDT/TIS (90:3:1:3:3; V_{tot} = 1 ml) for about 3 h, precipitated from ice-cold diethyl ether, recovered by centrifugation at 4°C for 6 min, washed four times with ice-cold diethyl ether, and dried *in vacuo*. The solid was dissolved in water and lyophilized. The purity and the identification of desired peptides were evaluated by analytical HPLC and MALDI-TOF-MS (Table 5 and Figure 6). The samples were prepared dissolving 0.2 mg of peptide in 150 μL of ACN/0.1%TFA in H₂O (25% and 75%, respectively).

Table 4. Sequences of synthetic substrates of HtrA.

<i>Name/Label</i>	<i>Sequence</i>
SubHtrA_QV	2-Abz-AQRVAF-Y (3-NO ₂)-NH ₂
SubHtrA_QA	2-Abz-AQRAAF-Y (3-NO ₂)-NH ₂
SubHtrA_KV	2-Abz-AKRVAF-Y (3-NO ₂)-NH ₂
SubHtrA_KA	2-Abz-AKRAAF-Y (3-NO ₂)-NH ₂

Table 5. Analytical characterization of the peptides.

Peptide label	M_{theor.}^a(Da)	(M-H)⁻_{found}^b (Da)	t_R^c (min)
SubHtrA_QV	1017.12	1016.03	28.4
SubHtrA_QA	989.06	987.91	26.8
SubHtrA_KV	1017.16	1016.23	27.1
SubHtrA_KA	989.11	988.31	25.7

a. Monoisotopic/Average

b. Measured by MALDI-TOF-MS (negative mode measurement)

c. HPLC gradient: 3% B for 8 min, 3-60% in 35 min, with A = 0.06% TFA in water and B = 0.05% TFA in acetonitrile

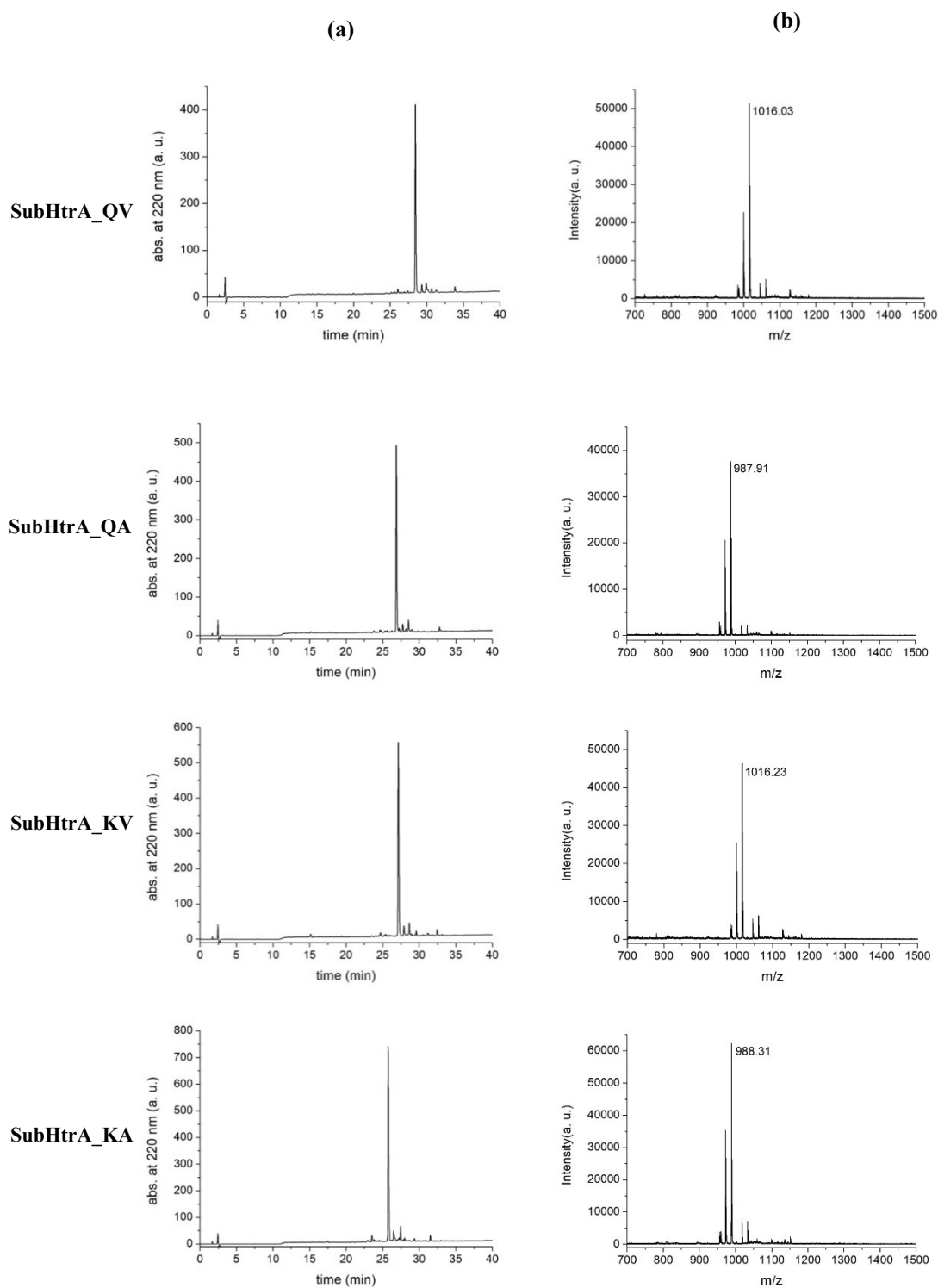


Figure 6. Analytical HPLC (a) and MALDI-TOF-MS (b) of synthesized peptides. The MS spectrum shows the characteristic MS fragmentation of the nitro group (-16 Da, -32 Da).

3. Results and Discussion

FRET technology is a methodology that allows continuous assays of protease activity and high-throughput screening of protease inhibitors. FRET peptide assay was developed from direct in-gel profiling of protease specificity (DIPPS) assay for HtrA [12]. The detected peptides were processed by HtrA. The data suggest that HtrA commonly cleaved peptides after the aliphatic residues V, I or A in position P1. Further, the P2 position is dominated by the basic amino acids R and K, P3 by R, P4 by A, P1' by A and K, P2' by Y (Figure 7, left panel). The detected characteristic AR/QRV↓AY confirmed the preference of HpHtrA to cleave between hydrophobic amino acids [12]. Moreover, it was suggested that AQPVEA linker region between the EC5 and the TMD of E-cadherin was a preferred cleavage site in E-cadherin for HpHtrA during the infection process, and this sequence is similar to the detected characteristic AR/QRV↓AY (Figure 7, right panel) [12].

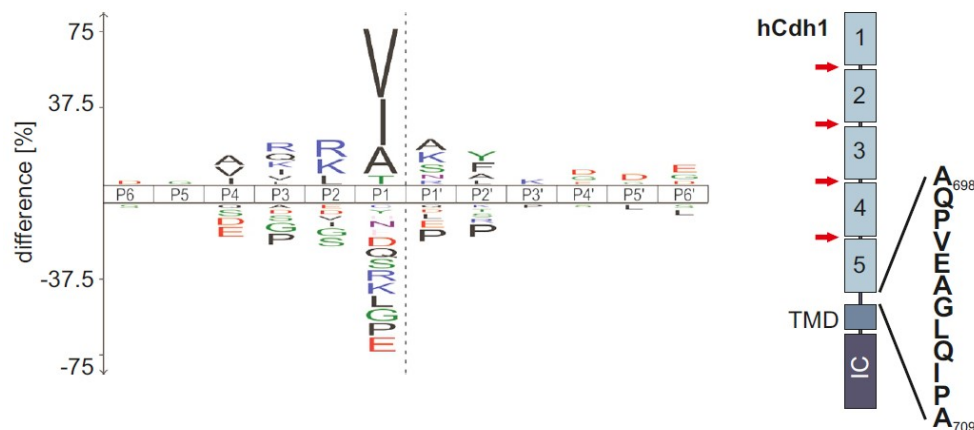


Figure 7. The cleavage specificity profile of HpHtrA obtained from DIPPS profiling (on the left) and the domain structure of human E-cadherin (hCdh1, on the right), composed of the extracellular domain (EC1–EC5), a transmembrane domain (TMD) and an intracellular domain (IC).

Based on these evidences, FRET peptides containing the N-terminal fluorophore 2-aminobenzoyl (2-Abz) and the C-terminal quencher 3-nitro-tyrosine Y(NO₂) were synthesized (Table 4). One of them, 2-Abz-AQRVAF-Y(3-NO₂)-NH₂, was selected and further tested to assess the activity of *H. pylori* HtrA. FRET-peptide was equally cleaved by trypsin with an R and by HpHtrA with a V in position P1 (Figure 8).

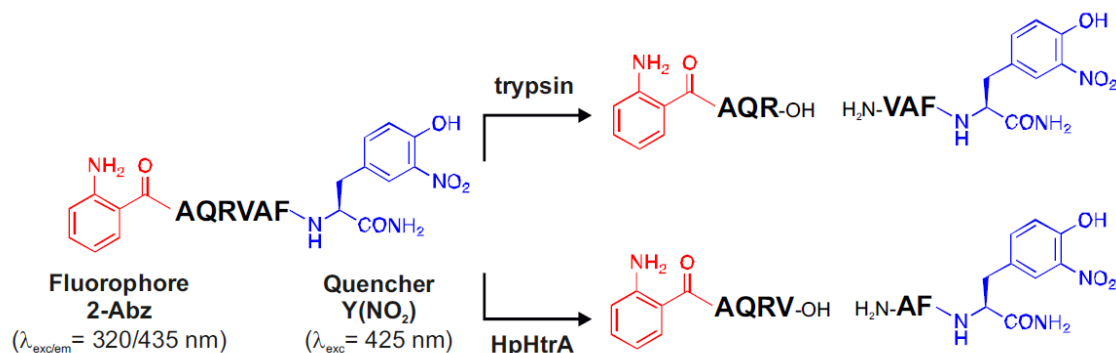


Figure 8. The sequence AQRVAF harbouring 2-aminobenzoyl (2-Abz) as fluorophore and 3-nitro-tyrosine Y(NO₂) as a quencher is hydrolyzed by trypsin with arginine (R) at position P1 and by HpHtrA with valine (V) at position P1 [12].

Intramolecular quenching of fluorescence of the FRET peptide was highly efficient (Figure 9).

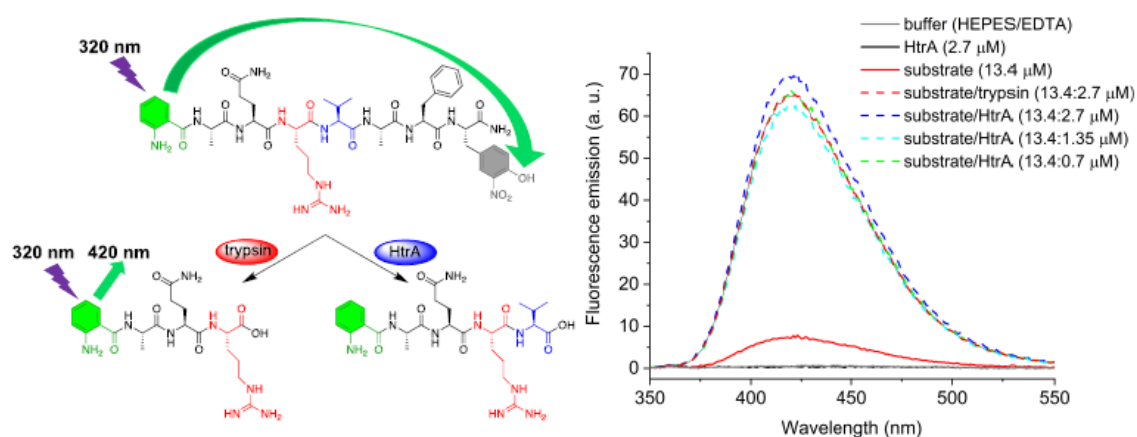


Figure 9. Intramolecular fluorescence quenching of the fluorogenic peptide 2-Abz-AQRVAF-Y(3-NO₂)-NH₂. To prove the intramolecular quenching of the 2-Abz fluorescence by 3-nitro-tyrosine, 120 μ l of a peptide solution (56 μ M in 50 mM phosphate buffer, pH 7.3) were diluted with 380 μ l of 50 mM HEPES/EDTA buffer (pH 7.4) to a final peptide concentration of 13.4 μ M. The peptide/protease mixtures were prepared by mixing 120 μ l of the peptide solution with trypsin or HpHtrA solutions: the final peptide concentration was 13.4 μ M, whereas the final protease concentrations were 2.7 μ M for trypsin, and 0.7 μ M, 1.35 μ M, and 2.7 μ M for HpHtrA. All samples were incubated overnight at 37°C. Then, the fluorescence emission spectra were recorded upon excitation at 320 nm at 24°C [12].

A fluorescence emission maximum for the 2-Abz moiety was observed at 420 nm, which showed ten times higher intensity in the presence of the protease, thus confirming the intramolecular quenching activity of 3-nitro-tyrosine on the 2-Abz group. No significant changes were observed between trypsin and HpHtrA or between the different HpHtrA concentrations [12].

A strong increase in emitted fluorescence was produced by the cleavage using trypsin and HtrA wild type (wt), while the inactive mutant of HtrA (SA) did not target the FRET substrate (Figure 10) [12].

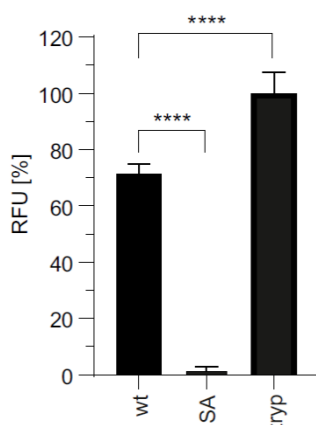


Figure 10. Emitted fluorescence by trypsin- or HpHtrA(wt)-mediated cleavage. 5 μ M of the FRET peptide were incubated with 250 nM of HpHtrA wild type (wt), its isogenic inactive mutant (SA), or 125 nM trypsin for 180 min in 50 mM HEPES buffer (pH 7.4) at 37 °C. The data represent the relative fluorescent units (RFU) \pm S.D. with the fluorescent signal obtained from trypsin-treated FRET peptide set as 100%. Asterisks indicate statistically significant differences (**** $p < 0.0001$).

Mass-spectrometry analyses demonstrated HtrA-specific cleavage with V in position P1 (Figure 11). The peptide was stable in the buffer in the absence of the protease as well as in the presence of the HpHtrA SA mutant. Instead, it was fully cleaved, preferentially after V in presence of the HpHtrA [12].

Figure 12 shows that the proteolytic activity of HpHtrA wt was concentration-dependent and the effective cleavage of the FRET peptide could occur at low concentrations compared to the inactive HtrA SA mutant [12].

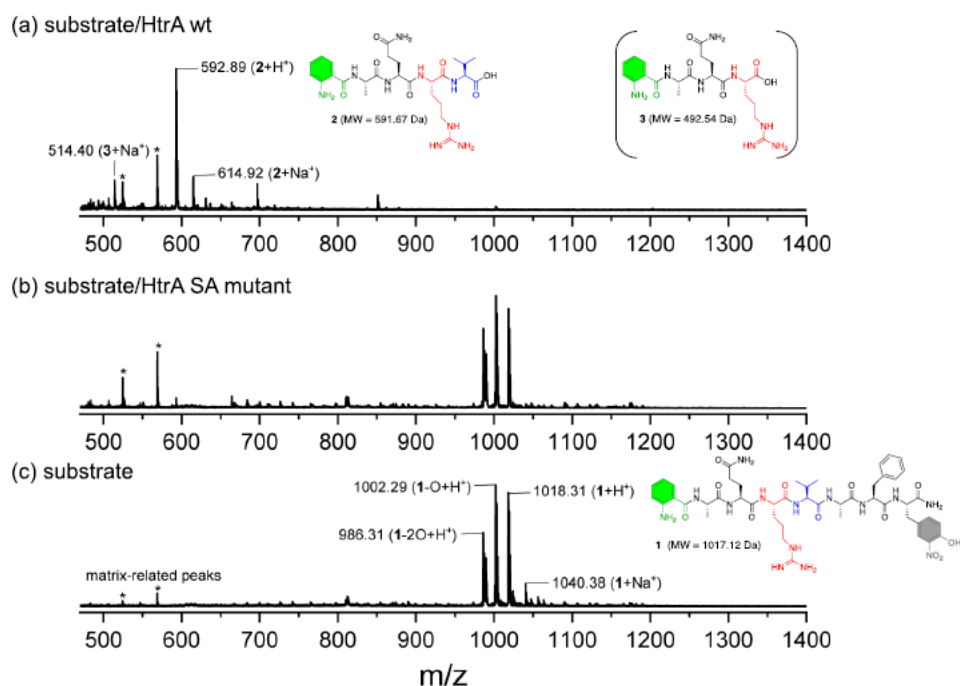


Figure 11. MS analysis of the HpHtrA-mediated cleavage products of 2-Abz-AQRVAF-Y(3-NO₂)-NH₂. The peptide was incubated alone or in the presence of HpHtrA wt or the inactive SA mutant at the 20:1 ratio in 50 mM HEPES buffer (pH 7.4) for 3 h at 37°C. The samples were desalted by using ZipTip® pipette tips (Merck Millipore) and measured by MALDI-TOF-MS.

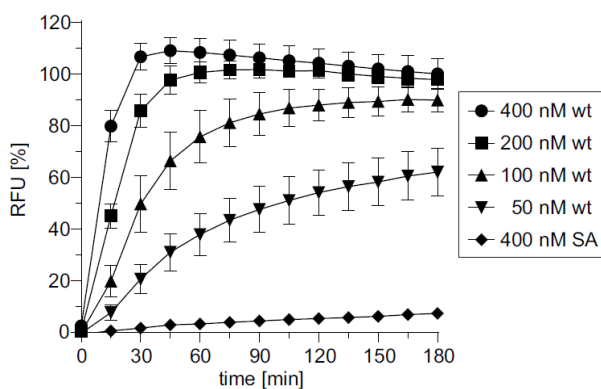


Figure 12. The kinetics of the proteolytic activity of increasing HpHtrA wt concentrations compared to the inactive HtrA SA mutant. 4 μM of the FRET peptide were incubated with indicated concentrations of HpHtrA wt or SA for 180 min at 37 °C in 50 mM HEPES buffer (pH 7.4). The data represent the RFU ± S.D. with the fluorescent signals obtained from FRET peptide treated with 400 nM HpHtrA wt for 180 min set as 100%.

Because of the evidence that Zn^{++} directly blocked the activity of serine proteases and potentiated moderate serine protease inhibitors, it was proven that Zn^{++} and Cu^{++} can block HtrA activity and could function as co-inhibitors of HtrA proteases [12].

These studies were conducted by *in vitro* experiments in which recombinant HpHtrA was incubated with casein or recombinant human E-cadherin (hCdh1) as a substrate, in presence of divalent cations (Figure 13A-B). The cleavage was analysed by coomassie-stained protein gels or Western blot. HpHtrA efficiently degraded casein or hCdh1 in absence of divalent cations. The presence of Zn^{++} and Cu^{++} strongly inhibited HtrA activity.

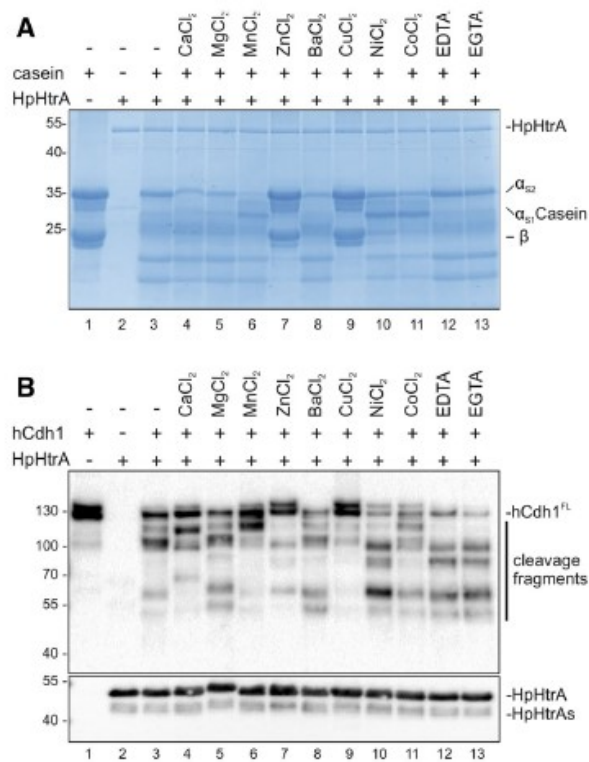


Figure 13. Divalent cations modulate the activity of HpHtrA on casein (A) or hCdh1 (B) substrates.

Zn^{++} - and Cu^{++} -mediated HtrA inactivation was validated using the FRET peptide assay, performing titration experiments to determine the concentrations of Zn^{++} and Cu^{++} that are required for HtrA inhibition [12]. The data suggested that increasing concentrations of Zn^{++} and Cu^{++} significantly interfered on HtrA activity (Figure 14). Moreover, the addition of Zn^{++} and Cu^{++} alone did not quench the fluorescent signal

(Figure 15) highlighting the specificity of the measurement and the broad application of the FRET peptide for future drug screening [12].

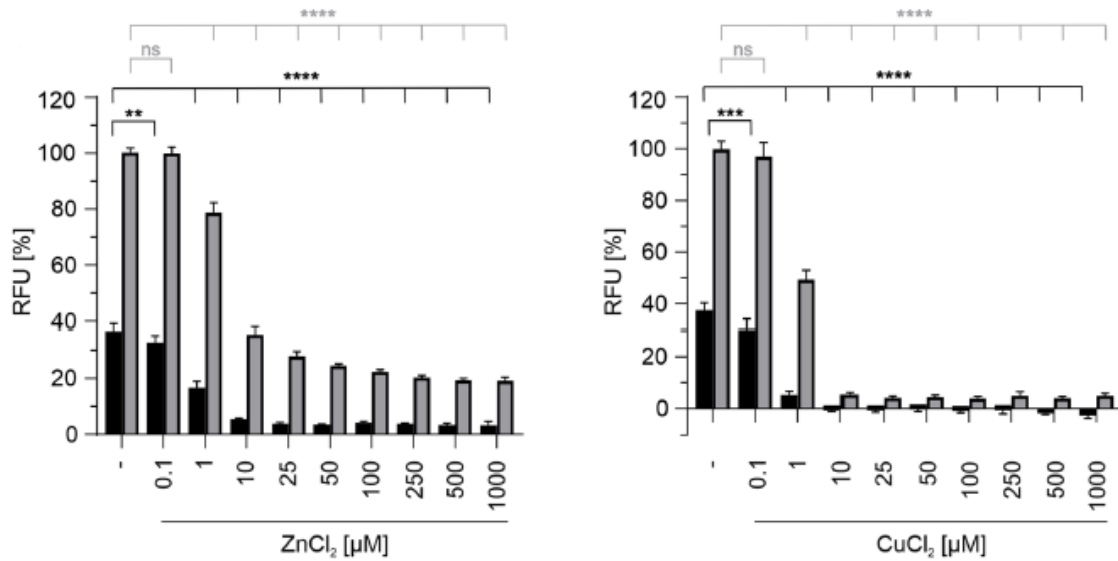


Figure 14. ZnCl₂ and CuCl₂ inhibit HpHtrA activity in a concentration-dependent manner [12]. 5 µM FRET peptide were incubated with 250 nM HpHtrA and increasing concentrations of ZnCl₂ (left panel) or CuCl₂ (right panel) for 15 min (black bars) and 180 min (grey bars) at 37°C in 50 mM HEPES buffer (pH 7.4). The data represent the relative fluorescence units (RFU) ± S.D. with fluorescent signals obtained from FRET peptide treated with HpHtrA wt set as 100%. Asterisks indicate statistically significant differences (*****p* < 0.0001; ns, non-significant).

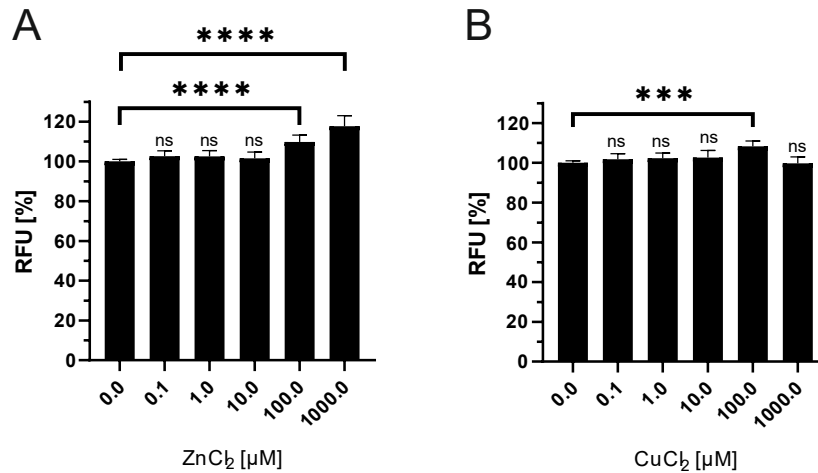


Figure 15. Divalent ions do not quench fluorophores [12]. The peptide was incubated with HpHtrA for 180 min at 37°C at a ratio of 20:1 in 50 mM HEPES buffer (pH7.4). The cleaved peptide was aliquoted and incubated with increasing concentrations of ZnCl₂ or CuCl₂ ranging from 0.1-1000 µM. After incubation for 30 minutes at RT in the dark, fluorescence of the cleaved peptides was measured. The data represent the relative fluorescent units (RFU) ± S.D. with fluorescent signals obtained from HpHtrA wt treated FRET peptide set as 100%. Asterisks indicate statistically significant differences (****p*=0.001; *****p* < 0.0001; ns, non-significant).

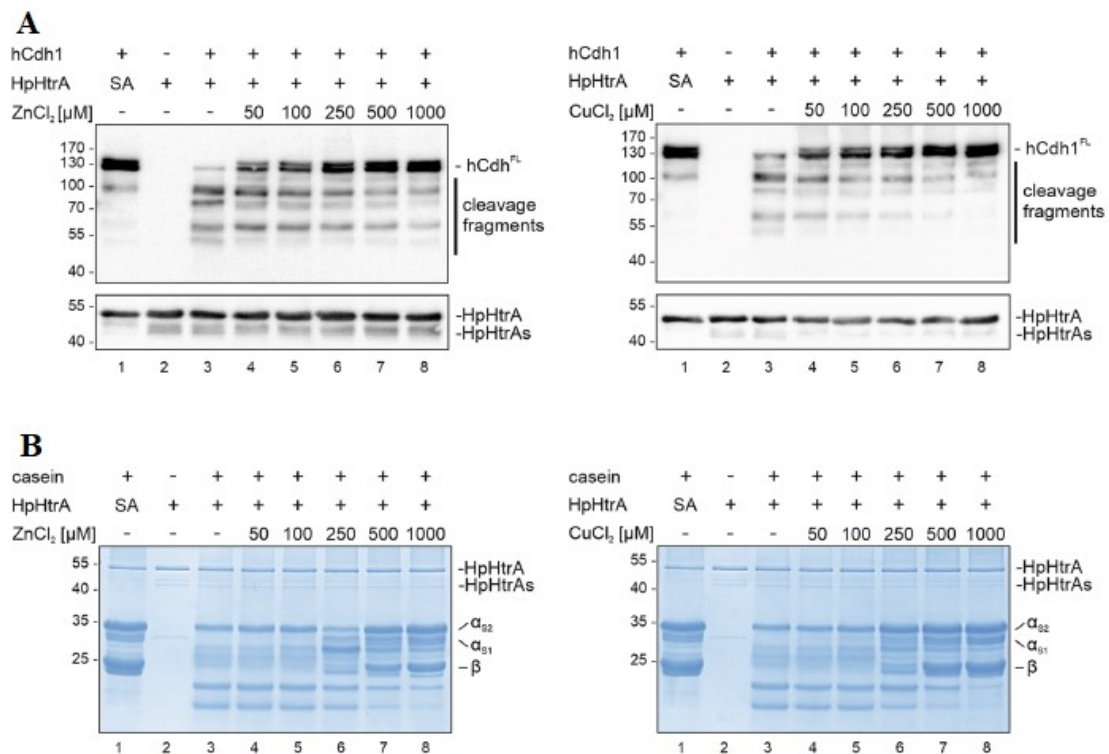


Figure 16. Concentration-dependent inhibitor effect of Zn⁺⁺ or Cu⁺⁺ on hCdh1 (A) and casein (B) [12]. The proteolytically inactive HpHtrA mutant (SA) does not process hCdh1 or casein and it was used as control. Zn⁺⁺ inhibited HpHtrA-mediated hCdh1 cleavage in a concentration-dependent manner. The caseinolytic activity of HpHtrA was not affected by low Zn⁺⁺ or Cu⁺⁺ concentrations. A slight inhibitory effect could be detected using 250 μM Zn⁺⁺ or Cu⁺⁺, which was further enhanced at increasing concentrations. An increase up to 500–1,000 μM was required to fully inhibit casein cleavage.

The inhibition of HpHtrA wt detected in the FRET peptide assay was also compared with *in vitro* cleavage experiments using casein or hCdh1 as substrates (Figure 16). Some differences in the concentrations required for efficient HpHtrA inhibition were detected in the FRET peptide assay and the *in vitro* cleavage experiment, which have been assigned to the increased accessibility of the FRET peptide, which contains a single, conformation-independent consensus cleavage site rather than folded complex proteins [12]. Comparing the different methods, we concluded that the FRET peptide as a substrate for HpHtrA is a highly sensitive and reliable approach to quantify HtrA activity [12].

References

1. Braun P, Gingras AC. History of protein-protein interactions: from egg-white to complex networks. *Proteomics*. 2012;12(10):1478-1498.
2. Azzarito V, Long K, Murphy NS, Wilson AJ. Inhibition of α -helix-mediated protein-protein interactions using designed molecules. *Nat Chem*. 2013;5(3):161-173.
3. Remaut H, Waksman G. Protein-protein interaction through beta-strand addition. *Trends Biochem Sci*. 2006;31(8):436-444.
4. Robinson JA, Moehle K. The protein epitope mimetic approach to protein-protein interaction inhibitors. *de Gruyter*. 2011. DOI:<https://doi.org/10.1515/9783110252361.fm>
5. Henchey LK, Jochim AL, Arora PS. Contemporary strategies for the stabilization of peptides in the alpha-helical conformation. *Curr Opin Chem Biol*. 2008;12(6):692-697.
6. Riemen AJ, Waters ML. Design of highly stabilized β -hairpin peptides through cation- π interactions of lysine and n-methyllysine with an aromatic pocket. *Biochemistry*. 2009;48(7):1525-1531.
7. de Vega MJ, Martín-Martínez M, González-Muñiz R. Modulation of protein-protein interactions by stabilizing/mimicking protein secondary structure elements. *Curr Top Med Chem*. 2007;7(1):33-62.
8. Falcigno L, D'Auria G, Calvanese L, Marasco D, Iacobelli R, Scognamiglio PL, Brun P, Danesin R, Pasqualin M, Castagliuolo I, Dettin M. Osteogenic properties of a short BMP-2 chimera peptide. *J Pept Sci*. 2015;21(9):700-709.
9. Roschger C, Cabrele C. The Id-protein family in developmental and cancer-associated pathways. *Cell Commun Signal*. 2017; 15(1):7.
10. Roschger C, Neukirchen S, Elsässer B, Schubert M, Maeding N, Verwanger T, Krammer B, Cabrele C. Targeting of a Helix-Loop-Helix Transcriptional Regulator by a Short Helical Peptide. *ChemMedChem*. 2017; 12(18):1497-1503.
11. Lee JH, Park SJ, Hariharasudhan G, Kim MJ, Jung SM, Jeong SY, Chang IY, Kim C, Kim E, Yu J, Bae S, You HJ. ID3 regulates the MDC1-mediated DNA damage response in order to maintain genome stability. *Nat Commun*. 2017;8(1):903.
12. Bernegger S, Brunner C, Vizovišek M, Fonovic M, Cuciniello G, **Giordano F**, Stanojlovic V, Jarzab M, Simister P, Feller SM, Obermeyer G, Posselt G, Turk B, Cabrele C, Schneider G, Wessler S. A novel FRET peptide assay reveals efficient *Helicobacter pylori* HtrA inhibition through zinc and copper binding. *Sci Rep*. 2020;10(1):10563.

Unit 3

**Design of novel formulations
containing H₂S-releasing corticosteroid hybrids**

1. Introduction

In this project molecular hybrids containing a pharmacologically active portion and an H₂S-releasing moiety have been synthesized and chemically/preclinically characterized with the aim to combine the pharmacological proprieties of native compounds and beneficial effects of H₂S. At the present, results about steroidal anti-inflammatory H₂S-releasing hybrids have been disclosed. As already reported in previous, although the major aim of my PhD work focused to the development of novel H₂S hybrids for the treatment of psoriasis, my studies have been also extended to the effects of the new entities in the therapy of asthma.

The project has been carried out in collaboration with the pharmaceutical industry Genetic s.p.a. in Fisciano (Italy), which presents an extensive experience in the production and development of pharmaceutical products.

During this experience I have expanded my skills and looked all the aspects of the development of pharmaceutical forms, including the development of analytical methods and their validation, thus the processes validation and finally the stability studies to ensure the safety, efficacy, and quality of a new drugs and to determinate their shelf-life. In Genetic I had the opportunity to learn the use of technical instruments in the R&D labs, applied on already active projects.

2. Aim

My training has been aimed to the design and the subsequential development of potential formulations containing the synthesized compounds that have shown more promising results.

In the first preliminarily phase I studied the characteristics of the main pharmaceutical forms for topical or respiratory use, under the supervision of the industrial tutor and the technicians of the research and development laboratories. Successively, the formulations have been designed for their application in the treatment of psoriasis and asthma, the latter in consideration of the interest of Genetic s.p.a. towards respiratory diseases. Further studies finalized to the evaluation of the active substances' stability, to the determination of the formulations physicochemical stability and to the

characterization of their *in vitro* performances will be carried out by Genetic s.p.a. on the developed formulations. In this unit, the characteristics of the selected pharmaceutical forms and the analyses that will be performed to assess the specific stability and safety profiles of formulations are argued.

3. Topical formulation for the treatment of psoriasis

Topical therapy is the most utilized treatment of psoriasis, especially in patients with mild disease [1]. Different vehicles are available for the correct penetration of medications: creams, lotions, foams, sprays, ointments, gels, solutions, shampoos, and so on [2]. The selection of a specific vehicle depends on different application sites on the body or patient compliance, that uses more gladly a less greasy preparation during the daytime than the night, in which can also use a less cosmetically appealing preparation, but more effective [1]. The most used topical preparations are semisolid dosage forms that include ointments, creams, lotions, and gels [3]. Topical formulations have the advantage to be easier administrated and are convenient in terms of portability. The development of a successful pharmaceutical dosage form for skin delivery requires pre-formulation and formulation studies, that have to consider the skin barrier structure, in order to overcome this or to interact with the barrier. Drug permeation depends on the nature of the active substance and the excipients [4]. The topical preparations may be designed to limit their activity on the surface of the skin with no stratum corneum penetration, and in such cases, excipients can be used to retain the drug on the surface layer of the skin, inhibiting skin penetration [3]. Furthermore, topical formulation may act locally or systemically, penetrating the stratum corneum [3]. Most of topical dermatologic preparations are designed to have local effects, but some of them also display a minor/negligible systemic effect, as a small amount of the drug is absorbed systemically [3]. Drug topical application must ensure the required therapeutic action at a specific target in the skin, via release of the active drug substance from the dosage form (drug release) and penetration/diffusion of the drug through the stratum corneum and other layers of skin, before giving the desired pharmacological effect at the site of action [5].

My attention has been focused to the development of creams as topical formulations to vehicle Triamcinolone acetonide hybrid derivatives and to promote their penetration and release in the skin.

3.1. Cream features

Creams are semisolid emulsions which contain one or more active substances dissolved or dispersed in a suitable base. A cream is therefore a biphasic system in which the dispersed or internal phase is uniformly dispersed in the continuous or external phase. According to the dispersed phase nature, it is possible to distinguish an oil-in-water cream (o/w or hydrophilic cream) or a water-in-oil cream (w/o or hydrophobic cream) [2, 6].

The design of a cream has the aim of developing a formulation which can achieve the therapeutic objectives and ensure the quality, remaining stable over the shelf life [4]. States of diseased skin, such as psoriasis, may have effects on the barrier property of skin, and this aspect must be considered in designing of topical formulations [3]. Drug properties such as solubility, partition coefficient (Log P), particle size, pKa, permeability, and melting point are important features to consider in the development of the cream [4]. Moreover, the selection of the excipients plays a central role, because they can influence the final product performance, manufacturability, and stability. Excipients may be used to improve drug solubility and to incorporate it at the target concentration (solvents), to control drug release and cream viscosity (thickeners), to improve drug skin permeability (chemical permeation enhancers), to enhance drug and formulation stability (antioxidants, emulsifiers, and buffers), and to prevent microbial growth and contamination (preservatives) [4].

The solvent choice is crucial for the solubilizing phase of the emulsion system and the skin permeation rate of the active substance. It can be selected according to drug physicochemical properties and aqueous or oily solubilizing phase nature of cream. Compatibility among excipients and active substance must be evaluated to predict any stability failures and possible incompatibilities in the final formulation [4]. These studies are important to select the suitable excipients to ensure drug stability, to identify degradation products and their formation pathway, and the stable storage conditions.

Therefore, the choice of excipients, their concentration, and characteristics can influence the drug product performance [4].

The oily phase can be made up by saturated and unsaturated fatty acids/fatty acid esters, hydrocarbons, and polyols. The oily excipient can contribute to the drug solubility, physical stability, and drug release performance and transport into the skin. They also act as penetration enhancers, and consistency or viscosity modifiers [4]. Humectant (polyols) promotes the retention of water in the system [3]. Thickeners and emulsifying agents contribute to stabilize the emulsion formulation consisting in two immiscible phases [4]. Thickeners influence cream viscosity and, consequently, skin retention of the topical dosage form and drug penetration. The emulsifying agents assist the emulsification process during cream manufacturing and ensure emulsion physical stability during the product shelf life. The type of emulsifying agent (anionic, cationic or nonionic), hydrophilic-lipophilic balance (HLB), Log P, and concentration are important parameters to consider for developing emulsion formulation. The nature of emulsifiers determines the emulsion type and stabilization. Ionic surfactants are used in o/w emulsions, whereas nonionic surfactants can be used in both o/w and w/o formulations. Permeation enhancer (such as Propylene glycol, Ethanol, Isopropyl Alcohol, Oleic acid, Polyethylene glycol) increases the permeation by promoting the diffusion, partitioning, or the drug solubility of an active ingredient through the stratum corneum [3]. Antioxidants and preservatives contribute to maintain the physicochemical properties of the emulsion and to prevent the microbial contamination, respectively [4]. The atmosphere oxidation results in degradation products and this can be prevented by introduction of excipients with antioxidant properties. The choice of antioxidant type and concentration depends on its efficacy and compatibility with other excipients, according to pharmacopeial information. Antimicrobial agents prevent any microorganism growth and must have a wide spectrum of bactericidal activity, low Log P, compatibility with other excipients, stability, and efficacy over a wide range of pH and temperatures. Acidifying/alkalizing/buffering agent can be added to maintain a proper pH for the dosage form [3].

3.2. Design and analysis of a cream for psoriasis disease treatment

The design of the specific pharmaceutical dosage has been preceded by an extensive retrospective analysis of the available literature on topical formulations for the treatment of psoriasis [7-9]. Based on the preclinical results obtained on H₂S releasing glucocorticoids and following the suggestions of Genetic s.p.a. we decided to develop a cream formulation containing Triamcinolone acetonide-HPI or Triamcinolone acetonide-HBTA (compounds **VI** and **VIII**, respectively) 0.1%, as active substances.

The designed formulations contain:

A) 0.100g Triamcinolone acetonide-H₂S donor per 100g, benzyl alcohol, cetylstearyl alcohol condensed with ethylene oxide, isopropyl palmitate, glycerin, sorbitol solution, lactic acid, purified water.

B) 0.100g Triamcinolone acetonide-H₂S donor per 100g, stearic acid, cetyl alcohol, stearyl alcohol, glyceryl monostearate, polyoxyl 20 cetyl ether, liquid paraffin, isopropyl myristate, dimethicone 350, ascorbic acid, disodium edta, glycerin, xanthan gum, sodium benzoate, citric acid monohydrate, purified water.

At the present the first three laboratory batches of the topical formulations have been set up for each compound.

After the validation of analytical methods, analyses to ensure the quality and stability of the products will be performed and compared with specification according to European Pharmacopeia and ICH guidelines. The analyses will consist in:

- Qualitative description, organoleptic qualities, and consistency of the drug product (i.e., change in the colour during storage);
- Visual test for homogeneity of drug product (i.e., ensuring no separation of phases);
- pH measurement of the cream on suitable pH-meter at 25°C;
- Evaluation of product viscosity;
- Evaluation of spreadability;
- Evaluation of tube extrudibility;
- Identification of active substance by HPLC, evaluating the retention time of the active substance peak in the chromatogram, and by UV;
- Determination of assay by HPLC;

- Preservative content by HPLC;
- Antioxidant content by HPLC;
- Impurity tests by HPLC;
- Microbial contamination test;
- Determination of minimum volume fill;
- Determination of residual solvent.

Studies on formulations stability will ensure the selection of the most promising formulation for the subsequential *in vitro* drug release and permeation testing, which will be realised through Franz diffusion cells using a synthetic membrane (such as silicone, polycarbonate, or cellulose) or skin membranes placed between the donor and the receptor compartments, respectively [4].

4. pMDI in the asthma therapy

Inhaled medications are preferred therapy for the treatment of asthma [10-11]. The major advantage of inhaled therapy is that medications are delivered directly into the site of action. The direct drug administration to the airways has many benefits, including rapid delivery of low doses and increased efficacy, with significantly reduction of systemic adverse effects.

There are different methods of delivering pulmonary drug aerosols to patients: pressurized metered dose inhalers (pMDI or MDIs), dry powered inhalers (DPIs) and nebulizers.

The development of a pharmaceutical formulation for pulmonary delivery involves different steps: *in vitro* performance characterization, testing and *in vivo* clinical studies in healthy volunteers or patients.

For the development of pulmonary inhalation products, it is important to assess the amount of drug that enters the lung, the location of deposition, the residence time at deposition sites and absorption into the systemic circulation [12]. This is important to determinate the fraction of drug contributing to the efficacy and whatever it leaves the lungs contributing to the systemic side effects. After inhalation, some fraction of administered dose of the drug is deposited in the mouth and adsorbed through the

gastrointestinal tract. Indeed, the drug deposited in the oropharynx and the portion absorbed from gastrointestinal tract get into systemic circulation and contribute only to side effects and not efficacy. Only the drug dose delivered directly to the lung contributes to the efficacy (Figure 1) [12].

Several techniques are available to describe lung deposition, including *in vitro* approaches (such as Multi-Stage Liquid Impinger or MSLI, Andersen Cascade Impactor or ACI and Next Generation Impactor or NGI), imaging approaches and pharmacokinetic studies [13-14].

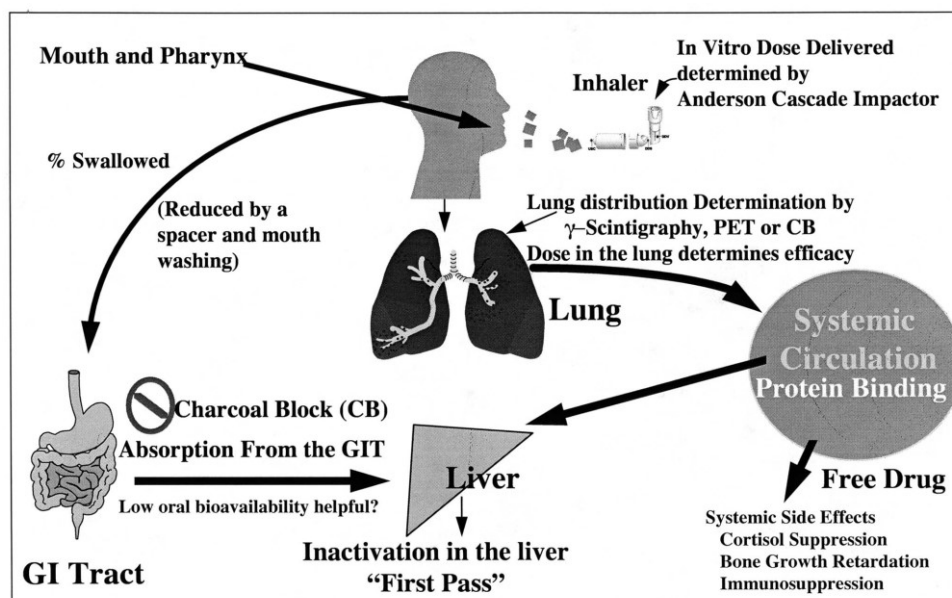


Figure 1. Deposition of an oral inhaled drug.

In vitro studies are important to establish the initial selection of doses that are then compared with *in vivo* ones using a pharmacokinetic study. Moreover, *in vitro* tests are designed as a demonstration of *in vivo* performance and they are useful for preliminary studies to give a good final formulation. Because the later clinical trials are often expensive and lengthy, these earlier tests represent a good point to ensure an efficient development program and successful outcome for the subsequent phases of formulation development as well as the clinical comparability in clinical trials [12].

For inhaled medications there are three important measures of performance which directly affect the delivery of the drug into the lungs and the site of action. They are the amount of drug contained within each pre-metered dose in the device - the *metered dose*- the amount of drug exiting the mouthpiece of the inhaler upon inhalation and entering the patient's respiratory tract - the *delivered dose* - and the amount of drug depositing in the lungs - the *fine particle dose* [15].

Once again, bearing in mind the preclinical results obtained on H₂S releasing glucocorticoids and merging these with the wide interest of the Company in the development of drugs for the treatment of respiratory diseases, my attention has been focused on the development of pMDI containing Triamcinolone acetonide-HPI as active substance.

4.1. pMDI features

Pressurized metered-dose inhaler is a portable, multi-dose, pressurized reservoir device system consisting of an aluminium canister within a plastic actuator, and which delivers drugs through an orifice in the actuator (Figure 2) [16]. It can be integrated by spacer and dose counter.

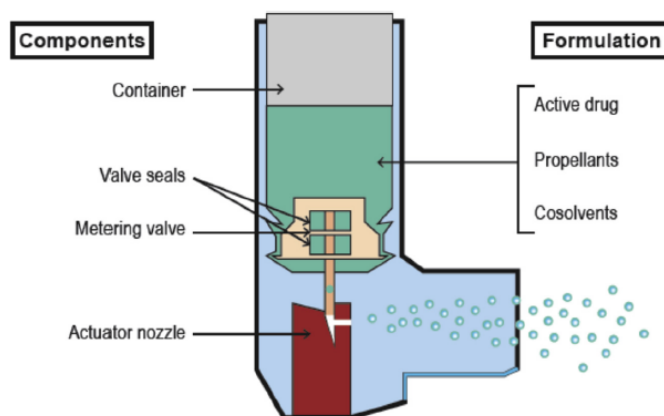


Figure 2. Components of a pMDI.

The pMDI use a propellant, usually an hydrofluroalkane (HFA), which is gaseous at atmospheric pressure and liquid when is in pMDI canister, to deliver a fixed volume of liquid solution or suspension to the patient in the form of an aerosol. The drug is

contained in the canister as a suspension of micronized crystals or a solution with a co-solvent. Suspension formulation can sometimes contain a surfactant, such as oleic acid or lectine, to reduce particle agglomeration [16]. Pressing the actuator, the formulation is released from the metering chamber of the valve into air via the actuator orifice.

Some important technical considerations need to be done in the development of pMDI. In fact, various factors can affect on performance of inhaled formulations and subsequent bioavailability of the delivered drugs, such as spray pattern and plume geometry, which depend by the size and shape of the actuator orifice, the design of the actuator, the size of the metering chamber, the size of the stem orifice of the valve, the vapor pressure in the container, and the nature of the formulation [17].

Some studies evidence as changes in the sump design for pressurized metered dose inhaler (pMDI) products, like orifice diameter, orifice length and sump chamber depth parameters, as well as variability introduced by canister, valve and formulation have the most significant effects on spray performance [17].

At the same time, the use of pMDI requires good coordination, technique, and actuation force. Conventional devices are not always suitable for elderly or paediatric users and many problems may occur because the patient is not able to coordinate inhalation of the drug with the emission following actuation. Spacers (or valved holding chambers) and newer breath-actuated pMDI can help in resolving these problems. The valved holding chamber (VHC) is a specific type of spacer, used as an add-on device for pMDI, which resolves some of the pMDI delivery problems. VCH geometrical and dimensional parameters also affect drug delivery to the patient [18].

4.2. Design and analysis of pMDI for the treatment of asthma

Our aim has been the development and *in vitro* testing of a formulation containing a microcrystalline suspension of Triamcinolone acetonide-HPI in the propellant HFA 134a using ethanol as a dispersing agent 1% w/w, based on the theoretical and practical knowledges acquired during my training in Genetic s.p.a.

In the development of a pMDI, aerosol delivery characteristics, portability, ease of use, device constituent part robustness, inclusion of a dose counter, appropriateness of a lockout, cleaning needs, and suitability to the patient population are important features

to consider [15]. The selection or design of the device constituent art (canister, valve components, actuator, and dose counter) is crucial for the correct delivery of drug [15]. The choice of excipients is important to minimize the potential for settling, creaming, or aggregation of the drug for suspension based pMDI [15]. In fact, they can be minimized if the active substance and the propellants have similar densities.

After preliminary optimization phases, the studies allowed the obtaining of a prototype device containing compound **VI**.

Several studies will be effectuated on the formulation with the aim to determinate the quality and stability of the pharmaceutical form. Analytical methods will be developed and validated. Analyses of the product will be done and compared with specification according to European Pharmacopeia.

The analyses will consist in:

- Evaluation of appearance of the container contents and components;
- pH measurement;
- Identification of active substance by HPLC, evaluating the retention time of the active substance peak in the chromatogram;
- Determination of assay by HPLC;
- Impurity tests by HPLC;
- Microbial test;
- Determination of minimum volume fill;
- Determination of residual solvent;
- Determination of water content;
- Test on spray pattern;
- Determination of number deliveries per inhaler;
- Determination of valve delivery (amount of formulation released per actuation, shot weight);
- Determination of uniformity of delivered dose (UDD), that consist in the measurement of the amount of drug discharged from the mouthpiece of pMDI, whit the dose collection apparatus (Dosage Unit Sampling Apparatus or DUSA, Figure 3);

- Determination of aerodynamic particle size distribution that allows to calculate the fine particle dose using the apparatus named Next Generation Impactor (NGI, Figure 4).

4.3. Dosage Unit Sampling Apparatus or DUSA

The dose collection apparatus (DUSA, Figure 3) must be capable of quantitatively capturing the delivered dose [2]. The apparatus consists of a filter-support base with an open-mesh filter-support, such as a stainless steel screen, a collection tube that is clamped or screwed to the filter-support base, and a mouthpiece adapter to ensure an airtight seal between the collection tube and mouthpiece. The vacuum connector is connected to a system comprising a vacuum source and flow regulator. The air flow rate is fixed at 28.3 L/min ($\pm 5\%$).

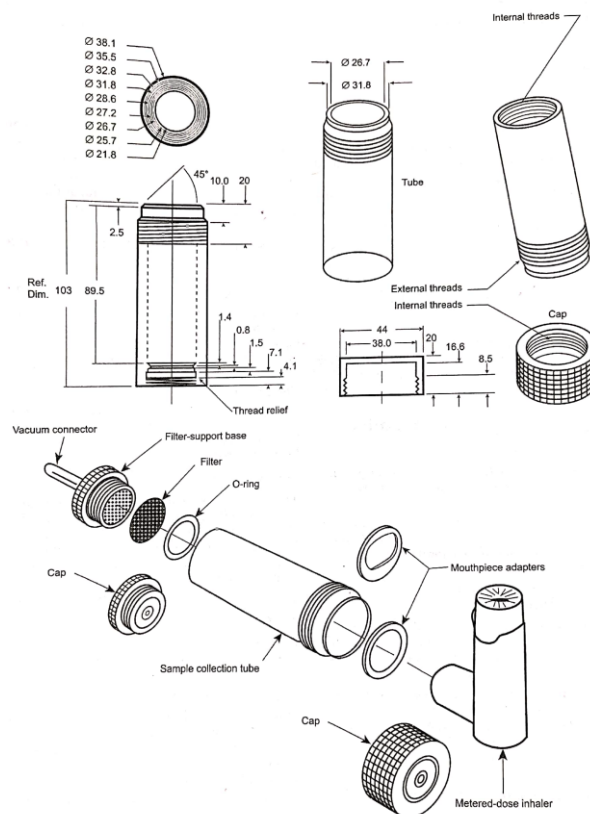


Figure 3. Dosage Unit Sampling Apparatus or DUSA.

The inhaler is shake for 5 s and one delivery dose is discharged to apparatus, depressing the valve for a sufficient time to ensure complete discharge. The procedure is repeated until the number of deliveries that constitute the minimum recommended dose have been sampled. After the dose is captured, the active drug is dissolved in solvent and an aliquot is then analyzed by HPLC to determinate the amount of active substance.

The preparation complies with the test in 9 out of 10 results lie between 75% and 125% of the average value and all lie between 65% and 135%. If 2 or 3 values lie outside the limits of 75% and 125%, the test must be repeated for 2 more inhalers. Not more than 3 of 30 values lie outside the limits of 75% and 125% and no value lies outside the limits of 65% and 135%.

4.4. Next Generation Impactor or NGI

The Next Generation Impactor (NGI) is used for aerodynamic particle size measurement for all inhalation products (Figure 4).

To be therapeutically effective, the particles should have an aerodynamic diameter in the range of 1 to 5 microns. Particles >5 microns generally impact in the oropharynx and be swallowed, whereas particles <1 micron remain entrained in the air stream and be exhaled [16].

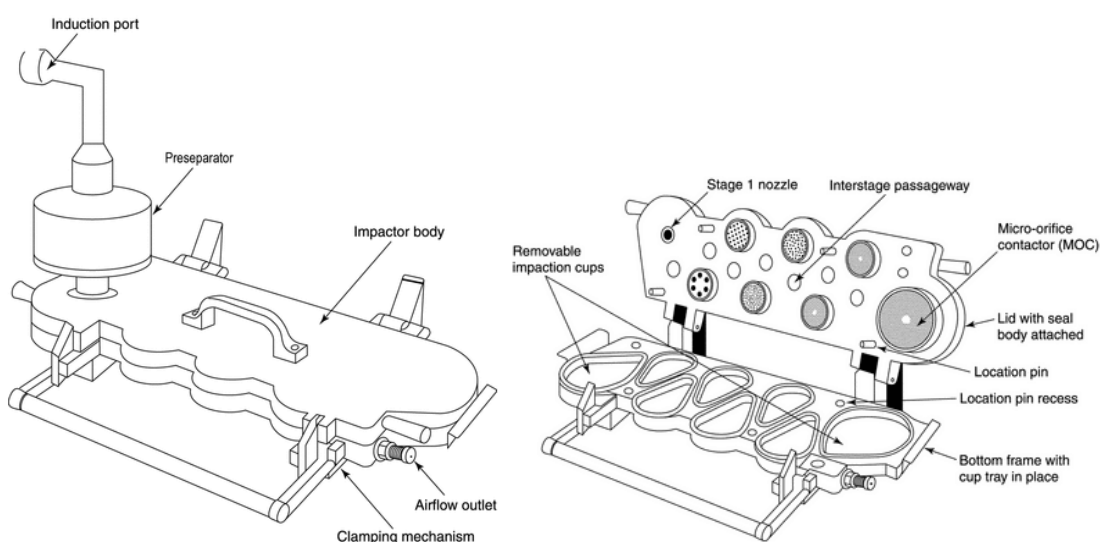


Figure 4. Next Generation Impactor or NGI.

NGI apparatus is a cascade impactor with 7 stages and a micro-orifice collector (MOC) (Figure 5). Over the flow rate range of 30 L/min to 100 L/min the 50 per cent-efficiency cut-off diameters (D_{50} values) range between 0.24 μm to 11.7 μm . In this flow range, there are always at least 5 stages with D_{50} values between 0.5 μm and 6.5 μm . The collection efficiency curves for each stage are sharp and minimize overlap between stages [19].

An induction port with internal dimensions (relevant to the airflow path) connects to the impactor inlet. A pre-separator can be added when required, typically with powder inhalers, and connects between the induction port and the impactor. A suitable mouthpiece adapter is used to provide an airtight seal between the inhaler and the induction port [19].

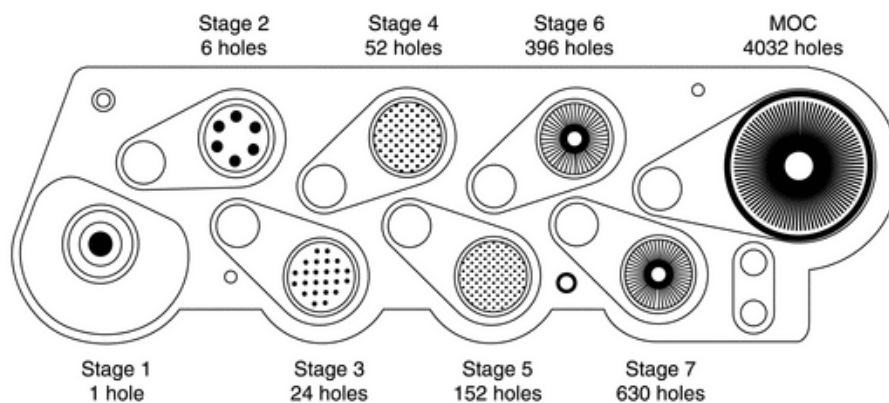


Figure 5. Nozzle configuration of NGI.

The apparatus is connected to a suitable pump and the air flow rate is fixed at 30 L/min ($\pm 5\%$). The inhaler is shaken for 5 s and one delivery dose is discharged to apparatus, depressing the valve for a sufficient time to ensure complete discharge, waiting 5 s before removing the assembled inhaler from the adapter. The procedure is repeated for maximum 10 times.

To recover the active substance the induction port and mouthpiece adapter are removed from the apparatus and the deposited active substance is recovered into an aliquot of solvent. Moreover, the active substance in each cup of the impactor is recovered into an aliquot of solvent. The quantity of active substance contained in each of the aliquots of solvent is determined by HPLC. The fine particle dose is then calculated according to the calculation in European Pharmacopeia.

References

1. Torsekar R, Gautam MM. Topical Therapies in Psoriasis. *Indian Dermatol Online J.* 2017;8(4):235-245.
2. European Pharmacopoeia (Ph. Eur.) 10th Edition, Volume 1, Monographs on dosage forms
3. Chang RK, Raw A, Lionberger R, Yu L. Generic development of topical dermatologic products: formulation development, process development, and testing of topical dermatologic products [published correction appears in *AAPS J.* 2015 Nov;17(6):1522]. *AAPS J.* 2013;15(1):41-52.
4. Simões A, Veiga F, Vitorino C, Figueiras A. A Tutorial for Developing a Topical Cream Formulation Based on the Quality by Design Approach. *J Pharm Sci.* 2018;107(10):2653-2662.
5. Shah VP, Yacobi A, Rădulescu FŞ, Miron DS, Lane ME. A science based approach to topical drug classification system (TCS). *Int J Pharm.* 2015;491(1-2):21-25.
6. United States Pharmacopeia (USP), General Chapters: <1151> Pharmaceutical dosage forms – creams.
7. United States Pharmacopeia (USP), Monographs: Triamcinolone acetonide cream.
8. Federman DG, Froelich CW, Kirsner RS. Topical psoriasis therapy. *Am Fam Physician.* 1999;59(4):957-964.
9. Muruganantham V, Sreedharan NKK, Jaykar B, Palanisamy P. Formulation development and evaluation of topical compositions comprising Arbutin, Tretinoin and Triamcinolone acetonide cream. *Journal of Pharmacy Research* 2014,8(10),1480-1490.
10. National Asthma Education and Prevention Program. National Asthma Education and Prevention Program. Expert Panel Report: Guidelines for the Diagnosis and Management of Asthma Update on Selected Topics--2002 [published correction appears in *J Allergy Clin Immunol.* 2003 Mar;111(3):466]. *J Allergy Clin Immunol.* 2002;110(5 Suppl):S141-S219.
11. Fabbri L, Pauwels RA, Hurd SS; GOLD Scientific Committee. Global Strategy for the Diagnosis, Management, and Prevention of Chronic Obstructive Pulmonary Disease: GOLD Executive Summary updated 2003. *COPD.* 2004;1(1):105-104.
12. Rhodes GR, Rohatagi S, Gillen MS, Deluccia F, Banerji DD, Chaikin P. In vitro and in vivo techniques used in drug development for evaluation of dose delivery of inhaled corticosteroids. *J Clin Pharmacol.* 2001;41(1):7-18.
13. Chrystyn H. Methods to identify drug deposition in the lungs following inhalation. *Br J Clin Pharmacol.* 2001;51(4):289-299.

14. Mobley C, Hochhaus G. Methods used to assess pulmonary deposition and absorption of drugs. *Drug Discov Today*. 2001;6(7):367-375.
15. Metered Dose Inhaler (MDI) and Dry Powder Inhaler (DPI) Drug Products--Quality Considerations. *Fda.gov*. [Online] 2018; <https://www.fda.gov/media/70851/download>.
16. Ferguson GT, Hickey AJ, Dwivedi S. Co-suspension delivery technology in pressurized metered-dose inhalers for multi-drug dosing in the treatment of respiratory diseases. *Respir Med*. 2018;134:16-23.
17. Liao L, Chauhan H, Newcomb A, L'Ecuyer T, Liu-Cordero S, Leveille C. Spray Pattern: A rapid and sensitive early development tool for respiratory drug products. *Proveris Scientific Corporation*. 2017.
18. Oliveira RF, Silva MV, Teixeira SFCF, Cabral-Marques HM, Teixeira JCF. Efficiency of Valved Holding Chambers: Experimental Full Dose Assessment. *Journal of Aerosol Medicine and Pulmonary Drug Delivery*. 2014; 28(4).
19. European Pharmacopoeia (Ph. Eur.) 10th Edition, Volume 1, 2.9.18 - apparatus E.